UNIVERSIDAD DEL PAÍS VASCO/EUSKAL HERRIKO UNIBERTSITATEA

Escuela de Ingeniería de Bilbao

Departamento de Ingeniería Química y del Medio Ambiente

# Integrated Hydrometallurgical process for Paval valorization

Dissertation submitted to fulfill the final requirements to obtain the degree of

Ph.D. in Engineering of Materials and Sustainable Processes

by:

**Ainhoa Ocio Eguiluz**

Thesis advisors:

**Prof. Dr. Pedro Luis Arias**

**Prof. Dr. José F. Cambra**

Bilbao, 2020

Durante los últimos años esta tesis ha ocupado buena parte de mi tiempo y energía, hasta el nivel de no saber hablar de otra cosa, y es el momento de reconocer el mérito que ha supuesto estar cerca de mí en este tiempo.

A mis directores de tesis, José y Pedro, por guiarme desde los inicios de mi camino en la investigación, animarme a hacer un doctorado, hacer posible conseguir una beca para ello, y tener siempre las puertas de vuestros despachos abiertas para prestarme vuestros conocimientos de ingeniería química, y de la vida en general.

A la gente de Befesa Aluminio, especialmente a Jessica Montero, por ser mi ventanita al I+D industrial desde la comodidad de la universidad.

A todos los veteranos de batalla, Kepa, Iker G, Aitziber, Naia, Solar, David, y a los que aún siguen por aquí, Maria, Ana, Paula, Juan Luis, Alberto, Nere, Mikel, por hacer más amenas las horas de laboratorio, y por los muy necesarios cafés.

A Marifeli Larisgoiti, con la que tuve la suerte de trabajar durante los primeros años de investigación y de la que aprendí muchísimo sobre todo tipo de equipos instrumentales, analítica, y, sobre todo, a no tenerle miedo a coger un manual desde la página 1, y estudiármelo.

A todo equipo de investigación de aguas, por regalarme conocimiento de técnicas instrumentales sin las que no existiría esta tesis, en especial a Miren.

A Javier Sangüesa del Departamento de Rocas y Minerales del servicio de Rayos X de la universidad, que ha realizado todos los análisis de FRX y DRX de esta investigación (que no son pocos) y siempre ha estado disponible para aclarar cualquier duda.

A los amigos que me han acompañado de cerca desde el otro lado del muro, Asier, Ione, Rubén, Garazi, Mikel, Unai, Imanol, que se que se alegrarán de saber que, si, parece que (por fin) he acabado de escribir.

A Sara, que comenzó siendo una gran compañera de laboratorio, y se ha convertido en una de mis personas preferidas.

A Gorka Gallastegui, la única persona que no tenía por qué, pero me ha pedido una copia física de la tesis y puede que de verdad se la lea.

A Iker, principal culpable de que se me vaya a poder llamar doctora en breves, y de mi felicidad durante estos años. Sin tu apoyo y ayuda *constante* no estaría escribiendo estos agradecimientos.

A mi familia, especialmente a mis padres y mi hermana, por estar siempre ahí, dispuestos a ayudarme en lo que necesite, y esperando pacientemente a que les informe de todos mis pequeños logros.

*A mis padres, por su apoyo absoluto y incondicional*

*A Maitane, somos un equipo*

*A Iker, que me metió en esto y luego me ayudó a salir*

# Table of contents

# Summary

This PhD thesis was carried out in the Sustainable Process Engineering (SuPrEn) research group of the Chemical and Environmental Engineering Department - Faculty of Engineering of Bilbao, University of the Basque Country, under the supervision of Prof. Dr. José Francisco Cambra Ibáñez and Prof. Dr. Pedro Luis Arias Ergueta.

Along these years, this work allowed to propose an integrated process for salt cake Paval valorization (through fluoride content reduction) *via* a hydrometallurgical process and the treatment of the generated effluent for its recycling, thus, reducing total waste production. This research is presented in eight chapters:

- Chapter 1 of this research provides a general overview of primary and secondary aluminum production, along with a brief description of the main wastes generated in these industries and their possible uses, including the production of Paval, the material of interest in this thesis.
- Chapter 2 of this PhD thesis consists on a description of the two main techniques for fluoride removal from solid matrixes: *(i)* Thermal treatments and *(ii)* hydrometallurgical treatments, such as chemical leaching.
- Chapter 3 of this PhD thesis sets the objectives and scope of this research, *i.e.* the design of a Paval valorization integrated process technically and economically viable to allow its industrial implementation.
- Chapter 4 summarizes the main experimental procedures used during the realization of this thesis to help the fluency of the following chapters dealing with the experimental results, discussion and conclusions.
- Chapter 5 studies the effect of the main operating parameters (acidic and basic leaching agents, temperature, pH, reaction time and solid/liquid ratio) on the selective fluoride leaching from industrial Paval samples. This was studied while minimizing aluminum removal *via* a Taguchi Design of experiments and an ANOVA analysis.
- Chapter 6 is a review of the industrially employed sulfate removal methods: *(i)* precipitation, *(ii)* membranes, *(iii)* ion exchange, *(iv)* adsorption, and *(v)* biological mechanisms.
- Chapter 7 studies the recyclability of the effluent produced in the hydrometallurgical process proposed in Chapter 5 to minimize the overall

waste production. In addition, some applications for the produced by-products are proposed.

- Chapter 8 summarizes the conclusions obtained after carrying out this PhD thesis, and proposes future research areas that could benefit from the present research.

# Resumen

Esta tesis doctoral se llevó a cabo en el grupo de investigación SuPrEn (Ingeniería de Procesos Sostenibles/Sustainable Process Engineering) del departamento de Ingeniería Química y del Medio Ambiente de la Escuela de Ingeniería de Bilbao de la UPV-EHU, bajo la supervisión del Prof. Dr. José Francisco Cambra Ibáñez y del Prof. Dr. Pedro Luis Arias Ergueta.

Tras estos años de trabajo se ha conseguido proponer un proceso integrado de valorización de Paval de escoria salina mediante la reducción de su contenido en flúor mediante tratamiento hidrometalúrgico, así como el posterior tratamiento y reintroducción del efluente obtenido y tratado al proceso hidrometalúrgico. Esta investigación se ha estructurado en ocho capítulos:

- El capítulo 1 proporciona una visión general de la producción de aluminio, junto con una breve descripción de los principales residuos generados en esta industria y sus actuales salidas, incluyendo la producción de Paval, el material de interés en esta tesis doctoral.
- El capítulo 2 describe las principales técnicas de eliminación de flúor en sólidos: *(i)* tratamientos térmicos, y *(ii)* tratamientos hidrometalúrgicos, especialmente la lixiviación química, y concluye, tras un análisis comparativo de estas técnicas, que la hidrometalurgia es la vía más indicada para la extracción de flúor de Paval.
- El capítulo 3 establece como objetivo de esta investigación el desarrollo de un proceso integrado de valorización de Paval que sea técnica y económicamente viable para su posterior implantación industrial, desarrollando este objetivo general en otros más concretos.
- El capítulo 4 contiene la descripción de los principales procedimientos experimentales utilizados en la realización de esta tesis doctoral, de forma que se agilice la comprensión de los siguientes capítulos, que contienen resultados experimentales, su discusión y las conclusiones.
- El capítulo 5 estudia el efecto de los principales parámetros de operación (agentes lixiviantes ácidos y básicos, temperatura, pH, tiempo de reacción y ratio sólido/líquido) en la lixiviación selectiva de flúor y aluminio de muestras industriales de Paval, con ayuda del Método Taguchi de diseño de experimentos y el análisis de la varianza (ANOVA).

- El capítulo 6 analiza y compara los principales métodos industriales de eliminación de sulfatos en efluentes, *(i)* precipitación, *(ii)* membranas, *(iii)* intercambio iónico, *(iv)* adsorción, and *(v)* métodos biológicos, y selecciona la precipitación química como la vía más indicada para el efluente obtenido en el capítulo 5.
- El capítulo 7 estudia la reciclabilidad del efluente producido en el capítulo 5, para minimizar la producción global de residuos, además de proponer posibles aplicaciones para los productos obtenidos en el proceso integrado.
- El capítulo 8 resume las conclusiones obtenidas en el transcurso de esta tesis doctoral, y propone futuras líneas de investigación que podrían beneficiarse de la investigación actual.

# Chapter 1

Introduction

# Table of contents

## 1.1 Introduction

This chapter provides a general overview of primary and secondary aluminum production, along with a brief description of the main residues generated in these industries and their possible uses, including the production of Paval, the material of interest in this PhD thesis.

## 1.2 Aluminum production

Aluminum is the most abundant metallic element in the Earth's crust and the third most abundant element by mass after oxygen and silicon. However, it is not found as pure metal in nature due to its strong tendency to form highly stable oxides. Consequently, its existence was not established until 1808. Bauxite, a clay-like ore, aluminum oxide rich material, was found in 1821 and became the primary source of aluminum. The industrial-scale production and use of aluminum are barely a century old, yet in that time, the industry has grown until it is second only to the iron and steel industry among metal producers. Primary aluminum is produced from virgin ore found in deposits in the Earth's crust and secondary aluminum refers to recycled aluminum, produced from scrap.[1–3]

### 1.2.1 Primary aluminum

In 1886 Charles Martin Hall in the United States and Paul Louis Héroult in France simultaneously and independently patented an identical process. In this process, known as Hall-Héroult process, aluminum ore is dissolved in a bath of molten cryolite ($Na_3AlF_6$) at 960 °C, and the aluminum is precipitated using electricity. It is still the most efficient method to produce aluminum in commercial quantities.[1,2,4]

The production of primary aluminum is accomplished in three stages:[1]

i. Mining the raw ore (fundamentally bauxite): The most important parameter used to determine bauxite suitability for primary aluminum production is its Total Available Alumina (TAA, g of extractable $Al_2O_3$ per g of material), often estimated *in situ* prior to mining, as it gives an idea of the aluminum that can

be extracted by the Bayer process.[5,6] Commercial bauxites typically present TAA 35–50%.[7]

ii. Production of alumina ($Al_2O_3$): In this step, bauxite ore, containing 30 to 60 % $Al_2O_3$) is refined to obtain smelter grade alumina of 99.5 % $Al_2O_3$). Karl Bayer developed a process (Figure 1.1) in which alumina contained in bauxite was selectively dissolved by heating in a sodium hydroxide solution under pressure to form a sodium aluminate solution, from which aluminum in hydroxide form precipitates. This precipitate was then filtered, washed, and calcined to produce high-purity crystalline alumina, and a caustic alkaline liquor to be recycled.[1,3,8] Although the Bayer process is the principal industrial means of refining bauxite to produce alumina ($Al_2O_3$) pure enough for aluminum electrolysis, there are three other alternatives: The Sinter process, the combined/parallel Bayer–Sinter process and the Nepheline-based process. These alternative processes, through which 17% of the world´s alumina is produced, mainly aim at accommodating different raw materials and improving the recovery rate of alumina.

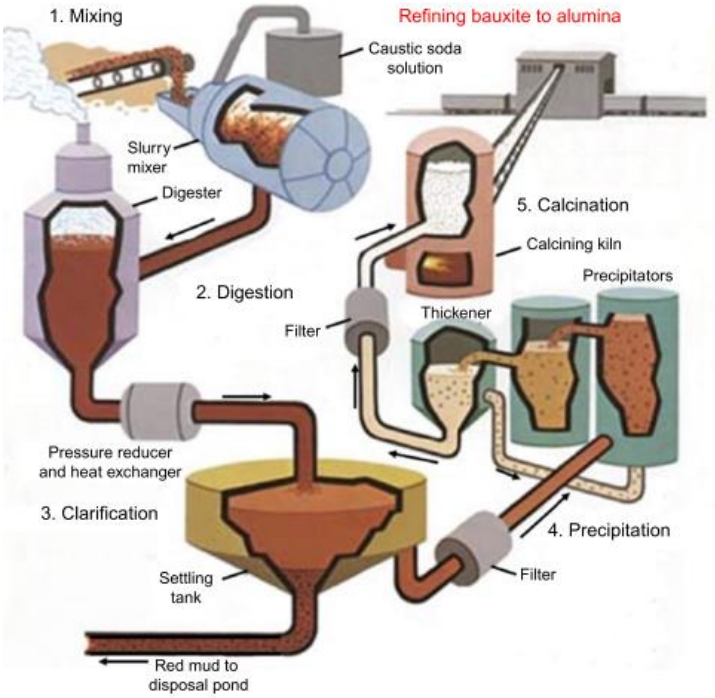


**Figure 1.1.-** Scheme of the Bayer process.[8]

iii. Conversion of alumina into metallic aluminum by Hall–Héroult process: The purified alumina is first dissolved in a bath of molten cryolite ($Na_3AlF_6$, 80-85 %), calcium fluoride ($CaF_2$, 5-7 %), aluminum fluoride ($AlF_3$, 5-7 %) and alumina ($Al_2O_3$, 2-8 %) at 960 ˚C and then reduced by electrolysis. Cryolite is used because it is the best fluxing agent for alumina, and $AlF_3$ and $CaF_2$ in order to lower the melting point of the electrolyte. The electrolytic reduction process requires high purity aluminum oxide, carbon, and electrical power. It takes place in carbon-lined (carbon lining serves as cathode of the cells) steel electrolytic Hall cells, or 'pots'.[1,2,4,8–13]

The end of life of the electrolytic cell is set as the voltage increases or iron starts to be detected in the aluminum metal. When this occurs, the potlining is removed and the shell is re-lined. The spent potlining (SPL) generated is listed by various environmental bodies as a hazardous material because of its leachable cyanide (up to 1 wt.%) and fluoride (up to 20 wt.%) contents. The production of 1 t of aluminum typically requires 420 kg of carbon, 1920 Kg of $Al_2O_3$, 16 kg of $AlF_3$, and approximately 13.200 kWh of electricity. On the other hand, as presented in Figure 1.2, 1 t of pure aluminum generates 1.42 Kg of gas ($CO_2$ + CO), 6.7–9.7 kWh of heat, and 22-50 Kg of SPL, depending on the smelter.[8–10,14–18] As SPL is related to this thesis target, it is further discussed in section 1.3.

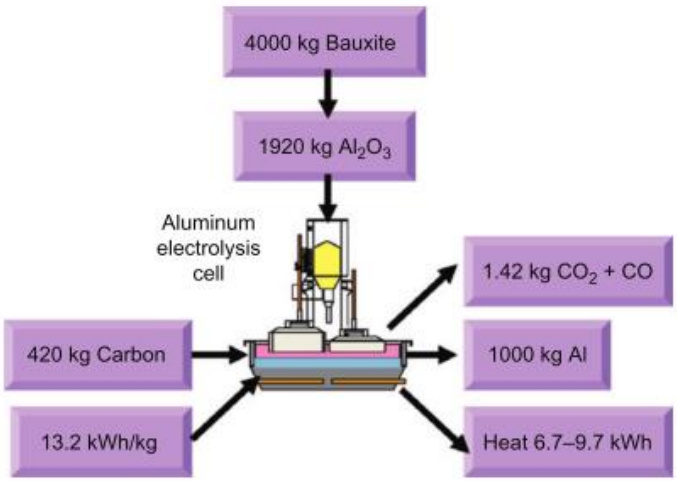


**Figure 1.2.-** Materials and energy consumption for the electrolytic production of 1 t aluminum.[8]

Due to the aluminum's attractive characteristics (high corrosion resistance, mechanical strength to mass ratio, excellent heat and electrical conductivity) aluminum alloys are used as a major structural material in aircrafts, buildings, machinery parts, beverage cans, and food wraps. Besides, the aluminum is the most recyclable of all materials, it is four times more valuable than any other recycled consumer materials. Moreover, aluminum's low melting temperature and Hall-Héroult process' high energy demand, makes its recycling 20 times more energy efficient and emits only 5% of the greenhouse gas as compared to its primary production.[1,2,8,19]

### 1.2.2 Secondary aluminum

In 1990, the secondary aluminum production was around 8 million metric tons (29 % of total aluminum production), in 2010 close to 18 million metric tons (32 % of total aluminum production), and it is estimated that by 2020 the secondary aluminum production will increase to 31 million metric tons (32 % of total aluminum production). Currently, more than half of the aluminum produced in Europe is obtained from recycled raw materials and that trend is clearly increasing.[20] Production of secondary aluminum is accomplished in two stages:

i. Scrap gathering: Scrap is divided in two categories: new and old scrap, according to its origin. If it comes from end of life products is called old scrap, and if it comes from the production process, new scrap [1]. Typical sources of aluminum new scrap are process scrap, extrusions, turnings, and of old scrap are commercial scraps, used beverage cans (UBCs), foils, and old rolled or cast metal. Today, around 50 % of the scrap is old scrap.[20]

ii. Melting of the scrap: A complex combination of all types of aluminum scraps collected is loaded into the melting furnaces, which are most likely to be either reverberatory or rotary furnaces. Regardless the furnace type, a salt flux is used to reduce the melting temperature, protect the molten aluminum pool from oxidation losses, absorb oxides and contaminants from the scrap, and improve the metal recovery from the scrap. Usual fluxes consist of a mixture of chloride, and fluoride compounds, as fluoride additions greatly reduce the surface tension of the molten flux on molten aluminum. The most

used fluoride compounds are cryolite ($Na_3AlF_6$), sodium fluoride (NaF), potassium fluoride (KF), or fluorspar ($CaF_2$).[2,19] Once aluminum is melted, the final alloy components compositions are adjusted to achieve the desired quality. By these means, the removal of oxides and impurities from molten aluminum is enhanced

In the secondary aluminum manufacture, two wastes are generated along with molten aluminum, *i.e.* off-gas and dross. Aluminum dross (also known as skim) is a semisolid mixture of molten aluminum and different oxides and chlorides, depending on the melting practice and used fluxes. Drosses can be classified as non-salt dross (also known as black dross in Europe, and white or gray dross in the United States) if no flux is employed in the melting process, or salt dross, when saline fluxes are used. Salt dross usually contains less than 20 % of aluminum metal, 30 to 50 % of aluminum oxide and 30 to 50 % of fluxing salt.[1,2]

Although salt dross can be thermally processed, it is a common practice to recover much of its aluminum by crushing and concentration. The remaining solid, called salt cake or salt slag, contains 3–9 wt.% of Al, 15–30 wt.% of $Al_2O_3$, 30–55% of NaCl, 15–30% of KCl and, depending on the scrap type may contain, carbides ($Al_4C_3$), nitrides (AlN), sulfides ($Al_2S_3$, $Na_2S$), phosphides ($Si_3P_4$), sulfates ($Na_2SO_4$), and also carbon and cryolite in smaller proportions.[1,2,7,19,21,22] As the salt cake is part of this thesis target, is further discussed in section 1.4.

## 1.3 Spent Potlining (SPL)

As described in section 1.2, SPL is a hazardous waste generated at the end-of-life of the carbon cathodes in aluminum smelting electrolysis cells or pots, *ergo*, produced by the primary aluminum industry. The cell's cathode is replaced when operational failure or poor cell performance, caused by carbon cathode lining degradation, forces the cell shutdown. Cathodes are discarded after 3-10 years, typically 5-6 years, and then named SPL. The SPL composition highly varies due to the differences in the cell lining components, dismantling procedures, and how long the pot has operated. Nevertheless, it usually includes aluminum (5-20 %), refractory bricks (20-50 %), fluorides (20 %),

carbon (5-50 %), sodium (7-20 %), calcium (1-3 %), cyanides (0.1-0.7 %), and polycyclic aromatic hydrocarbons (PAHs).[4,10–13,15,17,23–26] Thus, SPL is classified as a hazardous waste according to the European Waste Catalogue and Hazardous Waste List, (European Waste Code (EWC) 10 03 07*) and to the Environmental Protection Agency of the United States (EPA waste code K088).[18,27] It is considered highly flammable (H3-A[1]), corrosive (H8[2]) and leachable (H13[3]) due to its fluoride content.

A schematic diagram of an Electrolytic/Halt-Héroult cell is shown in Figure 1.3. SPL (Items 12, 15, 16, 18, 20 and 21) is usually classified into 1st cut (portion above the collector bars) and 2nd cut (fraction below the collector bar). The 1st cut is the cathode, which conducts electricity and consists mainly on carbonaceous material blocks with graphitized carbon. The refractory layer that is located below the cathode carbon layer is one of the main constituents of the 2nd cut lining.[15,28]

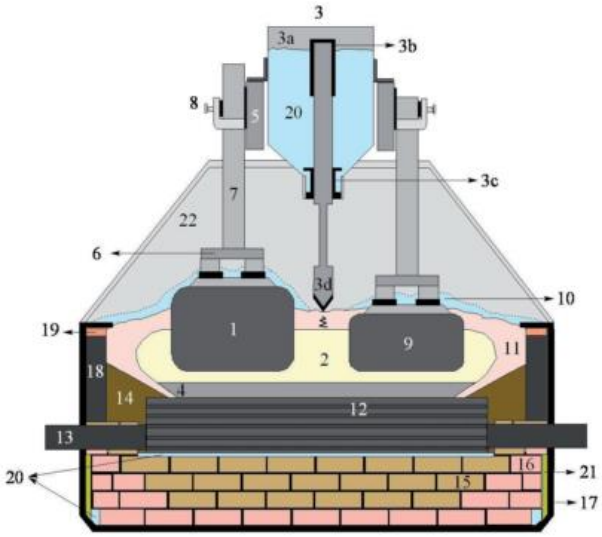


**Figure 1.3.-** Electrolytic/Halt-Héroult cell schematic diagram. (1) anode (prebaked); (2) electrolyte (bath); (3) Alumina point feeder, (3a) alumina hopper (3b) air cylinder, (3c) metering chamber, (3d) crust breaker; (4) aluminium pad; (5) anode beam (current supply); (6) anode yoke and stubs (iron); (7) anode rod (aluminium); (8) anode clamp; (9) spent anode (butt); (10) alumina crust/ cover; (11) crust (side ledge); (12) cathode carbon block; (13) current collector bar (steel); (14) ramming paste; (15) refractory; (16) insulation; (17) steel shell; (18) sidewall block; (19) cast able; (20) alumina; (21) rock wool and (22) gas collection hood (removable).[28]

[1]H3-A: substances and preparations which, in contact with water or damp air, evolve highly flammable gases in dangerous quantities.
[2]H8: substances and preparations which may destroy living tissue on contacts.
[3]H13: substances and preparations capable by any means, after disposal, of yielding another substance, *e.g.* a leachate, which possesses any of the characteristics listed above.

The 2nd cut is also separated according to the expected contamination degree, thus it is usual to find three different cuts:[26] *(i)* 1st Cut, the carbon liner, *(ii)* 2nd Cut,the part of the refractory material that was close to the carbon lining (Chamotte stone), and *(iii)* 3rd Cut, the part of the refractory expected to be least contaminated (Moler stone).

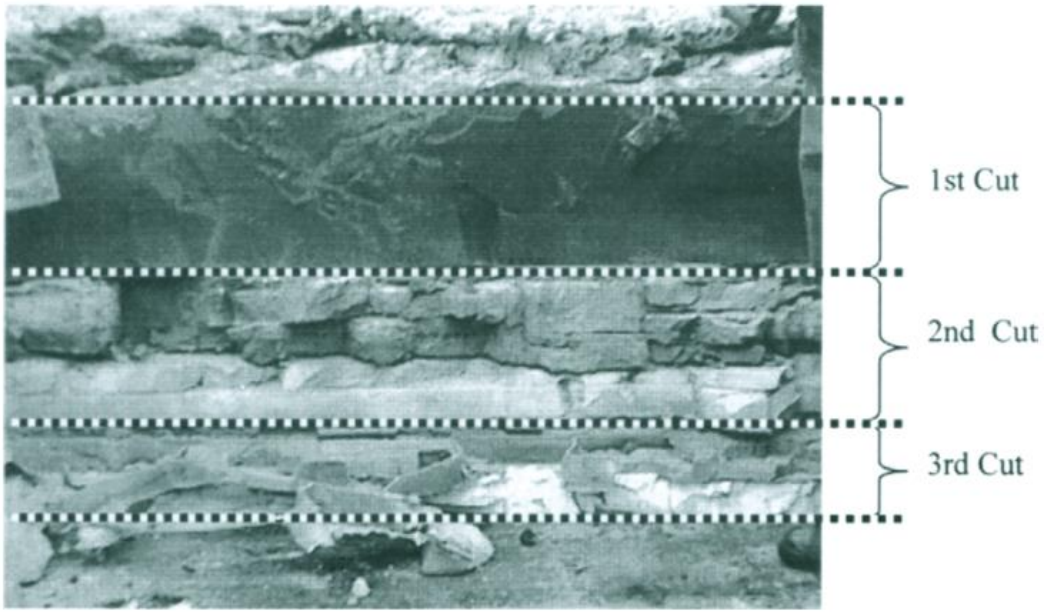


**Figure 1.4.-** SPL 3 cuts, carbon liner, Chamotte stone and Moler stone[26]

The fraction of interest in this PhD thesis is the second cut, as it is the fraction co-processed with salt slag by Befesa Aluminium and converted into Paval, which is the studied material.

### 1.3.1 2nd cut SPL chemical and mineralogical characteristics

The SPL composition highly varies due to the different technologies employed to build cell linings, and to the residual aluminum and flux remaining with the original cell lining components, which vary depending on the dismantling procedures. The composition also depends on how long the pot operated, as sodium and fluoride will have diffused deeper inside the lining for pots that have operated longer, increasing the sodium and fluoride content in SPL. This will also depend on the type of brick.[15] A typical composition of 2nd cut SPL is presented in Table 1.1.

**Table 1.1.-** 2nd cut SPL average elemental composition (wt%)[26]

| Al (total) | F | Si | Na | Fe | Ca | C | CN |
|---|---|---|---|---|---|---|---|
| 16-10 | 16-20 | 7-10 | 0.7-15 | 3 | 1-2 | 2 | 0.1-0.3 |

### 1.3.2 SPL management

As the SPL is subjected to high temperatures, some water reactive chemicals, such as cyanides, metals (Al, Li, and Na), reactive metal oxides ($Na_2O$), nitrides, and carbides, are generated and absorbed into the lining during the cell life. These compounds react with moisture and produce NaOH, $H_2$, $C_2H_4$, and $NH_3$.[12,15,17,18,24,26] It is well stablished that improper SPL disposal results in a substantial hazard to the environment due to migration, mobility and persistence of cyanides. Its management should, therefore, be carried out in compliance with current legislation.[16,24,26,27] In the past, the SPL water reactivity was used to break loose the lining by soaking the complete cell in water. However, because of health safety and environmental concerns, this practice is now abandoned, and today the lining is removed dry.[15] As the SPL is toxic, corrosive, and reactive with water, its processing is a tremendous challenge, along with its handling, transportation and storage.[15]

Although the SPL has been treated for many years just to minimize its fluoride leachability in water in order to enable its disposal in landfills[18,29–31], a number of SPL treatment technologies have been developed over the years mainly focused on recycling SPL. These can be classified into five categories: *(i)* recycling in other industries *e.g.* cement, mineral wool, iron and steel industries, *(ii)* physical separation methods, (*iii)* thermal treatment for the carbonaceous material *e.g.* fluidized bed combustion, pyrosulfolysis, and pyrohydrolysis, where the presence of $H_2O$ and HF at extreme temperatures cause corrosion problems,[32] *(iv)* chemical leaching approaches for cryolite recovery and *(v)* co-processing of SPL in third-party industries, where either its fluoride or carbon fraction can be used.[12,13,15–18,23,26,33] Two of the above mentioned technologies have been considered for development at industrial level, a thermal approach by Ausmelt Alcoa to produce $AlF_3$ and Alcan's caustic leaching to produce NaF or $CaF_2$.[23] As SPL is a hazardous waste, its treatment goals should include *(i)* minimum number of steps, to minimize cost and allow ease of implementation, *(ii)* recovery of valuable materials from SPL: graphite and fluorides (as $AlF_3$ or $CaF_2$), *(iii)* destruction of cyanides, *(iv)* generation of no further environmental problems, *(v)* low energy demand and *(vi)* recycling of virtually all chemical reagents employed.[34]

The co-processing of SPL with Salt Cake is one of the most promising approaches reported. Indeed, Befesa Aluminum found a synergy by blending salt slag and 2nd cut SPL that reduces the energy input to operate their water leach process to produce Paval, a sub-product suitable for the cement or mineral wool industry, which is the material studied in this PhD thesis.[15]

## 1.4 Salt Cake

As described in section 1.2, aluminum salt cake is produced by the secondary aluminum industry, during scrap/dross melting. Depending on the kind of furnace used and the raw mix of scrap being melted, the amount of salt slag produced per metric ton of secondary aluminum ranges from 200 to 600 kg,[2,19,22,35,36] and it contains 15–30 % of aluminum oxide, 30–55 % of sodium chloride, 15–30 % of potassium chloride, 5–7 % of metallic aluminum and impurities (carbides, nitrides, sulfides, phosphides, sulfates and cryolite).[1,2,7,19,22]

According to the European Waste Catalogue and Hazardous Waste List, salt cake is classified as a hazardous waste (European Waste Code (EWC) 10 03 08*).[27] It is considered highly flammable (H3-A[4]), irritant (H4[5]), harmful (H5[6]) and leachable (H13[7]).[27,37] It reacts with water or moist air to release an array of explosive and toxic gases, *e.g.* $CH_4$, $H_2$, $NH_3$, $PH_3$ and $H_2S$, in addition to leaching of toxic ions to the ground.[2,38] Its management should, therefore, be carried out in compliance with current legislation, which forbids landfill direct disposal in most European countries.[1,2]

[4] H3-A: substances and preparations which, in contact with water or damp air, evolve highly flammable gases in dangerous quantities

[5] H4: non-corrosive substances or preparations which through immediate prolonged or repeated contact with the skin or mucus membrane can cause inflammation

[6] H5: substances and preparations which, if they are inhaled or ingested or if they penetrate the skin, involve limited health risk

[7] H13: substances and preparations capable by any means, after disposal, of yielding another substance, e.g. a leachate, which possesses any of the characteristics listed above.

### 1.4.1 Salt Cake chemical and mineralogical characteristics

Salt cakes are complex mixtures of several compounds in different proportions depending on the production process variables and used raw materials.[38] This variability is highlighted by the different literature compositions showed in Table 1.2. Total aluminum concentration varies between 25 and 37%, from which aluminum metal is between 1 and 7%, as it has been previously removed from salt slag. Other typical major elements found in salt slag are chlorine, sodium, nitrogen, fluorine, potassium, magnesium, silica, iron and calcium.

**Table 1.2.-** Elemental composition (wt.%) of Salt slag samples from literature

| | Al (total) | Al (metallic) | Cl | Na | N | F | K | Mg | Si | Fe | Ca |
|---|---|---|---|---|---|---|---|---|---|---|---|
| Sample 1[39] | 25.5 | 3.04 | 0.59 | 0.66 | 0.54 | 3.87 | 0.49 | 6.69 | 3.40 | 1.58 | 1.23 |
| Sample 2[40] | 25 | 7.25 | - | 21.89 | 0.71 | - | 7.47 | 2.83 | 3.69 | 0.50 | 1.07 |
| Samples 3 | 37.2 | 1.22 | 9.39 | 8.52 | 7.53 | 5.15 | 3.18 | 2.59 | 2.07 | 0.82 | 0.72 |
| and 4[7,38,41] | 36.8 | 2.79 | 6.79 | 5.20 | 1.96 | 5.50 | 3.74 | 0.70 | 1.03 | 5.85 | - |

### 1.4.2 Salt Cake management

As salt cake direct/untreated disposal in landfills is either banned or too expensive, its treatment goals should include:[1,19,38]

i. An as low as possible cost and complexity for the process.
ii. A minimal environmental impact of the process.
    - Minimizing or eliminating the residue to be discarded.
    - Generating a nonhazardous residue that can be discarded if necessary.
iii. Recovering the salt content (NaCl and KCl) in the feed.
iv. Recovering the metallic aluminum in the feed.
v. Recovering alumina-containing compounds.
vi. Recovering hydrogen.

Some of the industrial plants that recycle salt slag are Engitec Technologies S.p.A., Berzelius Umwelt-Service AG (B.U.S.), Alustockach, Kali & Salz AG, RVA, Alumitech (Aleris), Alreco's (MHM Metals), Alcoa, ALNAK, Alsa, Alumaxm Reynolds, and Befesa Aluminium, which has plants in Spain, Germany and UK.[2,19,42]

Although there can be some variations, typical treatment includes the five steps described below and shown in Figure 1.5:[1,2,19]

i. Grinding and screening. This step is required to recover most of the aluminum metal. During the grinding process, while the salt slag compounds exhibit brittle behavior, the metallic aluminum exhibits plastic/malleable behavior, depending on the alloy, and is, thus, not reduced in size. Screening allows the coarse aluminum metal particles to be concentrated from the fine fractions, with a diameter of less than 3 mm, which tend to contain mainly metal oxides, other metal compounds, and flux salts. Although this is a usual step in salt slag recycling, a method which skips this step and still recovers 80% of the metallic aluminum has been reported.[1,2,19,38]

ii. Water leaching. It is also known as the reaction step. The water-soluble salts contained in the slag are dissolved and the reactive species decomposed. This step can be carried out at ambient temperature (taking into account that salt's dissolution heat rises temperature up to 60 °C) or at higher temperature and pressure (known as High-Temperature/High-Pressure Process), depending on the reactive compounds. As water will have to be removed later, a brine with 22-25% salt concentration is typically generated. As previously described, this process releases flammable gasses. Therefore, it is necessary to either maintain their concentration below the ignition point by air dilution or to prevent the entry of air.[1,2,7,19]

iii. Gas Treatment. According to Berzelius Umwelt-Service AG (B.U.S.), about 10 $Nm^3$ of $H_2$, $NH_3$, $PH_3$, $H_2S$, and $CH_4$ are produced per metric ton of feed material. $NH_3$ is scrubbed from the off-gas with a sulfuric acid solution and activated carbon filters are used to adsorb the toxic $PH_3$ and the $H_2S$ from the remaining off-gas. Kali & Salz AG purify the off-gases by transformation into ammonium sulfate, sodium phosphate and sodium sulfate. The cleaned gas consists mainly of $CH_4$ and $H_2$ and is used for heating in drying operations and for steam production (instead of natural gas).[2,19]

iv. Solid–Liquid Separation. The brine is then separated from the solid phase – non-metallic product (NMP) by filtering. A reduction in the amount of chlorides in the NMP is essential for its possible commercialization if the aluminum oxide containing material will be used in the production of cement, mineral fibers, and ceramic materials. In this regard, it is imperative to obtain chloride contents lower than 2 wt.% as the only possible outcome for materials with higher contents is landfill disposal. NMPs are marketed under various names, including Oxiton, Noval, Valoxy, Paval, and Serox. The samples of Paval and Serox used in this PhD thesis were provided by Befesa Aluminio.

v. Water removal. Usually water removal is achieved by an evaporator-crystallizer. Some alternative processes such as Freeze-Crystallization, Solvent/Antisolvent, Common Ion, and Electrodialysis have also been proposed. The result of crystallization is wet salt crystals that are subsequently air-dried and reused as flux. As KCl is preferentially vaporized during melting from the melting flux, the recovered salt from the brine has a higher NaCl/KCl ratio than the original flux, and fresh KCl must be added to bring the ratio to the desired values.

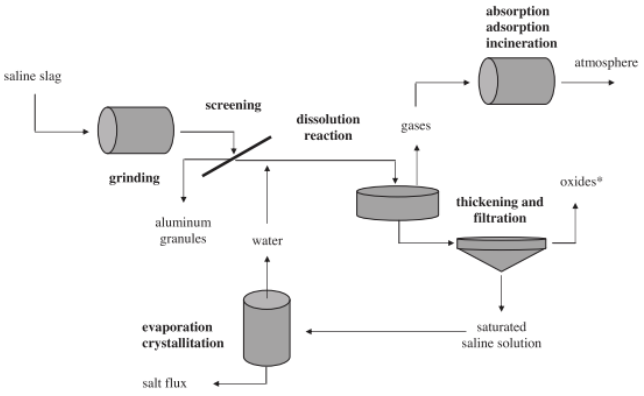


**Figure 1.5.-** Typical salt slag treatment flowchart.[19]

The Befesa's salt slag recycling process is almost identical to that described above: The first step is the mechanical crushing, in order to separate aluminum from the salt cake, and to reduce particle size to enhance reaction of the hazardous components in the next step. The second step is a water treatment in which salts are dissolved and hazardous components are eliminated. In order to control the gases emission during

leaching, the slurry is fed to reactors until the reaction is completed. Then, the brine is separated from the leach residue, by vacuum filtration. Finally, the NaCl and KCl contained in the brine are crystallized.

This process yields metal concentrates (Al) ready for melting, secondary oxide products (NMP), and flux salts to be recycled to the melting step. The NMP is called Paval by Befesa Aluminium and so will be in this thesis. This material mainly consist of alumina and other oxides, aluminum nitride and carbide[21] and is usually disposed in landfills as a nonhazardous material, sold to cement producers or used in calcium aluminate production.[1] As Paval is the material studied in this thesis, it will be further discussed in the next section.

## 1.5 Paval

Paval is the material studied in this PhD thesis. This denomination comprises a variety of materials resulting from primary and secondary aluminum industry residues (SPL and salt cake) valorization by Befesa in its four Salt Slags Recycling plants (Valladolid, Salzchlacke, Lunen and Whitchurch). In these plants 630.000 t/year of salt slag and SPL are valorized to produce 270.000 t/year of salt (a mixture of NaCl and KCl) and 360.000 t/year of Paval (also known as BFA, Serox, and BPL, depending on the country).

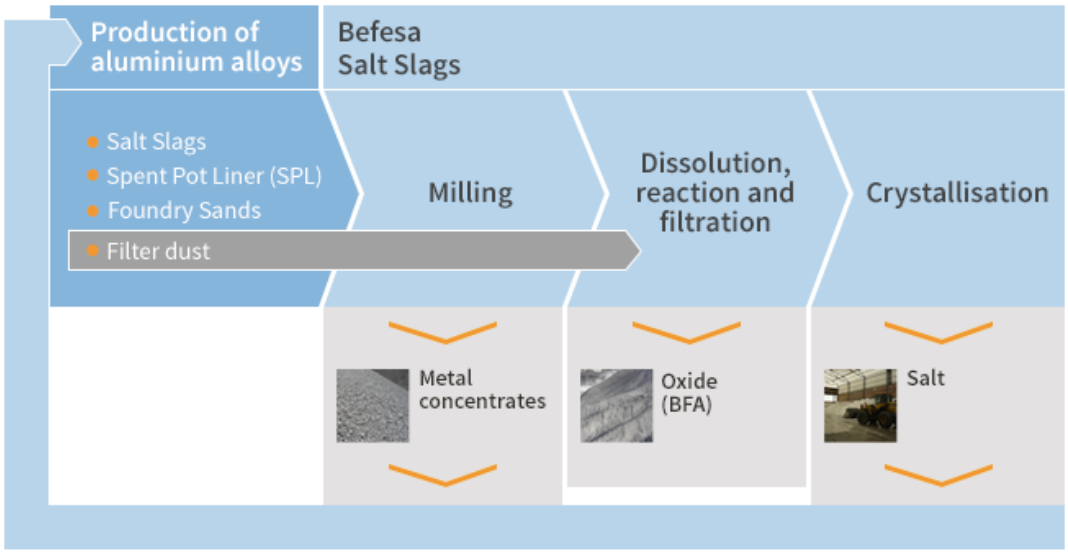


**Figure 1.6.-** Befesa's salt slag and SPL recycling services.[43]

The most usual direct applications for Paval-like materials are inert filling for construction, road paving, and mortar components. Some examples are listed below:[19]

i. Berzelius Umwelt-Service AG (B.U.S.), specify that their NMP containing primarily alumina and other alloying elements can be used, *after washing (or calcination)* in various industries (cement, ceramic, building industries).[2]

ii. Alsa Technologies, subsidiary of Germany's AGOR Group propose their NMP as a raw material in cement clinker, mineral wool, synthetic calcium aluminates, ceramics, refractory materials, abrasives, glass and as a filler.[2]

iii. Alustockach offer their NMP as a substitute for bauxite, and as a raw material for the cement, refractory, steel, and ceramics industries.[2]

iv. Kali & Salz AG in Germany affirms that their NMP (mainly aluminum oxide) is used to cover and foster tailings piles.[2]

v. RVA sells their NMP as raw material for cement or ceramic industries.[2]

vi. Alumitech (Aleris) further processes NMP for separate sale. NMP is divided in *i)* aluminum containing oxides, which are sold to the steel industry for use in exothermic compounds, de-oxidations materials and slag conditioner; and *ii)* aluminum free oxides, which are further processed to produce ceramic fibbers used as insulation in industrial applications, where temperatures can reach above 1100 °C.[2]

Befesa's current proposal for Paval potential industrial applications are similar to other companies:

i. Inorganic charge in plastic and rubber formulations.
ii. Flame retardant in rubber formulations.
iii. Alternative to Bauxite in refractory materials manufacturing.
iv. Raw material for ceramic materials, primary aluminum production, cement manufacturing, ceramics industry, chemical industry, metallurgical industry and agriculture.

One of the highest value-added applications for Paval is as raw material for calcined bauxite based refractory bricks production. However, in recent years, refractory manufacturers have limited the fluoride and sodium contents in the raw materials to avoid the formations of undesired compounds in the process.[14] The fluoride content has been limited to 1.0 wt% because, at the high temperatures involved in refractory manufacturing, fluoride containing gases would be produced and these emissions are limited by law. Some examples of refractory manufacturers that request this reduction in F content are Insertec, Refralia, Cerámica del Nalón, and Arciresa in Spain, and Imerys or Saint Gobain in Europe.

## 1.6 References


[1] M. E. Schlesinger, *Aluminum Recycling*, **2007**.
[2] P. E. E. Tsakiridis, *J. Hazard. Mater.* **2012**, *217–218*, 1–10.
[3] M. Authier-Martin, G. Forté, S. Ostap, J. See, *JOM* **2001**, 3–7.
[4] B. Mazumder, S. R. Devi, *Int. J. Eng. Sci.* **2014**, *4*.
[5] J. H. Bredell, *Econ. Geol.* **1985**, *78*.
[6] C. Light, M. Flagship, P. Crc, I. H. Solutions, C. Minerals, **2008**, 206–207.
[7] M. Davies, P. Smith, W. J. Bruckard, J. T. Woodcock, *Miner. Eng.* **2008**, *21*, 605–612.
[8] A. T. Tabereaux, R. D. Peterson, in *Treatise Process Metall.*, **2014**.
[9] E. Eby, F. Chanania, *Proposed Best Demonstrated Available Technology (BDAT) Background Document for Spent Aluminum Potliners K088*, Washington, DC, **2000**.
[10] T. K. Pong, R. J. Adrien, J. Besida, T. A. O 'donnell, D. G. Wood, *Inst. Chem. Eng.* **2000**, *78*, DOI 10.1205/095758200530646.
[11] J. F. Bush, *Halogen Recovery*, **1986**, 4,597,953.
[12] D. H. Jenkins, *Recovery of Aluminium and Fluoride Values from Spent Pot Lining*, **1994**, 5,352,419.
[13] B. I. Silveira, A. E. Dantas, J. E. Blasquez, R. K. P. Santos, *J. Hazard. Mater.* **2002**, DOI 10.1016/S0304-3894(01)00303-X.
[14] D. Mikša, M. Homšak, N. Samec, *Waste Manag. Res.* **2003**, DOI doi.org/10.1177/0734242X0302100509.
[15] G. Holywell, R. Breault, *Jom* **2013**, *65*, 1441–1451.
[16] Z. N. Shi, W. Li, X. W. Hu, B. J. Ren, B. L. Gao, Z. W. Wang, *Trans. Nonferrous Met. Soc. China (English Ed.* **2012**, *22*, 222–227.
[17] D. F. Lisbona, C. Somerfield, K. M. Steel, *Hydrometallurgy* **2013**, *134–135*, 132–143.
[18] R. S. Tabery, K. Dangtran, *Fluidized Bed Combustion of Aluminum Smelting Waste*, **1991**, 4,993,323.
[19] A. Gil, S. A. A. Korili, *Chem. Eng. J.* **2016**, *289*, 74–84.
[20] P. E. Tsakiridis, *J. Hazard. Mater.* **2012**, *217–218*, 1–10.
[21] J. W. Pickens, D. L. Stewart, R. Stephens, J. C. Daley, in *Recycl. Met. Eng. Mater.*, John Wiley & Sons, Inc., Hoboken, NJ, USA, **2000**, pp. 1195–1207.
[22] X.-L. Huang, A. El Badawy, M. Arambewela, R. Ford, M. Barlaz, T. Tolaymat, *J. Hazard. Mater.* **2014**, *273*, 192–199.
[23] D. F. Lisbona, K. M. Steel, *Sep. Purif. Technol.* **2008**, *61*, 182–192.
[24] Y. Courbariaux, J. Chaouki, C. Guy, *Ind. Eng. Chem. Res.* **2004**, *43*, 5828–5837.
[25] G. C. Holywell, M. Kimmerle, R. T. Gilles, R. J. Grolman, *Recycling of Spent Pot Linings*, **1995**, 5,470,559.
[26] I. Rustad, K. H. Karstensen, K. E. Odegard, *Found. Sci. Ind. Res.* **2000**, 617–632.
[27] European Communities, *Off. J. Eur. Communities* **2000**, *43*.
[28] O. Aljarod, Chemical Treatment and Characterization of Qatalum's 1st Cut Spent Pot Lining (SPL), **2015**.
[29] Q. C. Nguyen, H. J. Hittner, *Stabilization of Fluorides of Spent Potlining by Chemical Dispersion*, **1990**, 4,956,158.
[30] H. J. Hittner, Q. C. Nguyen, *Stabilization of Fluorides of Spent Potlining by Chemical Dispersion*, **1991**, 5,024,822.
[31] D. B. Banker, D. G. Brooks, E. R. Cutshall, D. D. Macauley, D. F. Strahan, *Detoxification of Aluminum Spent Potliner by Thermal Treatment, Lime Slurry Quench and Post-Kiln Treatment*, **1992**, 5,164,174.
[32] H. Kaaber, M. Mollgaard, *Process for Recovering Aluminium and Fluorine from Fluorine Containing Waste Materials*, **1996**, 5,558,847.
[33] C. G. Goodes, G. A. Wellwood, H. W. Hayden, *Recovery of Fluoride Values from Waste Materials*, **1990**, 4,900,535.
[34] D. F. Lisbona, K. M. Steel, *Miner. Met. Mater. Soc.* **2007**.
[35] European Aluminium Association (EAA), in *Alum. Recycl. Eur.*, **2004**.
[36] T. W. Unger, M. Beckmann, in *TMS Annu. Meet.*, San Diego, **1992**, pp. 1159–1162.
[37] H. Antrekowitsch, K. E. Lorber, in *2nd Int. Conf. Hazard. Ind. Waste Manag.*, Crete, **2010**, p. B.2.1.
[38] W. J. Bruckard, J. T. Woodcock, *Int. J. Miner. Process.* **2009**, *93*, 1–5.

[39] D. G. Graczyk, A. M. Essling, E. A. Huff, H. P. Smith, C. T. Snyder, F. P. Smith, *Light Met.* **1997**.
[40] F. A. López, E. Sáinz, A. Formoso, I. Alfaro, *Can. Metall. Q.* **1994**, *33*, 29–33.
[41] W. J. Bruckard, J. T. Woodcock, **2007**, *20*, 1376–1390.
[42] P. N. Papafingos, R. T. Lance, *Salt Cake Processing Method and Apparatus*, **1978**, 4,073,644.
[43] "http://www.befesaaluminium.com," **n.d.**

# Chapter 2

State of the art

# Table of contents

## 2.1 Introduction

As presented in Chapter 1, Paval has a high fluoride concentration that hinders its use as raw material for high value-added applications like the Bayer process and refractory manufacturing. Having the objective of reducing fluorine content in Paval-like materials, two main techniques were reported: *(i)* Thermal treatments (pyrohydrolysis, pyrosulfolysis, and fluidized bed combustion) and *(ii)* hydrometallurgical treatments such as chemical leaching. There is significantly more research performed on SPL recycling, including a significant number of US patents filed in the 80's and 90's proposing both thermal and hydrometallurgical processes to reduce SPL toxicity. It is probable that this results from SPL being considered a hazardous waste in the United States since 1988 (code K088). On the contrary, salt cake is still not considered hazardous and its disposal in landfills is permitted,[1] thus, not much research effort has been devoted to its recycling in the US.

## 2.2 Fluoride selective removal alternatives

The thermal treatments reported to reduce the fluoride and cyanide contents in SPL are combustion at temperatures higher than 1000 °C,[2–6] pyrohydrolysis, and pyrosulfolysis. Pyrohydrolysis involves contacting the SPL with $H_2O$ or steam at high temperatures to produce HF. A patented pyrohydrolysis process for SPL consisted in subjecting crushed SPL to 1150-1250 °C temperatures in the presence of water. NaF and HF vapor were recovered from the off-gases, and the solid residue immersed in a dilute caustic solution at 200 °C to leach out the alumina. This process requires very large and expensive reactors and their high capital and operating costs makes it uneconomical to operate. Moreover, although $AlF_3$ pyrohydrolysis is known to be relatively easy, the reaction of $CaF_2$ and NaF is challenging.[7–10]

Sulfolysis was also proposed and patented as a method to recover HF and $AlF_3$/cryolite from SPL. The process includes a first combustion step prior to the sulfolysis reaction for the carbonaceous material. Then, the oxidized material is attacked with a

sulfur source (as $H_2SO_4$ or $SO_2$) to produce HF.[11] Other patent consists on reacting SPL with $O_2$, $H_2O$ and $SO_2$ at 600 to 1200 °C to produce an HF enriched gas.[12]

Thermal approaches shared the setback of dealing with $H_2O$ and HF at extreme temperatures, which causes severe corrosion problems.[13] Hydrometallurgical processes, on top of not having these limitations, had a lower energy demand and therefore an smaller environmental impact. They were also susceptible to recycle the chemical reagents employed. Taking into account all of the mentioned above, this research was focused on removing fluoride from Paval by chemical leaching.

## 2.3 Fluoride selective leaching

As stated in the previous chapter, Paval is a material obtained from spent pot lining, salt slag or a mixture of them. Therefore, the literature concerning fluoride selective lixiviation can be divided into three mayor streams according to the matrix from which the fluoride is leached: *(i)* Spent pot lining (SPL), *(ii)* salt cake (also known as salt slag or saline slag), and *(iii)* other solid matrixes.

The elemental and phase composition of the materials is a critical variable in the leaching processes and therefore, the literature concerning fluoride leaching from salt cakes and SPL is presented in first place, and then the literature concerning fluoride leaching from other various matrixes.

### 2.3.1 Fluoride selective leaching from salt cake

The research concerning salt cake recycling is mainly focused on recovering metallic aluminum, sodium and potassium chlorides by wet treatments as well as removing other main compounds such as $Al_4C_3$, AlN, and $Al_5O_6N$. This processes usually release noxious gases such as $H_2$, $NH_3$, $CH_4$, $PH_3$, and $H_2S$.[14–16,18,19] The remaining residue, Paval, is employed in low-value applications or disposed in landfills,[15–17] therefore, there is little research about recycling it by hydrometallurgical processes.

To the best of our knowledge, the only hydrometallurgical process proposed in the literature to further recycle salt cake consists on a first aqueous leaching -which would

be the equivalent of Paval production from salt cake- and an alkaline leach at 60 °C. The proposed process consists of two steps: first, a water leach for 1 h at 25 °C, by which 90 % of the Cl, 55 % of the Na, and 45 % of the K can be leached. The same researchers proposed a modification to enhance the performance of the process consisting on further grinding in the water leach step, screening and filtering. Grinding enhanced fluoride extraction from 60 to 71 % and screening and filtering enhanced Al metal extraction. In the second step the material from the first step was put into contact with a 150 g/L NaOH aqueous solution for 15 min at 60 °C, and a S/L of 100 g/L.[18,19]

### 2.3.2 Fluoride selective leaching from SPL

The hydrometallurgical processes proposed in the literature can be divided in two main classes: Processes that include an initial aqueous treatment and processes that do not. This is an important distinction in this thesis because the material in this research is more similar to an aqueous washed SPL than to a SPL itself, as soluble fluoride compounds such as NaF are removed from the material in the water treatment.[20] The most common process in the literature to produce 'SPL Paval' consists on contacting <1.18 mm particle size SPL with milliQ grade water for 4 h at 25 °C, and S/L ratio of 240 g/L.[20–23]

Aluminum is widely used in fluoride leaching as they are known to form soluble and highly stable fluoro-aluminum complexes[24] which enhance fluoride leaching yields from fluoride-bearing materials, including $CaF_2$.[14,20,25–27] As a result, the three proposed leaching steps that follow the water treatment described above rely on aluminum affinity with fluoride. One of the methods leaches <1.18 mm particle size 'SPL Paval' with a 135 g/L of aluminum nitrate nonahydrate ($Al(NO_3)_3{\cdot}9H_2O$) aqueous solution for 24 h at 25 °C, and a S/L ratio of 150 g/L (the ratio is actually higher because the leaching losses in the water step are not taken into account).[21] A more aggressive alternative was proposed by adding 0.5 M $HNO_3$ to the $Al(NO_3)$ solution, raising the temperature to 60 °C, and reducing S/L ratio to 120 g/L. This allows the reaction time to be lowered to 4 h. The two proposed treatments aim to solubilize the cryolite ($Na_3AlF_6$) and fluorspar ($CaF_2$) present in SPL. While almost total cryolite leaching was achieved, solubilization of $CaF_2$ was only partial. Nonetheless, 96.3 wt% of the fluoride remaining after the water

wash step was extracted with this process.[20] Another process from literature used a mixture of $H_2SO_4$ 0.7 M and $Al^{3+}$ 0.20 M. The solution was put into contact with the SPL Paval for 4 h at 60 °C and using a S/L ratio 120 g/L (minus water leach losses) resulting in a fluoride removal of 83.2 wt%.[22,23]

A water leach at 20 to 70 °C and a S/L ratio between 250 and 333 g/L for 10 to 20 minutes was patented to dissolve all water-soluble fluorides in an SPL sample ground below 300 μm as previous step to an alkaline leaching process. The second step of this process used an aqueous solution of 30 to 40 g/L NaOH with a S/L ratio of 167 g/L for 40 to 80 minutes at 60 to 95 °C.[28]

Alternatively, a method to leach cryolite from SPL comprising $H_2SO_4$ and $Al_2(SO_4)_3$ was also patented. 93 %F extraction was achieved at 95 °C by maintaining the $Al_2(SO_4)_3/H_2SO_4$ ratio between 0.84 and 0.90, and the aluminum concentration below 0.1 M to avoid fluoride precipitation according to the authors.[29] Later, these researchers proposed an alkaline pretreatment to improve the results. The SPL was wet-ground to <100 μm in a 25 % slurry, and washed in counter current with a 14 g/L NaOH solution. 55 % of the fluoride present in the SPL was leached and the solution could be fed to a Bayer process. The solid was then filtered and fed to the $Al_2(SO_4)_3$-$H_2SO_4$ process described previously.[30]

Calcination is sometimes used prior to the hydrometallurgical treatments to destroy cyanides. In a reported work, after calcination, 30 g of SPL ashes were mixed with 12 g of concentrated $H_2SO_4$. Once homogenized, 3.7 g of $H_2O$ were added and the mixture was maintained at room temperature for 2 h. Then, a 74.5 g/L $Al_2(SO_4)_3 \cdot 18 \cdot H_2O$ aqueous solution was added, and the temperature risen to 93 °C for 1 h. The result was a fluoride extraction of 97 %.[31] Cyanides are also reported to be decomposed by heating the treated SPL to 160-220 °C.[32] In this case, the reported leaching solution was alkaline, and contained between 10 and 60 g/L of NaOH, which was put into contact with <600 μm SPL for 0.5 to 3 h at 60 to 90 °C and a S/L ratio from 100 to 120 g/L. In this process the cyanides were destroyed by heating the treated SPL at 160-220 °C.

Although the use of $Al^{3+}$ to dissolve fluorides in SPL is reported to be the key, it is not always necessary to add it externally, as it can be leached from the material.[13,27,33,34]

A process using the aluminum present in SPL was patented where < 7 mm SPL particles were leached with 0.5 M $H_2SO_4$ for 1 h at 90 °C and a S/L ratio of 100 g/L. Under these conditions, at the end of the reaction the $Al^{3+}$ concentration in the solution was 0.21 M, the F:Al atomic ratio 1.99, and the pH 2.2. The result was 93.3 % fluoride and 89.5 % aluminum leaching.[13] Another aluminum free treatment was a combination of acid and basic leaching steps. First, a NaOH 2.5 M solution was put into contact for 180 minutes at 100 °C, and a S/L ratio 220 g/L to dissolve $Na_3AlF_6$, NaF, and $Al_2O_3$ into the solution. Second, the filtered solid was mixed with HCl 9.7 M for 180 minutes at 90 °C and a S/L ratio 250 g/L to further dissolve the $CaF_2$ and $NaAl_{11}O_{17}$.[33]

Fluoride leaching was also studied using synthetic mixtures of the main fluoride species in SPL, *i.e.* NaF, $Na_3AlF_6$ and $CaF_2$. $Na_3AlF_6$ was found to be fully dissolved after 16 h reaction time with a 120 g/L $Al(NO_3)_3{\cdot}9H_2O$ solution at 25°C and a S/L ratio of 33 g/L. $CaF_2$, however, required a more concentrated leaching solution (150 g/L), two times higher leaching solution to liquid ratio (15 g/L) and longer reaction times (24 h). This results highlight the stability of the $CaF_2$ and, hence, its resistance to leaching.[35] $Na_3AlF_6$ solubility was further studied in an 107.7 g/L $Al_2(SO_4)_3$ aqueous solution at 95-98 °C. It was found that, due to $Na_2SO_4$ formation, fluoride solubility was lowered from 25 to 21 g/L.[36] A different approach to dissolve cryolite and fluorspar was reported, where fluoride compounds were used as leaching agents. It was based on the following reactions:

$$2\ Na_3AlF_6(s) + 3\ H_2SiF_6(aq) \rightarrow 2\ AlF_3\,(aq) + 3\ Na_2SiF_6(s) + 6\ HF(aq)$$

$$CaF_2(s) + H_2SiF_6 \rightarrow CaSiF_6(aq) + 2\ HF(aq)$$

Hexafluorosilicic acid ($H_2SiF_6$) digests cryolite and fluorspar forming hydrofluoric acid and soluble fluoride compounds.[24]

As fluoride leaching by hydrometallurgical processes is not a common research line, there is not a large amount of information available. Therefore, it was also considered interesting to research methods to leach fluoride from other solid matrixes.

### 2.3.3 Fluoride selective leaching from other solid matrixes

There is a need to reduce fluoride levels in other materials such as lead, zinc and copper sulfides prior to smelting because at levels above 100 ppm fluoride may interfere with the smelting process. A method for extracting fluoride from minerals or mineral species by lixiviation was patented in order to solve it. The patent was again based on the high stability of fluoride-aluminum complexes, several orders of magnitude above the bond strength of fluoride in minerals. If $Al_2(SO_4)_3$ and $H_2SO_4$ were employed, the pH was proposed to be between 3.0 and 4.3 because aluminum is soluble as aluminum sulfate and fluoride can exist in the free ionic $F^-$ state according to the inventors. On the other hand, if $AlCl_3$ and HCl were used, the pH was set between 1.0 and 2.0 due to the fluoride equilibrium between hydrogen fluoride and chloride. $Cl^-$ will compete with $F^-$ in the combination reaction with aluminum, and thus, reduce the efficiency of the fluoride removal reaction. The F:Al atomic ratio was set between 1:1 and 5:1, and preferably between 2:1 and 5:1 in order to minimize the formation of insoluble fluoride and aluminum species.[37]

In good agreement with this patent, the mixture of sulfuric acid and aluminum sulfate was reported to be efficient for the selective fluoride leaching from zinc concentrates: $CaF_2$ was successfully leached from a zinc concentrate (produced from zinc sulfide ore) following the patented method described above: $H_2SO_4$ and $Al_2(SO_4)_3$ maintaining a 3.3 pH and a F:Al ratio above 0.5.[19] Similarly, 92% fluoride removal from Double Leach Waelz Oxide (DLWO), a zinc concentrate produced by Befesa Zinc Aser S.A., was reported using a 70 g/L $Al_2(SO_4)_3$ solution maintaining the pH at 2 with a S/L ratio 240 g/L.[39]

The alternative mixture proposed in the previous patent, $AlCl_3$-HCl was useful to leach 99 % of the fluoride contained in a mixed rare earth concentrate. This concentrate was leached with a 4 M HCl and 1.5 M $AlCl_3$ mixture with a 50 g/L S/L ratio for 90 minutes at 85 °C.[40] When fluoride and the matrix containing it are not strongly bonded, the presence of aluminum may not be necessary. For example, HCl was used to leach fluoride from coal fly ash.[41] Fluoride in wastes produced by the pesticide industry is

typically found as NaF which can be leached with a 99 % yield by washing the waste with a NaOH solution with a S/L ratio of 25 g/L, for 4 h at 75 °C.[42]

**Table 3.1.-** Fluoride leaching conditions from literature

| Material | Leaching agent | Concentration (g/L) | t (h) | T (°C) | S/L (g/L) | [$Al^{+3}$] (M) | Particle size (μm) | F:Al | pH | wt. % F leached | wt. % Al leached | Ref |
|---|---|---|---|---|---|---|---|---|---|---|---|---|
| Salt Cake Paval[a] | NaOH | 150 | 0.25 | 60 | 100 | na | <2, <0.150 | na | na | 60-71 | 20 | [18,19] |
| SPL Paval[b] | $Al(NO_3)_3{\cdot}9H_2O$ | 135 | 24 | 25 | 150 | 0.36 | <1.18 | na | na | na | na | [21] |
| SPL Paval[b] | $Al(NO_3)_3{\cdot}9H_2O$ + $HNO_3$ | 135 $Al(NO_3)_3{\cdot}9H_2O$ 31.5 ($HNO_3$) | 4 | 60 | 120 | 0.36 | <1.18 | na | na | 96.3 | na | [20] |
| SPL Paval[b] | $H_2SO_4$ + $Al^{3+}$ | 68.6 | 4 | 60 | 120 | 0.20 | <1.18 | na | na | 83.2 | na | [22,23] |
| SPL[c] | NaOH | 20-50 | 0.7-1.3 | 60-95 | 50 | na | <0.300 | na | 7-10 | na | na | [28] |
| SPL | $H_2SO_4$ + $Al^{3+}$ | na | na | 95 | na | <0.1 | na | na | na | 93 | na | [29] |
| SPL | NaOH | 14 | na | na | na | na | <0.100 | na | na | na | na | [30] |
| SPL[d] | $Al_2(SO_4)_3{\cdot}18\ H_2O$ | 74.5 | 1 | 93 | 62 | 6.0 | <0.600 | na | na | na | na | [31] |
| SPL | NaOH | 10-60 | 0.5 – 3 | 60-90 | 100 – 120 | na | <0.600 | na | na | na | na | [32] |
| SPL | $H_2SO_4$ | 49 | 1 | 90 | 100 | 0.21 | <7 | 1.99 | 0-3 | 93.30 | 89.50 | [13] |
| SPL | NaOH | 100 | 3 | 100 | 220 | na | na | na | na | na | na | [33] |
| | HCl | 354 | 3 | 90 | 250 | na | na | na | na | na | na | |
| $CaF_2$, $Na_3AlF_6$ | $H_2SiF_6$ | 100-200 | na | na | na | na | na | na | na | na | na | [24] |
| $Na_3AlF_6$ | $Al_2(SO_4)_3$ | 107.7 | na | 95-98 | na | na | na | na | na | na | na | [36] |
| $CaF_2$, $Na_3AlF_6$ | $Al(NO_3)_3{\cdot}9H_2O$ | 120 ($Na_3AlF_6$) 150 ($CaF_2$) | 16 ($Na_3AlF_6$) 24 ($CaF_2$) | 25 | 33 ($Na_3AlF_6$) 15 ($CaF_2$) | na | na | na | na | na | na | [35] |
| Minerals and other matrixes | $Al_2(SO_4)_3$ + $H_2SO_4$ | na | na | na | na | na | na | 2-5 | 3.0-4.3 | na | na | [37] |
| | $Al_2(SO_4)_3$ + $H_2SO_4$ | na | na | na | na | na | na | >0.50 | 3.3 | na | na | [38] |
| | $Al_2(SO_4)_3$ | 70 | na | na | 240 | 5.7 | na | 8 | 2 | 92 | na | [39] |
| | HCl-$AlCl_3$ | 146 (HCl), 20 ($AlCl_3$) | 1.5 | 85 | 50 | 1.5 | na | na | na | 98.74 | na | [40] |
| | NaOH | na | 4 | 75 | 25 | na | na | na | 12 | 99 | na | [42] |
| | HCl | na | na | na | na | na | na | na | 2.5 | na | na | [41] |

a) Previously washed with milliQ, for 1 h at 25 °C, b) Previously washed with 240 g/L milliQ, for 4h, at 25 °C, c) Previously washed with 250-333 g/L milliQ, for 10-20 minutes, at 20-70 °C d)Previously calcined to destroy cyanides + acid treatment S/L= 30/15,7 g/g (1406 g$H_2SO_4$/L), 2h

## 2.4 References


[1] D. B. Banker, D. G. Brooks, E. R. Cutshall, D. D. Macauley, D. F. Strahan, *Detoxification of Aluminum Spent Potliner by Thermal Treatment, Lime Slurry Quench and Post-Kiln Treatment*, **1992**, 5,164,174.

[2] P. K. Davis, V. K. Kakaria, *Method of Treating Fluoride Contaminated Wastes*, **1988**, 4,735,784.

[3] G. W. Morgenthaler, J. L. Struthers, G. W. Carter, *Plasma Torch Furnace Processing of Spent Potliner from Aluminum Smelters*, **1993**, 5,222,448.

[4] J. G. Lindkvist, T. Johnses, *Method for Treatment of Potlining Residue from Primary Aluminum Smelters*, **1994**, 5,286,274.

[5] J. P. McGeer, V. V. Mirkovich, W. F. Phillips, *Recovery of Material from Aluminum Reduction Cell Lining*, **1958**, 2,858,198.

[6] R. S. Tabery, K. Dangtran, *Fluidized Bed Combustion of Aluminum Smelting Waste*, **1991**, 4,993,323.

[7] N. Bell, J. N. Andersen, H.-K. H. Lam, *Process for the Utilization of Waste Materials from Electrolytic Aluminum Reduction Systems*, **1978**, 4,113,832.

[8] J. N. Andersen, N. Bell, *Pyrohydrolysis System for Processing Fluorine-Containing Spent and Waste Materials*, **1979**, 4,158,701.

[9] J. N. Andersen, N. Bell, *Pyrohydrolysis Process for Spent Aluminum Reduction Cell Linings*, **1979**, 4,160,808.

[10] J. N. Andersen, N. Bell, *Modified Pyrohydrolysis Process for Spent Aluminum Reduction Cell Linings*, **1979**, 4,160,809.

[11] C. G. Goodes, G. A. Wellwood, H. W. Hayden, *Recovery of Fluoride Values from Waste Materials*, **1990**, 4,900,535.

[12] B. W. Gamson, H. W. Hayden, *Aluminum Electrolytic Cell Cathode Waste Recovery*, **1982**, 4,355,017.

[13] H. Kaaber, M. Mollgaard, *Process for Recovering Aluminium and Fluorine from Fluorine Containing Waste Materials*, **1996**, 5,558,847.

[14] W. J. Bruckard, J. T. Woodcock, *Int. J. Miner. Process.* **2009**, *93*, 1–5.

[15] P. E. E. Tsakiridis, *J. Hazard. Mater.* **2012**, *217–218*, 1–10.

[16] A. Gil, S. A. A. Korili, *Chem. Eng. J.* **2016**, *289*, 74–84.

[17] M. E. Schlesinger, *Aluminum Recycling*, **2007**.

[18] M. Davies, P. Smith, W. J. Bruckard, J. T. Woodcock, *Miner. Eng.* **2008**, *21*, 605–612.

[19] W. J. Bruckard, J. T. Woodcock, **2007**, *20*, 1376–1390.

[20] D. F. Lisbona, C. Somerfield, K. M. Steel, *Hydrometallurgy* **2013**, *134–135*, 132–143.

[21] D. F. Lisbona, K. M. Steel, *Sep. Purif. Technol.* **2008**, *61*, 182–192.

[22] D. F. Lisbona, C. Somerfield, K. M. Steel, *Ind. Eng. Chem. Res.* **2012**, *51*, 12712–12722.

[23] D. F. Lisbona, C. Somerfield, K. M. Steel, *Ind. Eng. Chem. Res.* **2012**, *51*, 8366–8377.

[24] T. K. Pong, R. J. Adrien, J. Besida, T. A. O 'donnell, D. G. Wood, *Inst. Chem. Eng.* **2000**, *78*, DOI 10.1205/095758200530646.

[25] R. Bruce Martin, *Coord. Chem. Rev.* **1996**, *141*, 23–32.

[26] R. P. Agarwal, E. C. Moreno, *Talanta* **1971**, *18*, 873–880.

[27] V. Schwemmer, *Process for the Recovery of Aluminum and Fluorine Compounds from the Worn-out Linings of the Electric Furnaces Employed for the Production of Aluminum*, **1937**, 2,186,433.

[28] V. Kasireddy, J.-L. Bernier, F. M. Kimmerle, *Recycling of Spent Pot Linings*, **2003**, 6,596,252 B2.

[29] J. F. Bush, *Halogen Recovery*, **1986**, 4,597,953.

[30] J. F. Bush, *Reclaiming Spent Potlining*, **1989**, 4,889,695.

[31] D. H. Jenkins, *Recovery of Aluminium and Fluoride Values from Spent Pot Lining*, **1994**, 5,352,419.

[32] G. C. Holywell, M. Kimmerle, R. T. Gilles, R. J. Grolman, *Recycling of Spent Pot Linings*, **1995**, 5,470,559.

[33] Z. N. Shi, W. Li, X. W. Hu, B. J. Ren, B. L. Gao, Z. W. Wang, *Trans. Nonferrous Met. Soc. China (English Ed.* **2012**, *22*, 222–227.

[34] R. J. Barnett, M. B. Mezner, *Method of Treating Spent Potliner Material from Aluminum Reduction Cells*, **1999**, 5,955,042.

[35] D. F. Lisbona, K. M. Steel, *Miner. Met. Mater. Soc.* **2007**.
[36] G. F. Gaydoski, J. F. Bush, *Aluminum-Fluorine Compound Manufacture*, **1985**, 4,508,689.
[37] K. Jomoto, T. C. Hughes, *Method of Extracting Fluorine from Minerals or Mineral Species*, **2001**, WO 95/01460.
[38] C. Torrisi, *Miner. Eng.* **2001**, *14*, 1637–1648.
[39] N. Antuñano, J. F. Cambra, P. L. Arias, *Hydrometallurgy* **2016**, *161*, 65–70.
[40] M. Li, X. Zhang, Z. Liu, Y. Hu, M. Wang, J. Liu, J. Yang, *Hydrometallurgy* **2013**, DOI 10.1016/j.hydromet.2013.09.004.
[41] R. Piekos, S. Paslawska, *Fluoride J.* **1998**, *31*, 188–192.
[42] Y. Li, H. Zhang, Z. Zhang, L. Shao, P. He, *J. Environ. Sci. (China)* **2015**, *31*, 21–29.

# Chapter 3

Objectives and scope of the thesis

In the first chapters of this Ph.D. thesis a general description of the aluminum production process was presented in order to contextualize the nature of the produced residues and its scale of production. Several applications of the Non-Metallic Product (Paval henceforth) were listed and the purification requirements for high-end applications such as refractory manufacturing (<1.0 wt% F) described. In chapter 2, a critical review of fluoride leaching processes was provided, showing the necessity of further research on fluoride selective leaching from this type of materials.

Against this background, the primary objective of this thesis is the design of a valorization process which selectively leaches fluoride from Paval and results in a treated material with a fluoride content below 1.0 wt%, while leaching the minimum aluminum possible. This process needs to be technically and economically viable to allow industrial implementation, hence, the following characteristics need to be part of the design: *(i)* simple process layout, *(ii)* low energy demand, *(iii)* minimum environmental impact, *(iv)* inexpensive chemical reagents, *(v)* mild reaction conditions in order to avoid expensive installations *(vi)* chemical reagents recycling, and/or *(vii)* value-added compounds recovery.

In order to achieve the primary objective of the thesis, a series of milestones need to be fulfilled.

- Selection of the most suitable leaching agent for selective fluoride removal. The literature review showed that many different leaching agents (acids and bases) have been used for fluoride selective leaching from different wastes; hence, the first objective should be the selection of the best one for our material.
- Optimization of the leaching conditions. The complexity of the raw Paval and the numerous parameters that play a role in fluoride and aluminum leaching result in a complex system whose study will be favored by the use of a Design of Experiments approach and an ANOVA analysis.
- Recyclability study of the generated by-product streams to reduce the inlet material requirements and material disposal costs.

The focus of this PhD thesis is a compromise between a rigorous academic approach and an industry-oriented research, which will contribute to the circular economy development through wastes transformation and their introduction as raw materials into other industrial manufacturing processes.

# Chapter 4

Experimental

# Table of contents

## 4.1. Introduction

This chapter will summarize the main experimental procedures used during the realization of this PhD thesis. This way, the technique used for the design of the experiments along with all the characterization and analytical details will be easy to find and it will help the fluency of the following chapters dealing with the experimental results, discussion and conclusions.

## 4.2. The Taguchi method for design of experiments and variance analysis

The traditional design of experiments (DOE), known as factorial design, is the technique of defining and investigating all possible conditions in an experiment involving multiple variables (called factors in DOE and henceforth). Taguchi DOE method uses the same principles as factorial design, in a simplified and standardized version. The most important differences between the traditional method and the Taguchi's one are the number of experiments and the approach to quality. A full factorial design needs $L^m$ experiments (where *L* is the number of levels for each factor, and *m* the number of factors), whereas Taguchi only needs a fraction of that number to obtain almost the same amount of information by using Orthogonal Arrays (OA). The main setback of DOE by OAs is that performance estimation at the optimum conditions can be inaccurate when there are strong nonlinear interactions between factors.

Moreover, traditional DOE is focused on how different design factors affect the average result level, whereas Taguchi's DOE studies how different parameters affect the mean and variance of a factor variation to achieve a robust design. As it can be observed in Figure 4.1, the traditional model for quality losses does not consider losses within the specification limits, and Taguchi's quality loss is zero only if the parameter is on target.

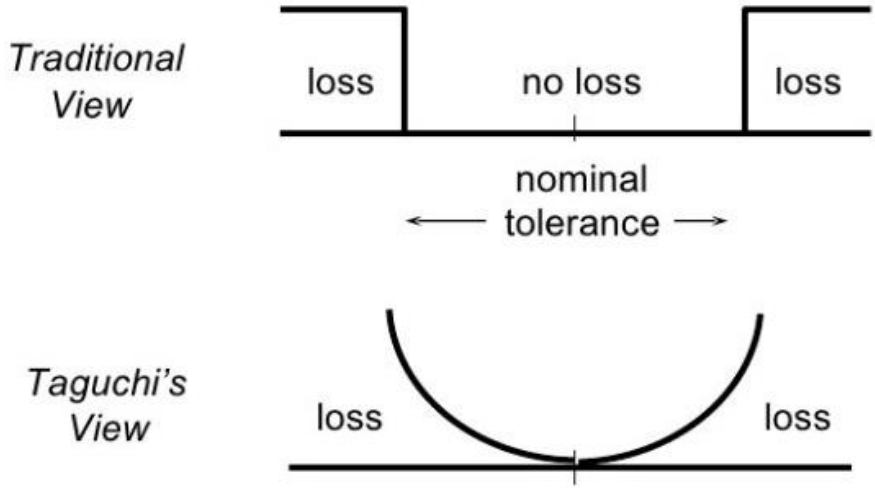


**Figure 4.1.-** Quality loss in Traditional and Taguchi´s view (Adapted from [1])

Taguchi's DOE is, therefore, an experimental method to achieve product and/or process quality through designing a system immune to uncontrolled variables (noise factors) based on statistical principles. It is an especially useful method when the number of variables is between 3 and 50, there are few interactions between variables, and only a small number of variables contribute significantly. The method is applied in four steps:

1. **Brainstorm the quality characteristics and design parameters important to the product/process.** Taguchi found brainstorming to be a necessary step for determining the full range of factors to be studied. In this PhD research, a number of preliminary experiments were carried out, based on the literature consulted for chapters number one and two (Introduction and State of the Art). Thus, the factors and levels to include in the Taguchi OA were determined, and the presence of interaction between factors evaluated.

2. **Design and conduct experiments**. In order to get an efficient design of the set of experiments, it is important to understand the *degrees of freedom* (DOF) concept, which is a measure of the amount of information (number of effects) that can be determined from a given set of data. For example, it is possible to estimate *n* effects with *n* data points. Each interaction consumes DOF equal to the number of levels minus one (*L*-1). Therefore, an interaction in a two-level factor design will consume

one DOF and, in a three-level factor, two DOF. In Figure 4.2 the most common OAs are presented. As it can be seen, the smallest OA for 2 levels is $L_4$, which can handle up to 3 factors with 2 levels. For 3 levels, the smallest OA is $L_9$, which can handle up to 4 factors with 3 levels.

| Array | Number of factors | Number of levels |
|---|---|---|
| $L_4(2^3)$ | 3 | 2 |
| $L_8(2^7)$ | 7 | 2 |
| $L_{12}(2^{11})$ | 11 | 2 |
| $L_{16}(2^{15})$ | 15 | 2 |
| $L_{32}(2^{31})$ | 31 | 2 |
| $L_9(3^4)$ | 4 | 3 |
| *$L_{18}(2^1,3^7)$ | 1 and 7 | 2 and 3 |
| $L_{27}(3^{13})$ | 13 | 3 |
| $L_{16}(4^5)$ | 5 | 4 |
| *$L_{32}(2^1,4^9)$ | 1 and 9 | 2 and 4 |
| $L_{64}(4^{21})$ | 21 | 4 |

*Mixed level arrays

**Figure 4.2.-** Common Orthogonal Arrays[1]

When possible, the tests should be run in random order to avoid the influence of the experimental setup. Besides, multiple runs of each test are recommended to increase the confidence of the results.

**3. Analyze the results to determine**:

**a. The optimum conditions:** In order to select the optimum level for each factor, the average performance of each level and factor is calculated. For example, the average performance of factor A at level 1 is obtained by adding all the results for trials including factor $A_1$, and dividing by the number of trials. To better compare average performances (also called main effects), they are usually plotted in a 2D graphic, where the factors and levels are in the X-axis and the response in the Y-axis. Then, following the corresponding criteria (the smaller the better, target is best, or the bigger the better) a probable optimum set of conditions is selected. When there are interactions

between factors, combined average effects are calculated and plotted to correct the previously selected levels if necessary.

**b. Which factors contribute to the results and how much**: The relative contributions of the factors, expressed in percentage, are determined by an analysis of variance (ANOVA). Variance measures the data distribution about the mean value of the data. In the Taguchi method, the deviation from the target is considered more significant than from the mean and thus, in Taguchi method the mean is replaced by the target value.

**Table 4.1.-** ANOVA definitions

| | | | | | |
|---|---|---|---|---|---|
| V | Mean squares (variance) | e | Error (experimental) | N | Number of trials |
| S | Sum of squares | F | Variance ratio* | CF | Correction factor |
| S’ | Pure sum of squares | P | Percent contribution | n | Total DOF |
| f | Degrees of Freedom | T | Total (of results) | r | Number of repetitions |

*Variance ratio is commonly known as the *F* statistic

Table 4.2.a is an example of the ANOVA table for a DOE with two three-level factors (A and B) and one interaction (AxB), and Table 4.2.b contains all the ANOVA formulae for the example:

**Table 4.2.a.-** ANOVA table for factors A and B and interaction AxB

| Factors | f | S | V | F | S' | P |
|---|---|---|---|---|---|---|
| **A** | $f_A$ | $S_A$ | $V_A$ | $F_A$ | $S'_A$ | $P_A$ |
| **B** | $f_B$ | $S_B$ | $V_B$ | $F_B$ | $S'_B$ | $P_B$ |
| **AxB** | $f_{AxB}$ | $S_{AxB}$ | $V_{AxB}$ | $F_{AxB}$ | $S'_{AxB}$ | $P_{AxB}$ |
| **error** | $f_e$ | $S_e$ | $V_e$ | $F_e$ | $S'_e$ | $P_e$ |
| **Totals** | $f_T$ | $S_T$ | | | | 100 |

**Table 4.2.b.-** ANOVA definitions table for factors A and B and interaction AxB

| Factors | f | S | V | F | S' | P |
|---|---|---|---|---|---|---|
| **A** | 3 – 1 | $\sum_{i=1}^{3}(A_i^2/N_{A_i}) - CF$ | $S_A/f_A$ | $V_A/V_e$ | $S_A-f_A*V_e$ | $S'_A/ S'_T*100$ |
| **B** | 3 – 1 | $\sum_{i=1}^{3}(B_i^2/N_{B_i}) - CF$ | $S_B/f_B$ | $V_B/V_e$ | $S_B-f_B*V_e$ | $S'_B/ S'_T*100$ |
| **AxB** | $f_A * f_B$ | $S_{AB}-S_A- S_B$ | $S_{AxB}/f_{AxB}$ | $V_{AxB}/V_e$ | $S_{AxB}-f_{AxB}*V_e$ | $S'_{AxB}/ S'_T*100$ |
| **error** | $f_T-f_A-f_B-f_{AxB}$ | $S_e$ | $S_e/f_e$ | 1 | $S_e+(f_A+f_B+f_{AxB})*V_e$ | $S'_e/ S'_T*100$ |
| **Totals** | N-1 | $S_e+S_A+S_B+S_{AxB}$ | | | $S'_T$ | 100 |

Where:

- CF = $T^2/N$
  - $T = \sum_{i=1}^{N}(Y_i - Y_0)$
    - $Y_i$ = result of test i
    - $Y_0$ = target value

- $S_{AB} = (\sum_{i=1}^{3}\sum_{j=1}^{3}(A_iB_j)/r_{ij}) - CF$
  - $r_{ij}$= number of test repetitions

When the contribution (P) of a factor is small, the factor is absorbed by the error, and therefore its f and S are added to $f_e$ and $S_e$. This process is known as Pooling, and is recommended when a factor is determined to be insignificant. Taguchi recommends pooling factors until the error DOF is approximately half the total DOF of the experiment. Increasing the DOF for the error term, as a result of pooling, increases the confidence level of the significant factors.[2]

c. **What will be the expected result at the optimum conditions:** Performance at the optimum condition is estimated only from the significant factors. It is the sum of the mean of all gathered responses, plus the difference between the average response of the optimum level for each significant factor and the media of all gathered responses. Following the example from Table 6.4, if only factors A and B are significant, and the optimum levels are $A_1$ and $B_2$, the expected result (ER) at the optimum condition will be:

$$ER = \overline{T} + (\overline{A_1} - \overline{T}) + (\overline{B_2} - \overline{T})$$

4. **Run a corroborative test(s) using the optimum conditions**. As Taguchi design includes only a small set of the full factorial experiments, the optimum set of conditions is usually not one of the trial runs. Thus, when the optimum set of conditions has not been tested, confirmation testing is a necessary and important step as direct proof of the methodology.[1]

## 4.3. Experimental set-ups

### 4.3.1. Sample preparation

Paval samples were dried for 24 h in an oven at 100 °C, crushed in a ceramic mortar, sieved below 1 mm, and stored in a desiccator with silica gel, which was regenerated once a day.

Effluent samples were stored in polypropylene sample containers at room temperature. Before use, they were homogenized and filtered if necessary.

### 4.3.2. Hydrometallurgical tests

In Figure 4.3 a scheme of the leaching set-up for fixed temperatures from 25 °C and up to 100 °C is shown. The leaching tests were carried out in a flat-bottom borate glass flask, placed in a silicon bath, heated by a hot plate. A magnetic PTFE stirrer was placed in the glass flask and controlled by the magnetic stirring plate to achieve a vigorous stirring. In order to control the temperature, a glass thermometer was placed in one of the flask necks. In the other opening, a glass reflux condenser connected to tap water was place, in order to avoid vapor leaks.

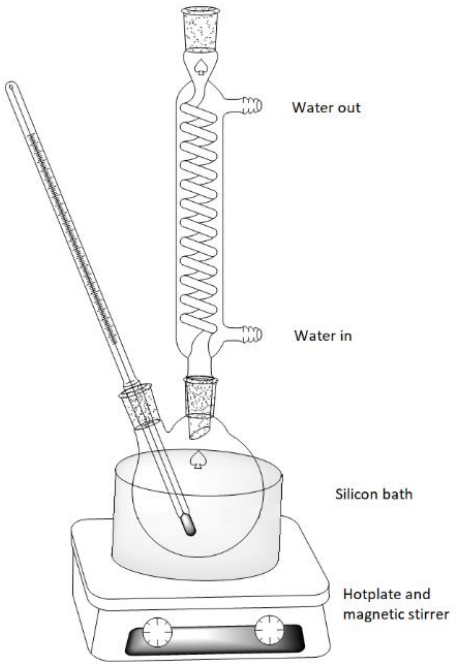


**Figure 4.3.-** Hydrometallurgical tests set-up

The Paval was weighed and fed to the flask, then, the liquid and the magnetic stirrer were introduced. The flask was placed in the preheated silicon bath, stirring adjusted, and the reaction time started once the slurry had achieved the target temperature. Once the reaction time ended, the flask was externally cooled with water and ice to stop the leaching reactions, and the slurry filtered immediately.

### 4.3.3. Set-up for precipitation tests

Precipitation tests were carried out at room temperature (25 °C) in an Erlenmeyer flask, on a magnetic stirrer. The precipitating agents were slowly added to the stirred solution with the aid of a funnel and a beaker. The reaction time started when all the reactants were in the Erlenmeyer. Once the reaction time ended, the slurry was filtered immediately.

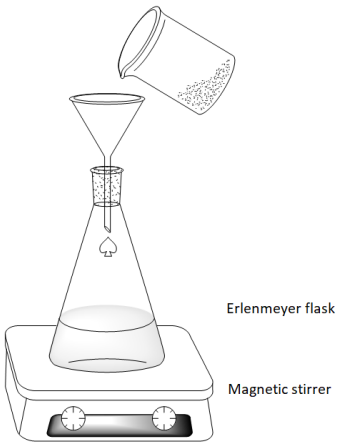


**Figure 4.4.-** Precipitation tests set-up

### 4.3.4. Solid/liquid filtration

Solid and liquid phases were filtered in a Millipore Sigma™ 142 mm Hazardous Waste Pressure Filter System lined with a PTFE coating which prevents heavy metal contamination and equipment deterioration. The filters used for all the solid/liquid separations were 0.45 µm pore size membrane filters from Merck (HAWP14250) together with glass fiber prefilters (AP2012450). The filtrations were carried out under 5 bar g of compressed air.

## 4.4. Analytical and instrumental techniques

#### 4.4.1. pH and conductivity electrodes

The pH was measured with a Crison pHmeter 50 14 T, equipped with a temperature sensor Pt 100 which allows pH measuring at temperatures up to 100 ˚C . Calibration was carried out daily before use, with Crysolit pH buffers 4.01, 7.00 and 9.21.

Conductivity was determined with a Crison conductivimeter EC-Metro GLP 31. Calibration was carried out daily before use, with Crysolit standards 147 µS/cm, 1413 µS/cm y 12.88 mS/cm.

### 4.4.2. Ion-Selective Electrodes

Fluoride and chloride contents in liquid samples were measured with a pH & Ion-Meter GLP 22+ equipped with a Ag/AgCl reference electrode, a 96 55 fluoride selective electrode, and a 96 52 chloride selective electrode.

Fluoride selective electrode was used together with a Total Ionic Strength Adjustment Buffer (TISAB) specific for fluoride determination in samples with a high $Al^{3+}$ content, known as TISAB D.[3] It is composed by 230 g disodium tartrate dihydrate, 242 g tris, and 84 mL 37 % HCl per liter of solution. By adding 10 mL of TISAB D to 40 mL of sample, it measures 100 % of the fluoride ions when both $Al^{3+}$ and $Ca^{2+}$ concentration are below 100 mg/L, and above 98 % when $Mg^{2+}$ concentration is below 50 mg/L. The electrode was calibrated daily before its use with freshly prepared NaF standards.

Chloride selective electrode was used together with 5 M $NaNO_3$ as TISAB, and calibrated daily before its use with freshly prepared NaCl standards.

### 4.4.3. Ion Chromatography

The sulfate concentrations were analyzed using a liquid chromatograph Dionex IC 3000 equipped with a conductivity detector operating at 35 °C, a guard column Ion Pac AG19 (4x50 mm) and a column Ion Pac AS19 (4x250 mm), which separates $F^-$, $Cl^-$, $NO_2^-$, $NO_3^-$, $SO_4^=$, and $PO_4^{3-}$. As eluent, 14 mM NaOH was used in isocratic conditions, and the suppressor, Thermo Scientific Dionex DRS 600, was set at 35 mA to neutralize its conductivity.

### 4.4.4. Alkalinity titration

Carbonate content in aqueous solution was determined by alkalinity analysis from pH 10.8 to 4.3 by titration with 0.01 N HCl and a pHmeter was used to accurately identify the endpoints. In Figure 4.5 the species involved in an aqueous solution as a function of the pH are presented.

As observed, $OH^-$ is the responsible for the solution alkalinity (caustic alkalinity) above pH 10.8 and therefore the protons needed to decrease the pH from the starting point to 10.8 are used to neutralize $OH^-$. From 10.3 to 8.3, alkalinity is due to $CO_3^=$, and from 8.3 to 4.3 due to $HCO_3^-$. Although alkalinity is usually expressed in meq/L of $OH^-$, $HCO_3^-$ or $CO_3^=$, in this PhD thesis total carbonate concentration was needed, and the result was given as mol $CO_3^=$/L.

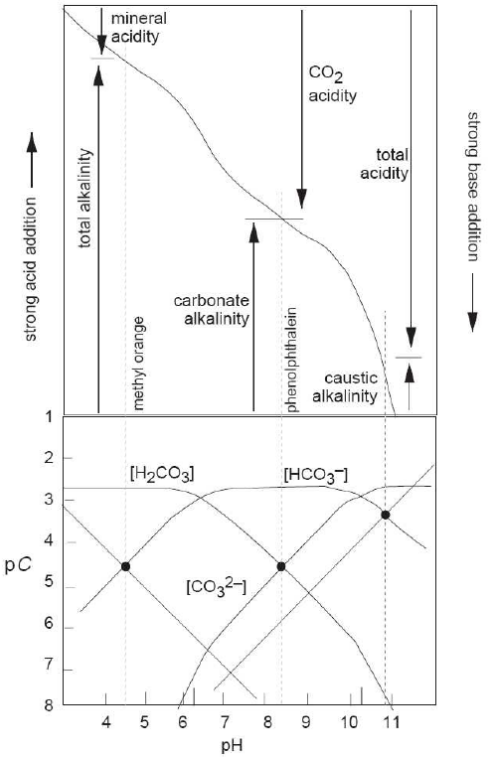


**Figure 4.5.-** Species affecting alkalinity and titration curves

### 4.4.5. Inductively Coupled Plasma Optical Emision Spectrometry

Elemental analysis was determined by inductively coupled plasma optical emission spectroscopy (ICP-OES) on a Perkin Elmer Optima 2000 OV device. The measured elements were calibrated daily before use.

### 4.4.6. X-Ray Fluorescence

The powdered Paval samples were mixed with Spectromelt A12 flux from Merck in a proportion of 20:1 and melted in an induction micro-oven to prepare a boron glass pearl for the analysis. The pearl chemical analysis was performed under vacuum with an AXIOS wavelength dispersion X Ray fluorescence sequential spectrometer from PANalytical, equipped with a Rh tube and three detectors: gas flow, scintillation, and sealed Xe. The calibration was made with international rock and mineral standards. The loss of ignition (LOI) was measured by calcining a portion of each sample in a muffle

oven at 1050 °C for an hour. The elements typically found in rocks were analyzed at a quantitative level, and Cl, F, and S at a semiquantitative level.

### 4.4.7. X-Ray Diffraction analysis

The powdered samples phase analysis was carried out by X-Ray Diffraction (XRD) with a PANalytical Xpert PRO diffractometer equipped with a copper tube ($\lambda Cu K\alpha mean$=1,5418 Å, $\lambda Cu K\alpha 1$=1,54060 Å and $\lambda Cu K\alpha 2$=1,54439 Å), a vertical Bragg-Brentano goniometer, a programmable divergence slit, an autosampler, a graphite secondary monochromator, and a PixCel detector. The PANalytical X´pert HighScore software combined with the database PDF2 from ICDD were used for data treatment and phase identification.

## 4.5. References

[1] R. K. Roy, Society of Manufacturing Engineers., *A Primer on the Taguchi Method*, Society Of Manufacturing Engineers, **1990**.

[2] A. Al-Refaie, M.-H. Li, *J. Simul.* **2010**, *4*, 143–148.

[3] S. Borjigin, Y. Ashimura, T. Yoshioka, T. Mizoguchi, *Japan Soc. Anal. Chem.* **2009**, *25*, DOI 10.2116/analsci.25.1437.

# Chapter 5

Hydrometallurgical process

# Table of contents

## 5.1. Introduction

In this chapter, the process to selectively leach fluoride from Paval or similar residues is studied. In order to rigorously consider and analyze all the influencing factors, the design of experiments methodology will be employed. In Chapter 4, the Taguchi method has been presented, as it is the selected method to design the experiments in this PhD thesis. The first step in the Taguchi method is a brainstorming to identify all the possible factors involved in the process to be studied. In this case, the factor and level determination were based on literature and preliminary tests. Once all factors and levels were determined, the optimum Orthogonal Array (OA) was selected and the tests were carried out. The elemental composition of all the samples employed in this chapter is collected in Table 5.13 in Appendix 5.1.

## 5.2. Taguchi design of experiments

### 5.2.1. Factors contemplated in the literature

In Chapter 2, the methods to leach fluorine from Paval-like materials (salt cake and SPL both treated with water and untreated) have been described. It is common to find that separate researchers study different parameters; nevertheless, a number of variables such as leaching agent and its concentration, time and temperature of reaction, and solid to liquid ratio (S/L) are most frequent. In Table 5.1, the leaching conditions reported in the literature, from Table 2.1, are summarized.

**Table 5.1.-** Summary of fluoride leaching conditions from literature

| Leaching agent | Concentration (g/L) | t (h) | T (°C) | S/L (g/L) | $[Al^{+3}]$ (M) | F/Al | pH | Ref |
|---|---|---|---|---|---|---|---|---|
| NaOH | 10-150 | 0.25-4 | 60-100 | 25-220 | - | - | 12 | [1–6] |
| $H_2SO_4$ | 49-68.6 | 1-4 | 60-98 | 62-240 | 0.1-6 | 0.5-8 | 0-4.3 | [7–15] |
| $Al(NO_3)_3$ | 31.5-150 | 4-24 | 25-60 | 15-150 | 0.36 | - | - | [16–18] |
| HCl | 146-354 | 1.5-3 | 85-90 | 50-250 | 1.5 | - | - | [5,19] |
| $H_2SiF_6$ | 100-200 | - | - | - | - | - | - | [20] |

Particle size has also been considered to be an important parameter, as fluoride leaching results are enhanced for lower particle size. Significantly better results have been reported for the same hydrometallurgical process for particle size below 150 µm compared to 2 mm.[1,2] Yet, another study suggested that no further improvements were achieved when reducing the particle size below 1.18 mm and down to 53 µm.[17] Based on this evidence, particle size was set below 1.00 mm in order to favor solid interaction with the solution.

Considering the number of different reaction conditions proposed in the literature, a series of tests was conducted to reduce the amount of factors to include in the DOE to a manageable number. Although a DOE could be designed to fit all the parameters from the literature, it would require an excessive amount of experiments. Moreover, that kind of broad DOE approach would likely not provide detailed enough results and, probably, a second more specific DOE would be necessary.

### 5.2.2. Preliminary tests with Paval

As presented in Table 5.2, the parameters commonly studied in the literature for designing hydrometallurgical processes are the leaching agent and its concentration, time and temperature of reaction, solid to liquid ratio (S/L), pH, aluminum concentration and aluminum to fluorine ratio in the leaching solution (Al/F). In order to best adapt these variables to the researched material and process, a number of tests were carried out. First, the effect of aluminum addition was studied in order to determine, on the one hand, if it was viable to maintain a fixed Al/F ratio; and, on the other hand, if it was necessary to externally add aluminum as Paval already contains it. To assess these issues, a series of tests was designed based on a patent.[13] For these tests, sample SCP01 (1.5 wt% F, 40.5 wt% Al) was treated for 20 minutes with two aluminum containing solutions ($AlCl_3$-HCl and $Al_2(SO_4)_3$-$H_2SO_4$) at a very low S/L ratio (4 g/L) in order to avoid saturation limitations. The selected pH was 1.5 for $AlCl_3$-HCl solution and 3.0 for $Al_2(SO_4)_3$-$H_2SO_4$, adding NaOH to maintain it.

The results from these tests are presented in Table 5.2. As it can be observed, at the tested conditions aluminum is leached from the sample, which results in higher Al/F ratios in solution than the intended ones.

**Table 5.2.-** Conditions and results for aluminum addition tests

| Medium | Al/F $_{Nominal}$ | $pH_{initial}$-$pH_{final}$ | Al/F $_{Measured}$ | % $F_{leached}$ | % $Al_{leached}$ |
|---|---|---|---|---|---|
| HCl-$AlCl_3$ | 3 | 1.5-1.8 | 17 | 12.8 | 8.5 |
| HCl-$AlCl_3$ | 5 | 1.5-1.7 | 53 | 8.0 | 9.4 |
| $H_2SO_4$-$Al_2(SO_4)_3$ | 3 | 1.9-3.0 | 31 | 5.8 | 7.7 |
| $H_2SO_4$-$Al_2(SO_4)_3$ | 5 | 3.0-3.0 | 52 | 18.0 | 9.5 |

A second set of tests was performed with lower amounts of aluminum salts to achieve the Al/F ratio proposed in the patent. The results are presented in Table 5.3:

**Table 5.3.-** Conditions and results for aluminum addition tests

| Medium | $g_{salt}$/ $g_{sample}$ | Al/F $_{Measured}$ | pH | % $F_{leached}$ | % $Al_{leached}$ |
|---|---|---|---|---|---|
| HCl 0.5 M-$AlCl_3$ | 0.0 | 2.2 | 1.5 | 5.2 | 0.7 |
| HCl 0.5 M -$AlCl_3$ | 0.1 | 5.1 | 1.5 | 6.9 | 0.0 |
| HCl 0.5 M -$AlCl_3$ | 0.2 | 8.7 | 1.5 | 7.4 | 0.0 |
| $H_2SO_4$ 0.5 M -$Al_2(SO_4)_3$ | 0.0 | 1.7 | 3.5 | 4.4 | 0.5 |
| $H_2SO_4$ 0.5 M -$Al_2(SO_4)_3$ | 0.1 | 5.0 | 3.5 | 6.8 | 0.3 |
| $H_2SO_4$ 0.5 M -$Al_2(SO_4)_3$ | 0.2 | 9.7 | 3.5 | 5.9 | 0.0 |

From the very low fluorine reduction in these experiments, it can be inferred that the conditions are too mild for the studied material. Additionally, the required external aluminum amount is minimal since part of the aluminum from the sample is dissolved into the acid medium. Based on these results, it was decided that 1) enough aluminum is leached from the material even at mild conditions and the addition of an aluminum salt was not necessary for Paval, which would most likely result in a more economical and environmentally friendlier design, and 2) as aluminum is extracted from the material, its concentration and therefore, Al/F ratio was not a factor to be included in the DOE.

Then, four aluminum-free leaching agents can be found in the literature: Sodium hydroxide (NaOH), sulfuric acid ($H_2SO_4$), hydrochloric acid (HCl), and hexafluorosilicic acid ($H_2SiF_6$). First, $H_2SiF_6$ was tested in order to evaluate the viability of the chemical reaction proposed by the authors,[20] as it is the rarest and most expensive leaching agent from literature. The proposed leaching treatment is focused on leaching cryolite ($Na_3AlF_6$) and calcium fluoride ($CaF_2$), which are the two main fluoride phases found in the Paval. It is well-known that cryolite is more easily leached by acids and bases than

$CaF_2$, which is considered almost insoluble.[17] Thus, $H_2SiF_6$ would be considered as leaching agent to treat Paval if it was proved as a good solvent for $CaF_2$.

$$CaF_2(s) + H_2SiF_6\ (aq) \rightarrow CaSiF_6\ (aq) + 2\ HF\ (aq)$$

A test was performed contacting $CaF_2$ with $H_2SiF_6$ acid, in 20 % stoichiometric excess, for 24 h at room temperature resulting in only 11 wt% solid leaching. Considering its high price, environmental and health risks, and low performance, $H_2SiF_6$ was discarded as a viable leaching agent.

Second, the harsher processes from literature and 1 M *aqua regia* (a solution containing $HNO_3$ 0.25 M and HCl 0.75 M) were tested with different Paval samples (with different fluoride contents) as a preliminary screening of their adequacy to selectively leach fluoride. At this stage of the experimental work, aluminum and fluorine leaching were the two selected parameters to compare the processes, as fluoride leaching should be as high as possible while maintaining aluminum leaching at a minimum.

The results from these tests are listed in Table 5.4 and displayed in Figures 5.1.a and 5.1.b for an easier comparison. Figure 5.1.a presents the relationship between the leached and the fed fluorine amounts normalized by the added leaching agent amount. In Figure 5.1.b similar ratios are used to show the aluminum leaching. Thereby, the fluorine and aluminum leaching capacity of the leaching agents can be compared, independently of the fluorine and aluminum content in the sample and leaching agent concentration. Both graphics are in logarithmic scale, and lines representing 25, 50 and 100 % leaching (Figure 5.1.a, F) or 1, 10, 25 and 100 % leaching (Figure 5.1.b, Al) have been added for an easier reading.

**Table 5.4.-** Leaching agent screening tests

| Sample | Leaching agent | t (min) | T (°C) | S/L (g/L) | % $F_{sample}$ | % $Al_{sample}$ | % $F_{leached}$ | % $Al_{leached}$ |
|---|---|---|---|---|---|---|---|---|
| SPL[5] | NaOH 2.5 M | 180 | 90 | 250 | - | - | - | - |
| SCP11 | NaOH 2.5 M | 180 | 90 | 250 | 0.57 | 25.9 | 22.2 | 0.7 |
| SCP01 | NaOH 2.5 M | 180 | 90 | 250 | 1.51 | 40.5 | 24.9 | 33.6 |
| MP04 | NaOH 2.5 M | 180 | 90 | 250 | 5.87 | 29.0 | 55.5 | 35.4 |
| SPLP01 | NaOH 2.5 M | 180 | 90 | 250 | 15.3 | 20.8 | 39.0 | 2.2 |
| SPLP02 | NaOH 2.5 M | 180 | 90 | 250 | 19.1 | 25.9 | 20.1 | 3.1 |
| SPL[5] | NaOH 2.5 M (180 min, 90 °C) + HCl 9.7 M (180 min, 100 °C) | | | 250 | - | - | - | - |
| SCP11 | NaOH 2.5 M (180 min, 90 °C) | | | 250 | 0.57 | 25.9 | 29.3 | - |
| SPLP01 | + HCl 9.7 M (180 min, 100 °C) | | | 250 | 15.3 | 20.8 | 45.2 | 64.3 |
| SCP01 | HCl 0.5 M | 90 | 100 | 100 | 1.51 | 40.5 | 39.0 | 61.0 |
| SCP01 | HCl 2.5 M | 90 | 100 | 100 | 1.51 | 40.5 | 72.0 | 96.0 |
| SCP01 | HCl 0.5 M | 90 | 25 | 100 | 1.51 | 40.5 | 31.0 | 18.0 |
| SCP01 | HCl 2.5 M | 90 | 25 | 100 | 1.51 | 40.5 | 41.0 | 38.0 |
| SCP01 | 0.3 M | 120 | 50 | 250 | 1.51 | 40.5 | 31.1 | 5.8 |
| MP04 | $HNO_3$+ | 120 | 50 | 250 | 5.87 | 29.0 | 53.2 | 11.0 |
| SPLP02 | 0.7 M HCl | 120 | 50 | 250 | 19.1 | 35.5 | 16.4 | 7.3 |
| SPL[7,8] | $H_2SO_4$ 0.7 M | 240 | 60 | 120 | - | - | - | - |
| SCP06 | $H_2SO_4$ 0.5 M | 90 | 50 | 250 | 0.68 | 36.9 | 35.5 | 7.5 |
| SCP05 | $H_2SO_4$ 0.5 M | 90 | 50 | 250 | 1.57 | 33.1 | 37.7 | 10.5 |
| MP01 | $H_2SO_4$ 0.5 M | 90 | 50 | 250 | 2.16 | 34.5 | 32.6 | 4.1 |
| MP03 | $H_2SO_4$ 0.5 M | 90 | 50 | 250 | 3.54 | 39.6 | 38.1 | 1.4 |
| MP02 | $H_2SO_4$ 0.5 M | 90 | 50 | 250 | 3.69 | 38.5 | 54.2 | 0.0 |
| SPL[11] | $H_2SO_4$ 0.5 M | 60 | 90 | 100 | - | - | 93.3 | 89.5 |
| SCP01 | $H_2SO_4$ 0.5 M | 90 | 100 | 100 | 1.51 | 40.5 | 49.5 | 29.8 |
| SCP01 | $H_2SO_4$ 2.5 M | 90 | 100 | 100 | 1.51 | 40.5 | 72.2 | 60.7 |
| SCP01 | $H_2SO_4$ 0.5 M | 90 | 25 | 100 | 1.51 | 40.5 | 33.0 | 26.0 |
| SCP01 | $H_2SO_4$ 2.5 M | 90 | 25 | 100 | 1.51 | 40.5 | 45.0 | 35.0 |

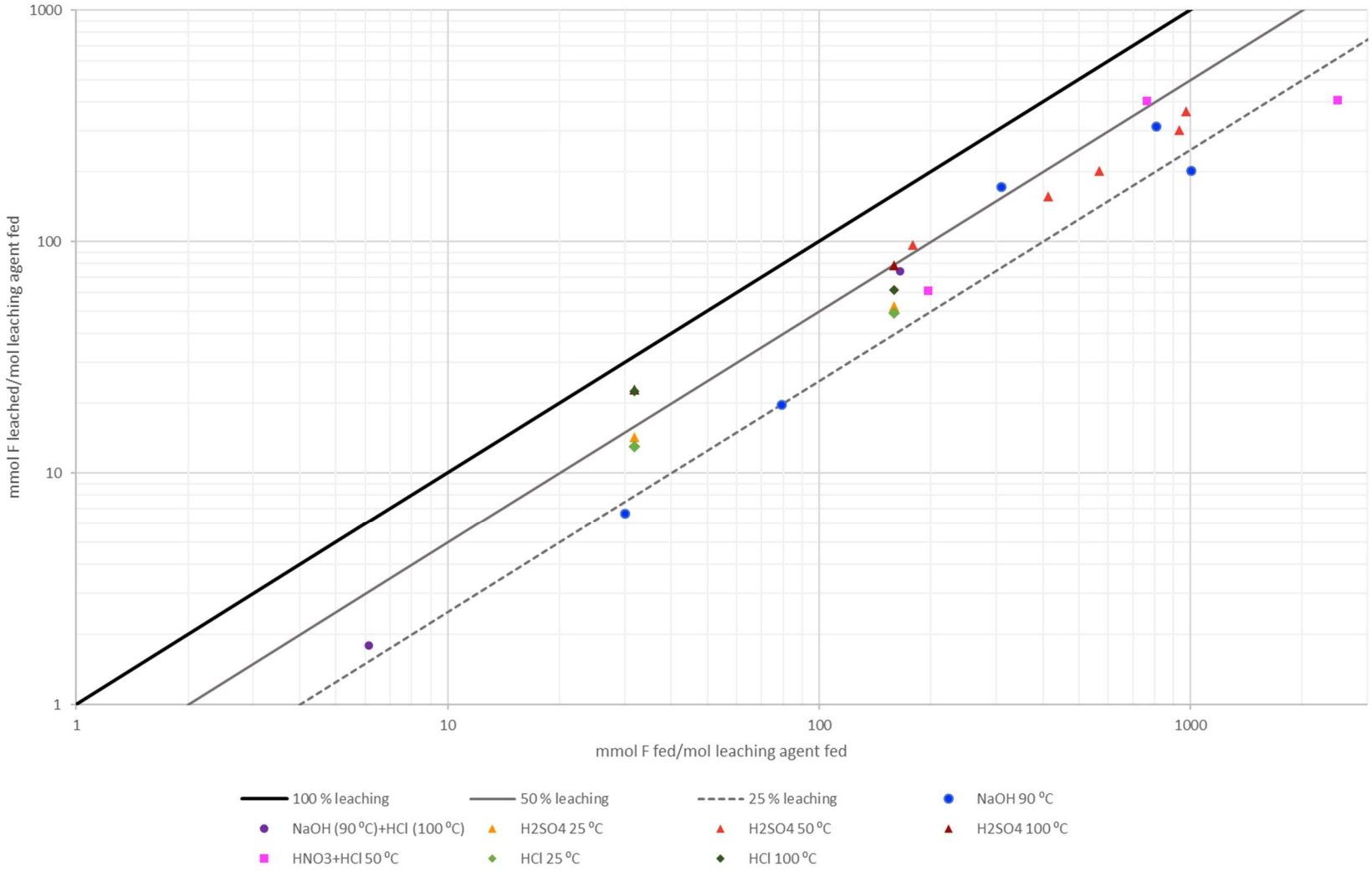


**Figure 5.1.a.-** Leaching agents screening for fluoride leaching

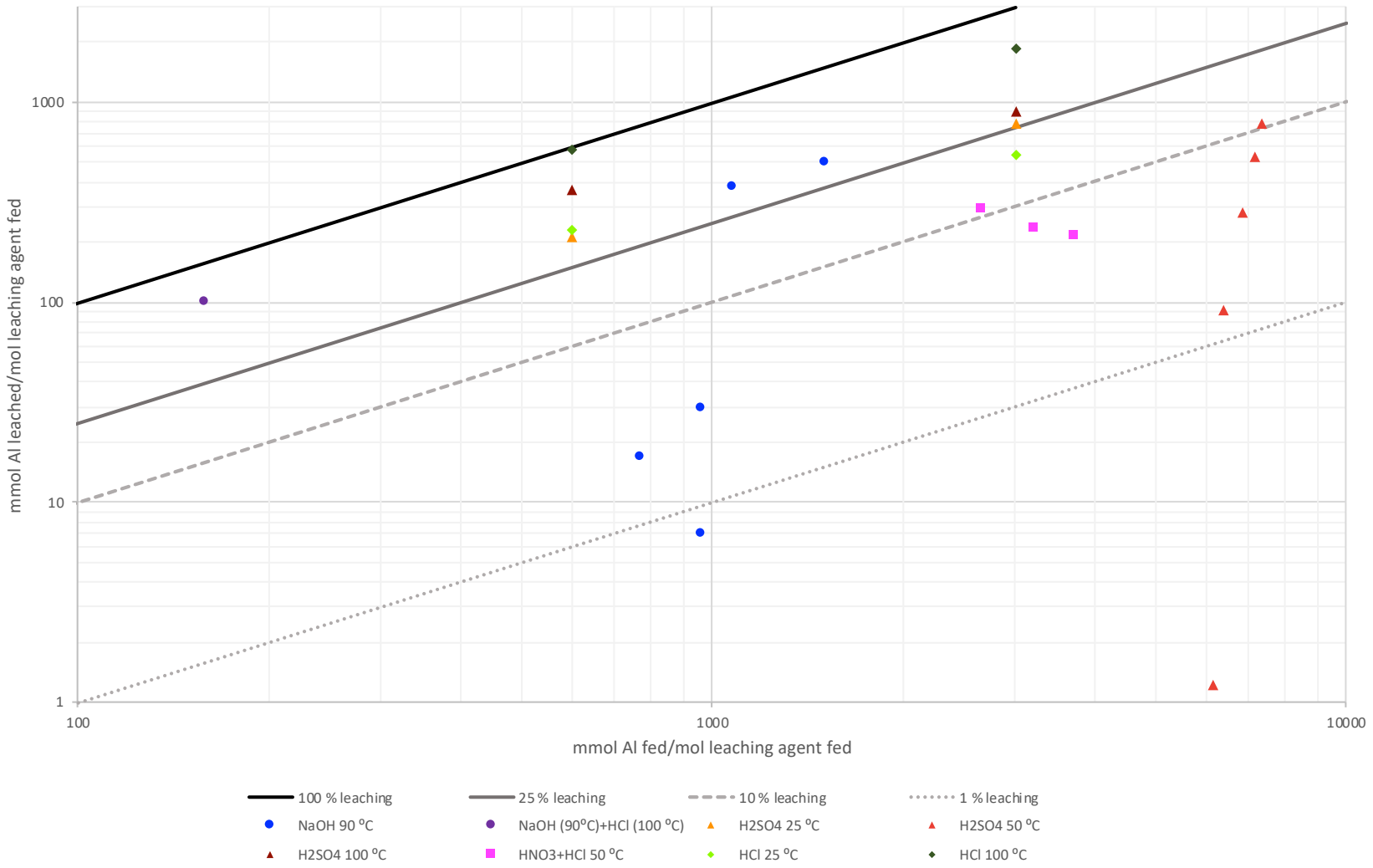


**Figure 5.1.b.-** Leaching agents screening for aluminum leaching

High values on the *x*-axis represent high element (F in Figure 5.1.a and Al in Figure 5.1.b) to leaching agent ratios, what would be desired from the process economic point of view. On the *y*-axis, high values represent high leaching capacities for the chemical and the operating conditions. In the case of fluorine leaching, the most desired area for the results would be high *x* and *y* values, as it represents situations where low leaching agent to fluorine ratios are very effective for its removal. In the case of aluminum leaching, the desired situation would be the opposite, meaning that even at high leaching agent to aluminum ratios (low range in the *x*-axis), low aluminum removal efficiency is achieved (low *y* values). As the viability of the leaching procedure would be dependent on both the fluoride and aluminum removal efficiencies, the results from the experiments will be discussed considering these two variables simultaneously.

As it can be observed in Figures 5.1.a and 5.1.b, the two-step leaching process including NaOH 2.5 M and HCl 9.7 M, while being the most aggressive treatment (in terms of concentration/pH, temperature and time), showed low fluoride leaching capacity and high aluminum leaching capacity, which is the opposite to the process target. When only the first NaOH step was carried out, fluorine removal results widely varied depending on the sample, with the *mmol F leached/mol leaching agent fed* ratio ranging from 7 at favorable conditions (low *fluorine/leaching agent ratio*) to 315 at conditions one order of magnitude less favorable. Similar variability was observed in aluminum leaching results varying this same ratio between 7 and 504 for similar aluminum/leaching agent ratios. Comparing these results, the HCl 9.7 M step only increased in a 15 % fluoride leaching, while enhancing aluminum leaching by 2800 %, thus, this step proved to be inadequate for the purpose of this research/process.

As 9.7 M HCl at 100 °C is a very aggressive environment, milder sets of conditions were tested for HCl. When maintaining 100 °C and using either HCl 0.5 or 2.5 M concentrations, both fluoride and aluminum leaching capacities remained similar to HCl 9.7 M. When testing HCl at 25 °C, fluoride, and aluminum leaching capacities decreased accordingly, although maintaining a high aluminum leaching selectivity. HCl was thus discarded as leaching agent as it was proven to be a more selective leaching agent for aluminum than fluoride. Alternatively, HCl combination with $HNO_3$ (as 1 M *aqua regia*) significantly modified its leaching behavior, allowing enhanced fluoride leaching efficiencies in addition to lower aluminum removal efficiencies at 50 °C.

$H_2SO_4$ was the last leaching agent to be studied. First, 0.5 M $H_2SO_4$ was tested at 50 °C showing only small variations in fluorine removal with almost one order of magnitude difference in the *fluorine/leaching agent* ratio: from 366 to 97 *mmol F leached/mol leaching agent fed* at the less favorable conditions. Aluminum leaching varied from 1 to 772 *mmol Al leached/mol leaching agent fed* for similar *aluminum/leaching agent* ratios in different samples. At the same temperature, a mixture of 1 M *aqua regia* resulted in similar fluoride leaching capacity and variability; however, aluminum leaching capacity was higher and more stable when using 1 M *aqua regia* than 0.5 M $H_2SO_4$. For the purpose of this research, high aluminum leaching variability with similar fluorine removal capacities is interesting as it could allow for leaching conditions optimization yielding high fluorine and low aluminum leaching process.

As the leaching characteristics of $H_2SO_4$ were the most desirable amongst the tested agents, 2.5 M $H_2SO_4$ was also tested at 25 and 100 °C. For the same Paval sample, at 100 °C fluoride leaching increased from 50 to 72 % when increasing $H_2SO_4$ concentration from 0.5 to 2.5, accordingly with aluminum leaching, which increased from 30 to 60 %.

- The fact that $H_2SO_4$ leaches less aluminum than HCl or *aqua regia* for similar fluoride leaching yields, makes $H_2SO_4$ the best leaching agent alternative. Besides, lower temperatures seem to be more appropriate, as the aluminum leaching capacity of $H_2SO_4$ is triggered at higher temperatures significantly more than fluoride leaching is. Taking into account the results obtained from the leaching agents screening, five main conclusions were obtained: *(i)* HCl was discarded as leaching agent as it tends to selectively leach aluminum. Moreover, chlorides would be more difficult to remove from the process effluent, which is part of this PhD thesis, than sulfates. *(ii)* NaOH was discarded as leaching agent as its selective fluorine leaching capacity is inferior to the one of $H_2SO_4$. *(iii)* $H_2SO_4$ was selected as the most promising leaching agent attending at its high fluoride removal selectivity and the possibility for fluoride and aluminum leaching optimization as well as its high availability and comparatively low price and environmental impact. *(iv)* Fluoride removal results varied depending on the sample nature rather than its fluoride content. Thus, in order to compare, the next tests would be performed with Salt Cake Paval (SCP) samples, as it is the main type of Paval

produced by Befesa. In Table 5.5 the typical SCP composition is presented. *(v)* The factors selected at this point to be studied by the Taguchi method are $H_2SO_4$ concentration, reaction time, and temperature.

**Table 5.5.-** Typical elemental composition of SCP

| Element | F | Cl | Al | Si | Fe | Ca | Mg | Na | K |
|---|---|---|---|---|---|---|---|---|---|
| wt% | 0.3-1.6 | 0.2-1.1 | 34-45 | 2-6 | 1-2.5 | 0.8-2.6 | 3.3-6.6 | 0.03-1.7 | 0-1.3 |

Once the leaching agent and the relevant factors for the Taguchi method were selected, a series of experiments were carried out to determine the range in which each variable should be studied.

First, a series of tests were carried out at different reaction times to explore the kinetics of the process. In the literature reaction times widely vary between methods from 15 min to 24 h. More specifically, when $H_2SO_4$ is employed reaction time vary between 1 and 4 h. Taking all into account, four different SCP samples (SCP04, SCP06, SCP07 and SCP08) were put in contact with 0.5 M $H_2SO_4$ with S/L ratio 250 g/L at 50 °C for 20, 45 and 90 min, in order to assure the consistency of the conclusions among different SPC samples. The results are shown in Figure 5.2.a and 5.2.b:

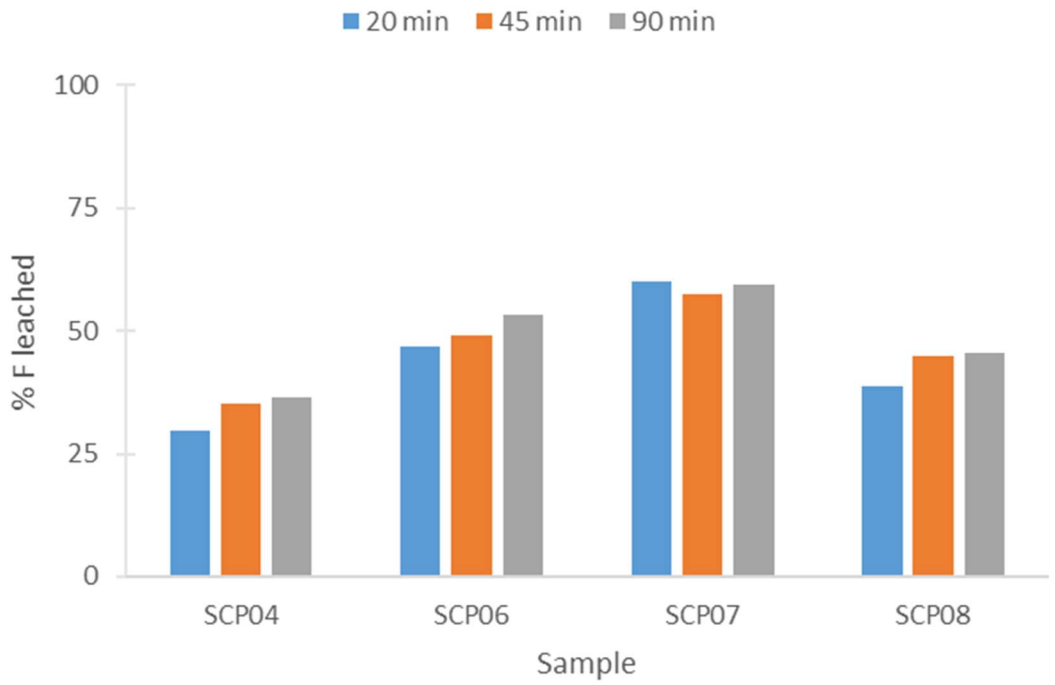


**Figure 5.2.a-** % F leached from samples at 20, 45 and 90 min

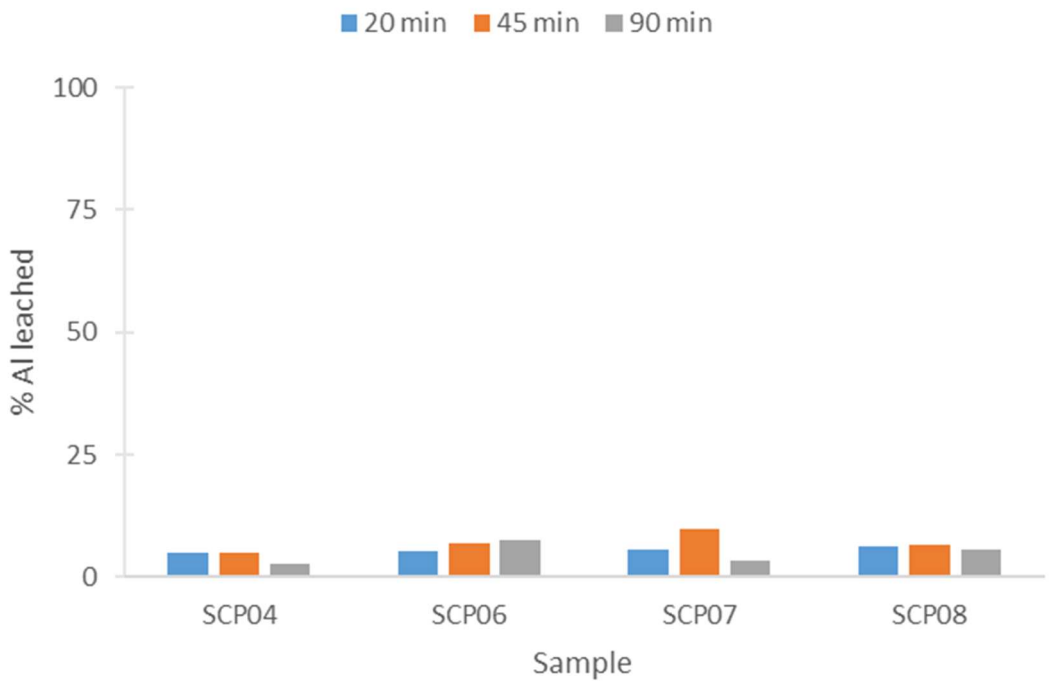


**Figure 5.2.b-** % Al leached from samples at 20, 45 and 90 min

As can be observed, when increasing reaction time from 20 to 45 min, both the F and the Al leaching increased for almost all the samples. When the contact time was further increased to 90 min, however, small leaching differences were observed only in some samples, while almost identical leaching results were achieved for the rest of the samples. Thus, it was decided not to test higher reaction times, as the small change between 45 and 90 min suggested that the leaching reactions were close to equilibrium after just 45 min.

Second, a series of tests was carried out to determine the range of concentrations that will be included in the design of experiments. SCP03 samples were put in contact with different $H_2SO_4$ concentration solutions at 25°C for 90 minutes, and a S/L of 250 g/L. The fluoride and aluminum leaching results are presented in Figure 5.3:

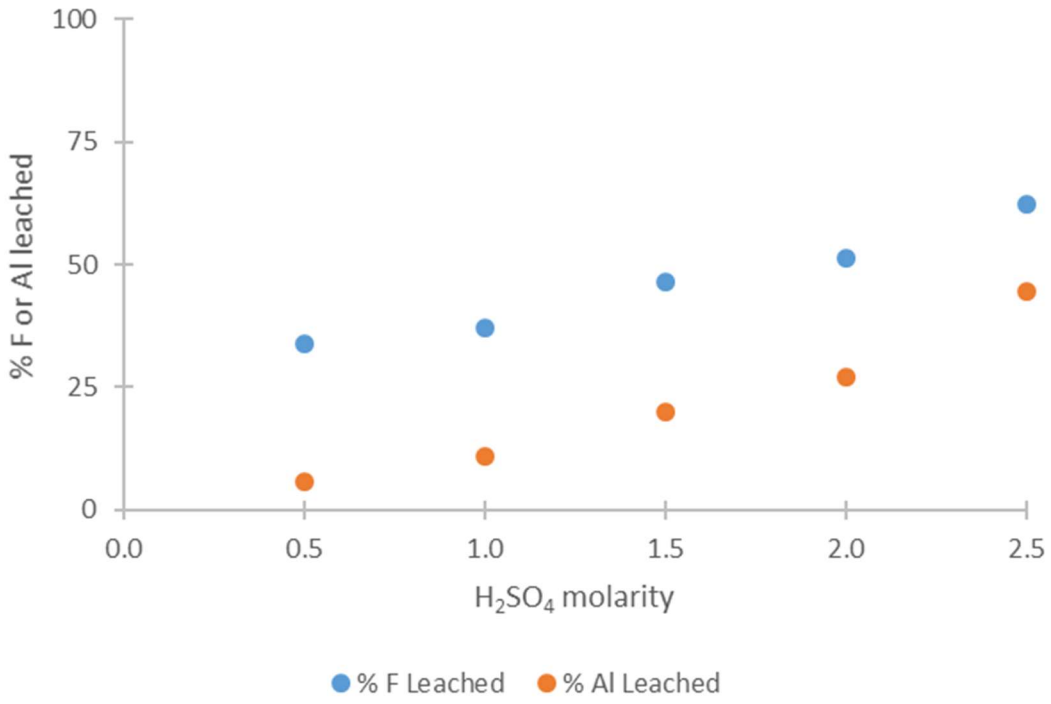


**Figure 5.3.-** Leaching tests results at different $H_2SO_4$ concentrations in mol/L

As expected, when higher acid concentrations were used, higher leaching results for both fluorine and aluminum were obtained. However, aluminum leaching increased faster with the increase in concentration than fluoride leaching. Therefore, a compromise will be requires in order to achieve the best leaching results with the lowest acid concentration possible.

Third, the solid to liquid ratio was studied at different concentrations and temperatures using sample SCP01 and 90 min reaction time. An adequate S/L ratio is important to avoid leaching limitations by saturation and stirring mechanical problems. If there is not enough liquid, there will not be a good phase contact and the leaching yield will be low even at extreme conditions of temperature and concentration. Moreover, if the leaching agent is rapidly saturated, it will not be able to extract as much fluorine as it could with a lower S/L ratio. On the contrary, if excessive liquid is employed, an unnecessary amount of $H_2SO_4$ will be used, generating larger amounts of effluent and resulting in an economically and environmentally worse process. The tested S/L ratios were 40 and 100 g/L for 25 °C, and 100 and 250 g/L for 50 and 100 °C, as solubility is typically enhanced at higher temperatures. Fluorine and aluminum leaching results are shown in Figure 5.4.a and 5.4.b:

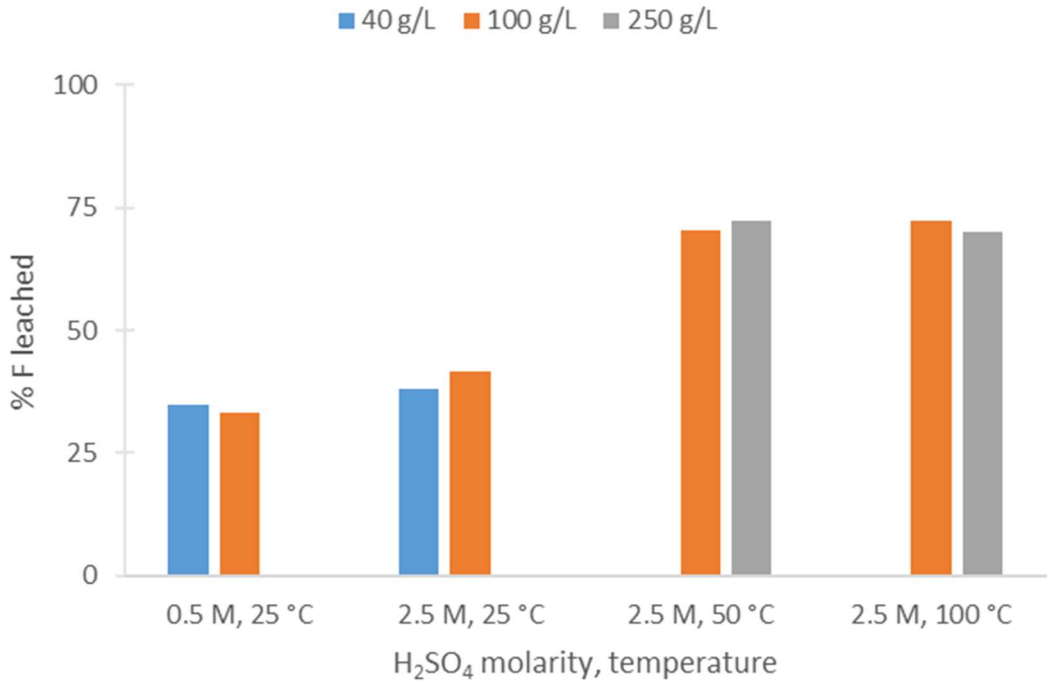


**Figure 5.4.a.-** Fluoride leaching tests results for different S/L ratios

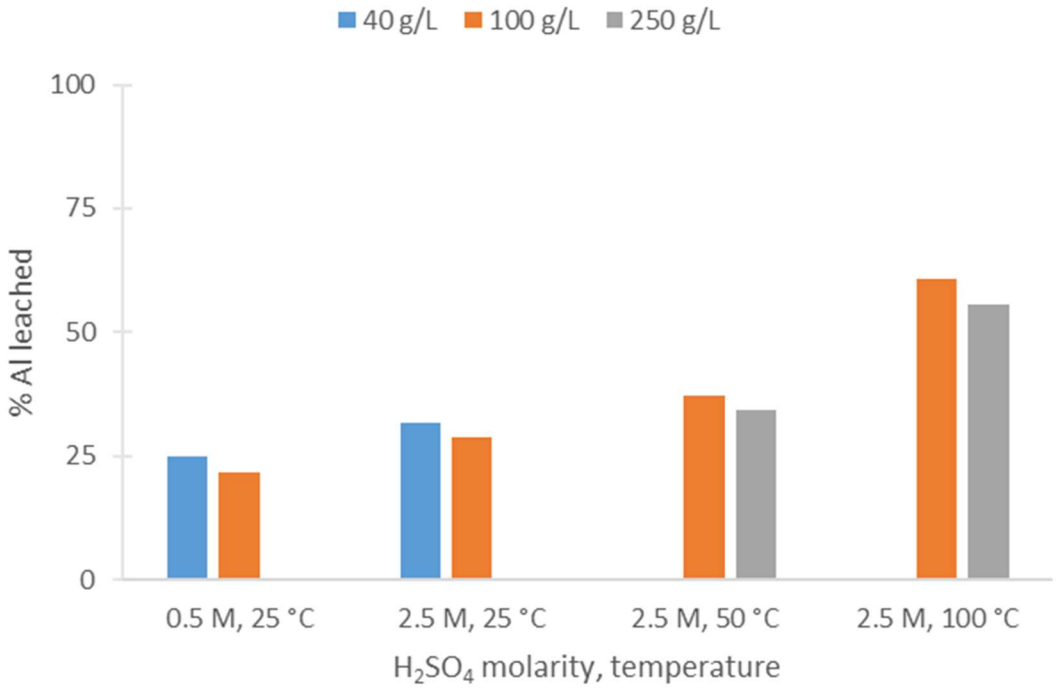


**Figure 5.4.b.-** Aluminum leaching tests results for different S/L ratios

These results confirm that temperature effect is more important than S/L ratio effect as neither fluoride nor aluminum leaching results showed a high enhancement when decreasing the S/L ratio from 250 to 100 g/L, or 100 to 40 g/L. Thus, solubility was not considered a limiting variable if a S/L ratio of 250 g/L was employed in the process. When

testing higher S/L ratios the generated slurry was difficult to stir, and the contact between solid and liquid inadequate. Therefore, all the following tests were performed with a S/L ratio of 250 g/L.

An important aspect of the Taguchi method is the assumption of a good process knowledge. It is especially critical when there are interactions between variables, as if they are not properly included in the design, the results will not be accurate (this can be verified when the confirmation run does not corroborate the expected result at optimum conditions). From the tests performed up until this point of the research, it is hypothesized that temperature and concentration are not independent factors, and therefore interact with each other. If there are interactions between factors, they must be included in the Taguchi design. When two variables are independent their effects are additive, and when they are dependent due to an interaction, their effects are not additive. The fastest way to test the dependence of two variables is by graphing them. Figures 5.6.a and 5.6.b show the interaction between temperature and $H_2SO_4$ concentration, and Figure 5.7.a and 5.7.b the interaction between S/L ratio and temperature.

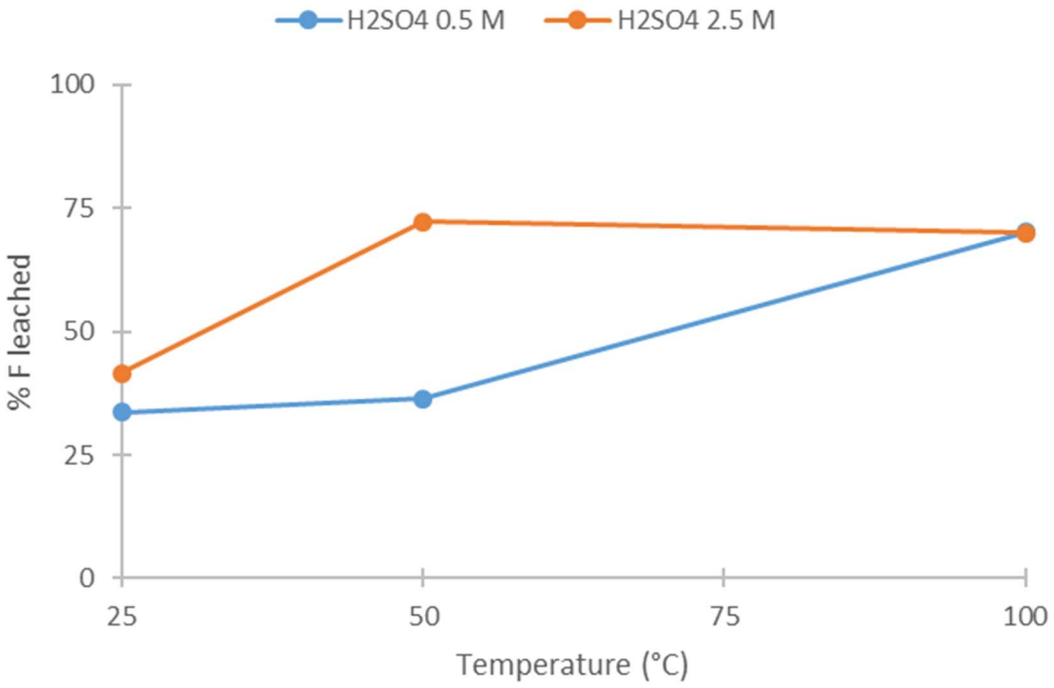


**Figure 5.6.a.-** Fluoride leaching results for temperature and $H_2SO_4$ concentration interaction

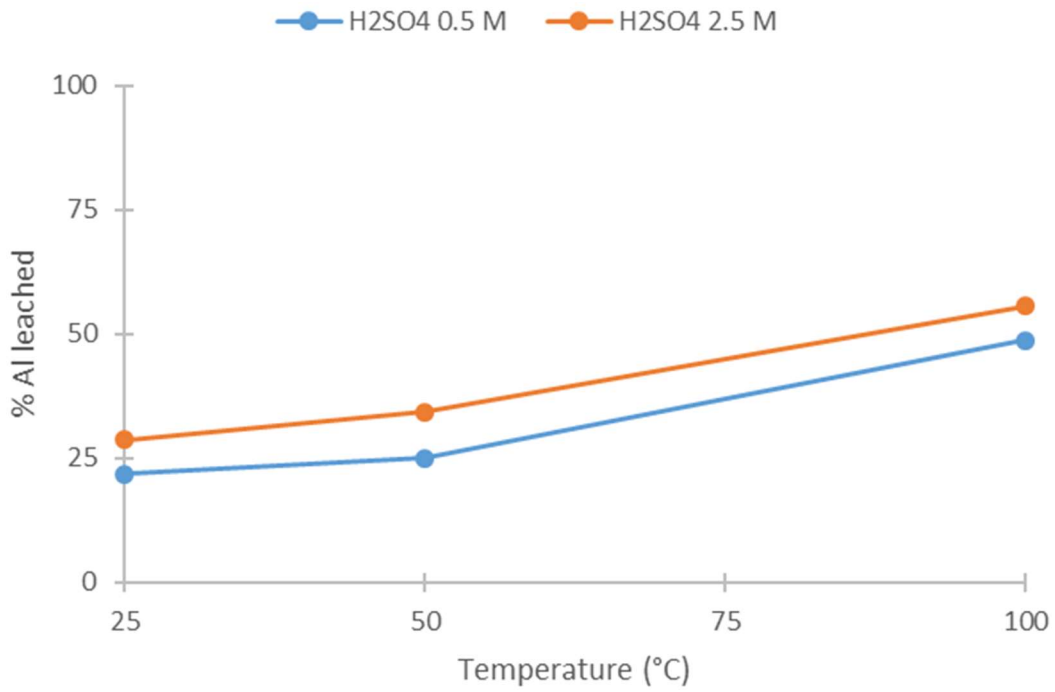


**Figure 5.6.b.-** Aluminum leaching results for temperature and $H_2SO_4$ concentration interaction

Fluoride leaching results show a synergetic effect between temperature and $H_2SO_4$ concentration, while aluminum leaching results do not. This was identified as a potentially important characteristic to further study, as ideally aluminum leaching should be as low as possible, and fluorine as high as possible. Finding a set of conditions where fluorine leaching was maximized while aluminum leaching was minimized was this thesis scope.

In Figures 5.7 (a and b) and 5.8 (a and b), no indication of an interaction between the other variables is found. The values for the different operating conditions were sufficiently close to be considered equal within the experimental error.

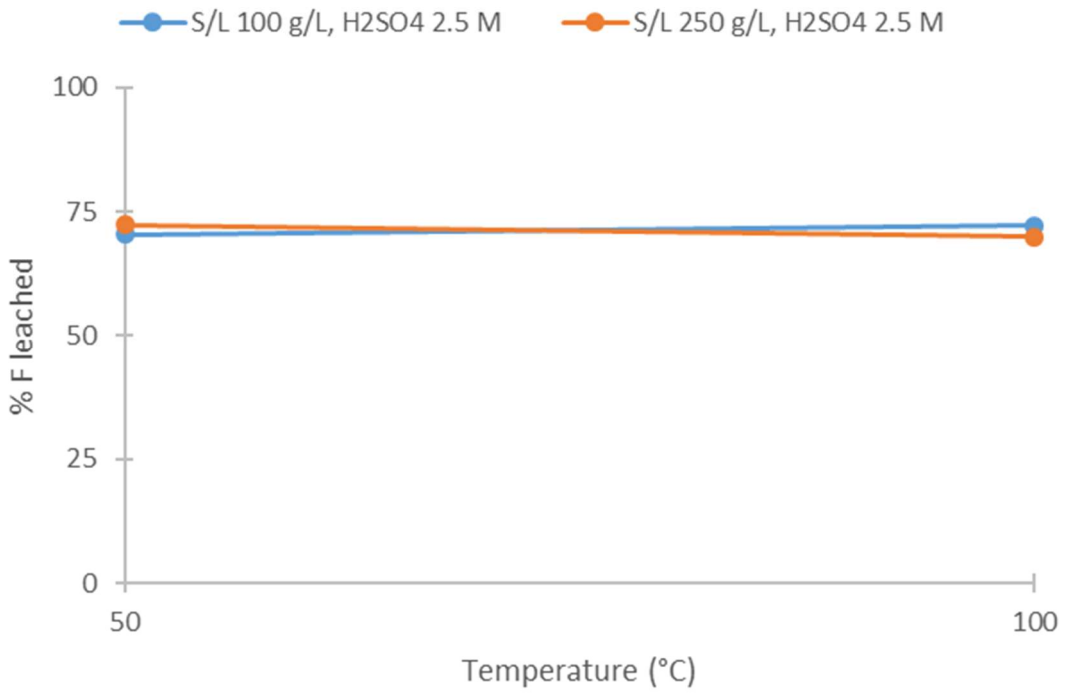


**Figure 5.7.a.-** Fluoride leaching results for temperature and S/L interaction

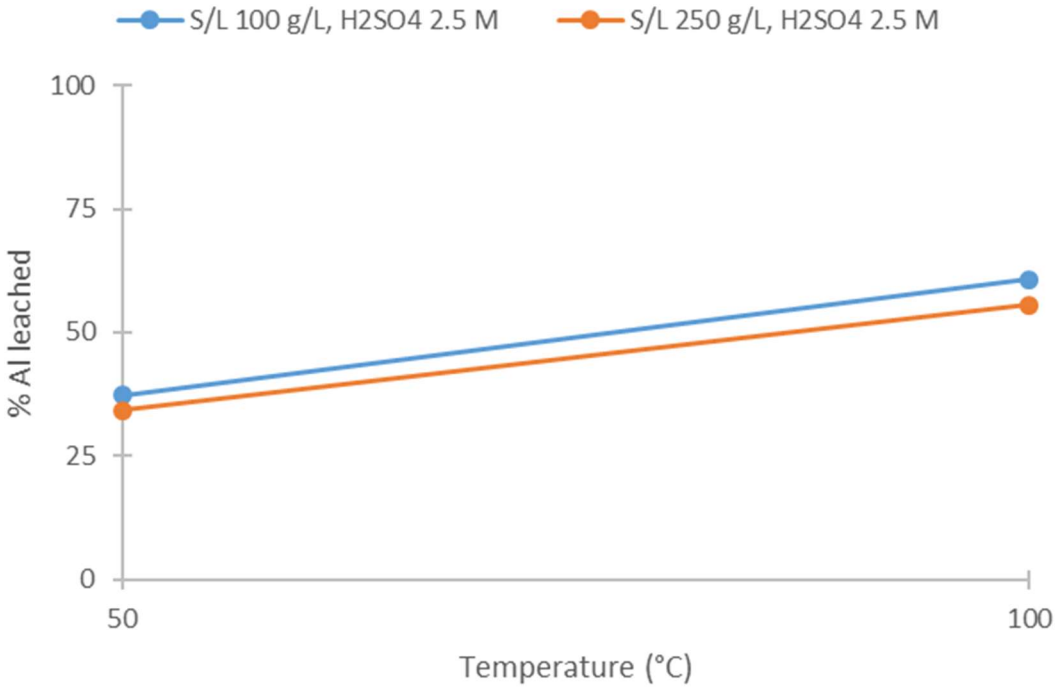


**Figure 5.7.b.-** Aluminum leaching results for temperature and S/L interaction

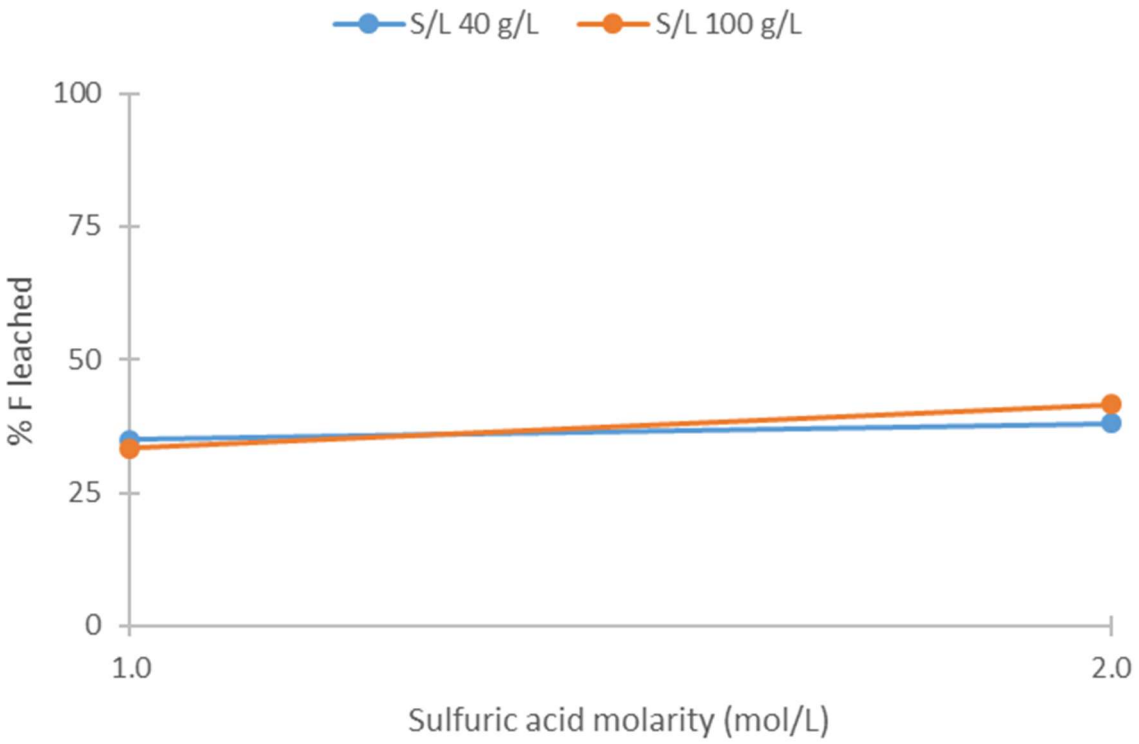


**Figure 5.8.a.-** Fluoride leaching results for S/L and $H_2SO_4$ concentration interaction

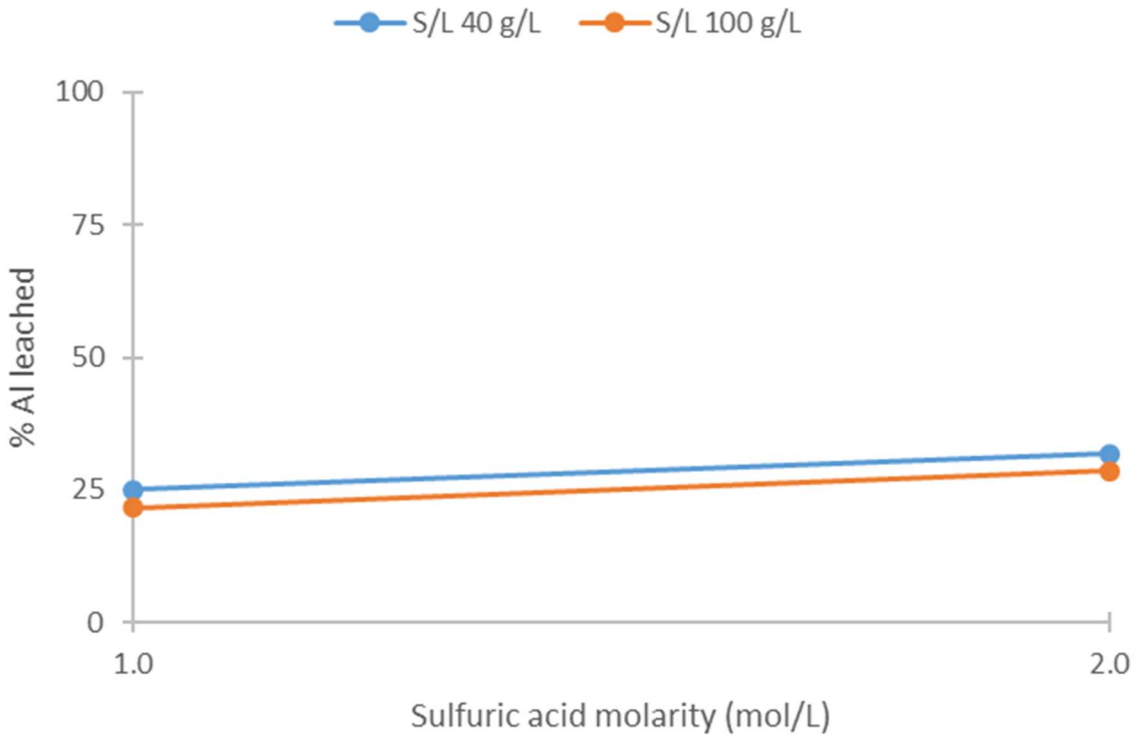


**Figure 5.8.b.-** Aluminum leaching results for S/L and $H_2SO_4$ concentration interaction

Taking in account all of the above, the $L_9$ Taguchi Orthogonal Array (OA) was selected for the study (Table 5.6.a). It is a 3-level OA, which was more appropriate than a

two-level OA due to the suspected interaction between temperature and concentration. This interaction could result in nonlinear results, and a third level allows us to verify it, whereas if two levels were considered only linear outputs can be obtained. Each interaction consumes 2 degrees of freedom (DOF), leaving the design as a 3x3 full factorial. Thus, $H_2SO_4$ concentration (Factor A), temperature (Factor B), and their interaction (AxB) were studied at a constant S/L ratio of 250 g/L and 90 min contact time. As shown in Table 5.6.b, the design levels for Factor A ($H_2SO_4$ concentration) were 0.5, 1.5 and 2.5 M; and for Factor B (temperature) were 25, 50 and 100 °C.

**Table 5.6.a.-** Taguchi's $L_9$ OA

| $L_9$ ($3^4$) | | A | B | C | D |
|---|---|---|---|---|---|
| Set of conditions | 1 | 1 | 1 | 1 | 1 |
| | 2 | 1 | 2 | 2 | 2 |
| | 3 | 1 | 3 | 3 | 3 |
| | 4 | 2 | 1 | 2 | 3 |
| | 5 | 2 | 2 | 3 | 1 |
| | 6 | 2 | 3 | 1 | 2 |
| | 7 | 3 | 1 | 3 | 2 |
| | 8 | 3 | 2 | 1 | 3 |
| | 9 | 3 | 3 | 2 | 1 |

→

**Table 5.6.b.-** Taguchi's $L_9$ for 2, 3-level factors and 1 interaction

| Test | [$H_2SO_4$] | T (°C) | S/L (g/L) | t (min) |
|---|---|---|---|---|
| 1 | 0.5 | 25 | 250 | 90 |
| 2 | 0.5 | 50 | | |
| 3 | 0.5 | 100 | | |
| 4 | 1.5 | 25 | | |
| 5 | 1.5 | 50 | | |
| 6 | 1.5 | 100 | | |
| 7 | 2.5 | 25 | | |
| 8 | 2.5 | 50 | | |
| 9 | 2.5 | 100 | | |

## 5.3. Hydrometallurgical experiments

Once the set of experiments was designed, they were carried out in duplicate as described in Chapter 4 of this PhD thesis. In Table 5.7 the results of the experiments (wt% total mass, and elemental leaching) are shown along with the calculated mass balance error (MBe) from liquid and solid analysis.

**Table 5.7.-** Results of the Taguchi experiments

| Test | [$H_2SO_4$] | T | S/L | t | % $mass_{leach}$ | $F_{leach}$ | $F_{MBe}$ | $Al_{leach}$ | $Al_{MBe}$ | $Ca_{leach}$ | $Ca_{MBe}$ | $Mg_{leach}$ | $Mg_{MBe}$ | $Fe_{leach}$ | $Fe_{MBe}$ | $Si_{leach}$ | $Si_{MBe}$ | $Na_{leach}$ | $Na_{MBe}$ | $K_{leach}$ | $K_{MBe}$ |
|---|---|---|---|---|---|---|---|---|---|---|---|---|---|---|---|---|---|---|---|---|---|
| 1 | 0.5 | 25 | 250 | 90 | 9.2 | 24.7 | 8.1 | 5.9 | 3.3 | 25.7 | 14.3 | 15.9 | 22.1 | 50.3 | 24.1 | 27.4 | 5.6 | 68.5 | 19.1 | 63.8 | 11.2 |
| | | | | | 9.2 | 22.7 | 14.7 | 5.8 | 3.6 | 23.2 | 16.9 | 13.2 | 31.4 | 55.0 | 12.1 | 27.3 | 9.6 | 73.4 | 5.8 | 62.2 | 3.6 |
| 2 | 0.5 | 50 | | | 10.0 | 38.9 | 10.4 | 6.2 | 3.1 | 28.2 | 18.2 | 16.2 | 23.0 | 56.9 | 21.1 | 13.2 | 11.9 | 69.7 | 9.5 | 65.5 | 10.5 |
| | | | | | 11.8 | 38.7 | 10.0 | 6.0 | 0.6 | 24.3 | 2.9 | 23.2 | 20.1 | 59.3 | 8.3 | 20.5 | 3.8 | 60.7 | 21.2 | 52.2 | 3.7 |
| 3 | 0.5 | 100 | | | 2.6 | 23.3 | 10.0 | 2.9 | 0.4 | 26.8 | 5.9 | 23.1 | 14.3 | 65.9 | 18.0 | 5.5 | 2.5 | 26.8 | 1.9 | 1.3 | 7.2 |
| | | | | | 1.0 | 21.2 | 6.9 | 2.4 | 1.4 | 22.8 | 0.7 | 23.5 | 20.5 | 66.3 | 16.3 | 8.9 | 3.5 | 50.2 | 23.7 | 68.4 | 67.4 |
| 4 | 1.5 | 25 | | | 19.8 | 31.2 | 4.3 | 14.2 | 5.1 | 25.8 | 8.5 | 22.2 | 17.2 | 76.7 | 14.0 | 28.9 | 0.4 | 67.7 | 4.4 | 58.3 | 1.8 |
| | | | | | 18.6 | 28.8 | 5.0 | 12.7 | 0.2 | 21.6 | 0.9 | 21.7 | 27.5 | 76.3 | 8.9 | 28.0 | 5.7 | 67.7 | 14.2 | 53.6 | 2.1 |
| 5 | 1.5 | 50 | | | 26.6 | 41.1 | 18.0 | 21.1 | 6.0 | 29.0 | 9.8 | 22.6 | 19.5 | 79.3 | 20.8 | 29.9 | 6.3 | 69.1 | 1.6 | 60.3 | 3.0 |
| | | | | | 27.6 | 35.6 | 17.6 | 21.3 | 3.3 | 20.8 | 12.2 | 26.4 | 23.6 | 82.1 | 6.0 | 27.9 | 0.9 | 68.2 | 1.3 | 49.5 | 9.6 |
| 6 | 1.5 | 100 | | | 23.6 | 48.0 | 13.1 | 24.3 | 8.4 | 29.4 | 1.5 | 27.1 | 16.0 | 83.0 | 19.3 | 4.8 | 3.8 | 13.6 | 21.7 | 1.2 | 5.8 |
| | | | | | 25.2 | 53.4 | 1.3 | 27.3 | 1.2 | 26.4 | 1.6 | 29.1 | 25.9 | 84.0 | 11.8 | 4.3 | 7.6 | 27.6 | 8.9 | 0.0 | 2.4 |
| 7 | 2.5 | 25 | | | 23.2 | 29.2 | 0.3 | 17.5 | 6.5 | 17.4 | 6.6 | 19.2 | 21.3 | 79.0 | 6.4 | 21.5 | 15.4 | 62.7 | 3.2 | 52.7 | 7.3 |
| | | | | | 21.8 | 33.7 | 5.9 | 15.5 | 0.6 | 13.2 | 8.6 | 26.9 | 30.5 | 75.9 | 16.4 | 23.7 | 3.6 | 68.8 | 14.7 | 51.0 | 1.4 |
| 8 | 2.5 | 50 | | | 35.2 | 40.6 | 3.4 | 29.8 | 6.5 | 21.4 | 3.7 | 25.5 | 18.2 | 81.7 | 11.7 | 24.2 | 0.6 | 66.2 | 0.5 | 54.8 | 4.3 |
| | | | | | 35.0 | 38.0 | 4.6 | 29.3 | 8.0 | 19.2 | 9.5 | 23.7 | 24.3 | 83.3 | 4.6 | 19.9 | 17.0 | 59.8 | 10.4 | 41.6 | 23.1 |
| 9 | 2.5 | 100 | | | 45.6 | 37.3 | 44.2 | 59.7 | 7.6 | 19.8 | 7.9 | 29.4 | 24.5 | 86.5 | 0.1 | 19.5 | 12.4 | 59.2 | 10.4 | 42.8 | 24.1 |
| | | | | | 47.6 | 39.0 | 37.5 | 60.7 | 6.8 | 17.1 | 0.7 | 32.5 | 15.7 | 86.6 | 10.1 | 22.3 | 3.5 | 65.1 | 2.0 | 55.0 | 9.7 |

As described in Chapter 4, ANOVA provides the relative contributions of the factors (P) considered in the design of experioments and an error contribution from relevant and omited factors or random variations or errors.[21] If the relative contribution of the error was equal or higher than other relative contributions, it could mean that at least one significant factor was not considered in the DOE. Therefore, it is interesting to confirm the relevance and completeness of the selected factors through variance analysis before selecting the optimum set of conditions, as an incomplete or erroneous parameter selection would produce misleading results.

As the main objective of this PhD thesis is to selectively leach fluoride while maintanining aluminum leaching at minimum, ANOVA was applied to the results twice: first to study fluoride leaching (target 100 %), and then to study aluminum leaching (target 0 %). In Table 5.8 and Figure 5.9 F and Al leaching ANOVA table and factor percent contribution are shown.

**Table 5.8.-** ANOVA table for F and Al leaching

| | | **F leaching** | | | | | **Al leaching** | | | | |
|---|---|---|---|---|---|---|---|---|---|---|---|
| Factors | f | S | V | F | S' | **P** | S | V | F | S' | **P** |
| [$H_2SO_4$] | 2 | 917.3 | 458.6 | 64.2 | 458.6 | **40.9** | 2809.5 | 1404.7 | 1510.4 | 1404.7 | **49.9** |
| Temperature | 2 | 440.8 | 220.4 | 30.8 | 220.4 | **19.7** | 943.2 | 471.6 | 507.1 | 471.6 | **16.8** |
| Interaction | 4 | 512.6 | 128.1 | 17.9 | 384.4 | **34.3** | 1238.8 | 309.7 | 333.0 | 929.1 | **33.0** |
| error | 9 | 64.3 | 7.1 | 1.0 | 57.2 | **5.1** | 8.4 | 0.9 | 1.0 | 7.4 | **0.3** |
| Totals | 17 | 1935.0 | | | 1120.6 | 100.0 | 4999.9 | | | 2812.9 | 100.0 |

*f = degrees of freedom; S = sum of squares; V = mean squares; F= variance ratio;
S' = pure sum of squares; P = percent contribution

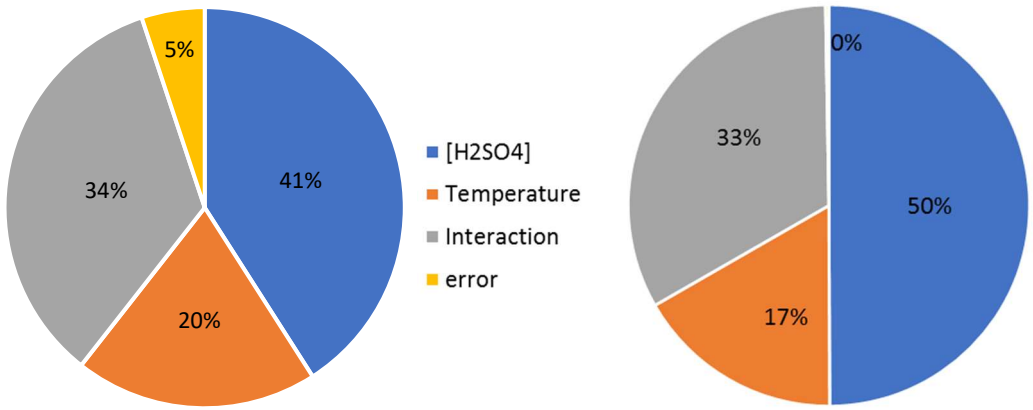


**Figure 5.9.-** Factor percent contribution to F leaching (left) and Al leaching (right)

The selected factors contributed to nearly 95 % to the fluoride leaching variance, whereas the remaining 5 % variation was caused by the experimental error and other factors not included in the study. In the analysis of Al leaching, the percent contribution of the error was nearly 0 %. Also, it sould be noticed that if the interaction was not considered in the ANOVA analysis, its percent contribution was practically added to the error percent contribution in both cases, rising from 5.1 to 55 % in the analysis for F leaching, and from 0.3 to 38 % in the analysis for Al leaching. Therefore, it was concluded that the selected factors ($H_2SO_4$ concentration, temperature and their interaction) were the main variables affecting both fluoride and aluminum leaching.

Once the results reliability was set, the optimum conditions were selected considering both main effects and interactions. The results were analyzed twice, first for F leaching, in which the criterium was *the bigger the better* and second for Al leaching, in which the criteria was *the smaller the better* instead.

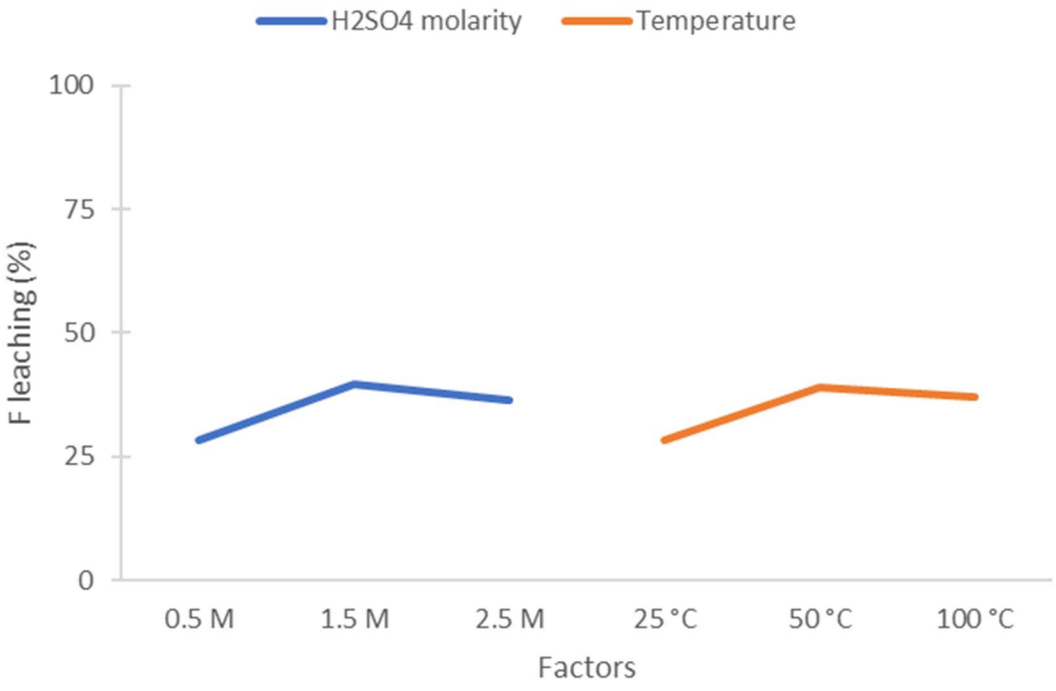


**Figure 5.10.a.-** Main effects for F leachig

Regarding the main effects for F leaching, the optimum values would be 1.5 M and 50 °C as the criteria was *the bigger the better*.

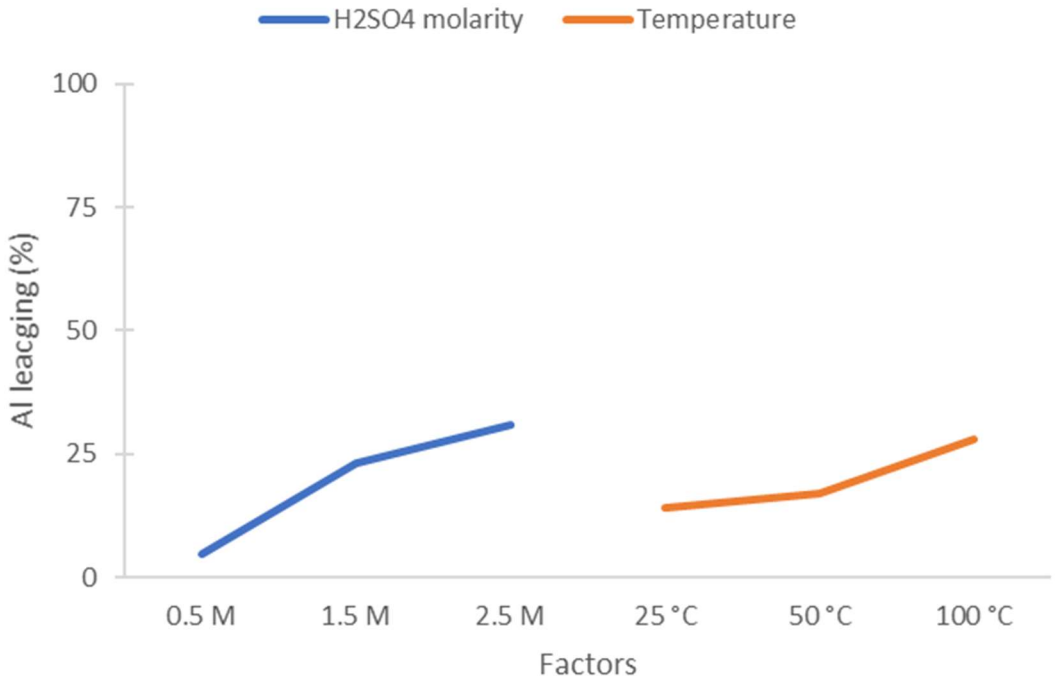


**Figure 5.10.b.-** Main effects for Al leaching

Regarding the main effects for Al leaching, the optimum values would be 0.5 M and 25 °C as the criteria was *the smaller the better*.

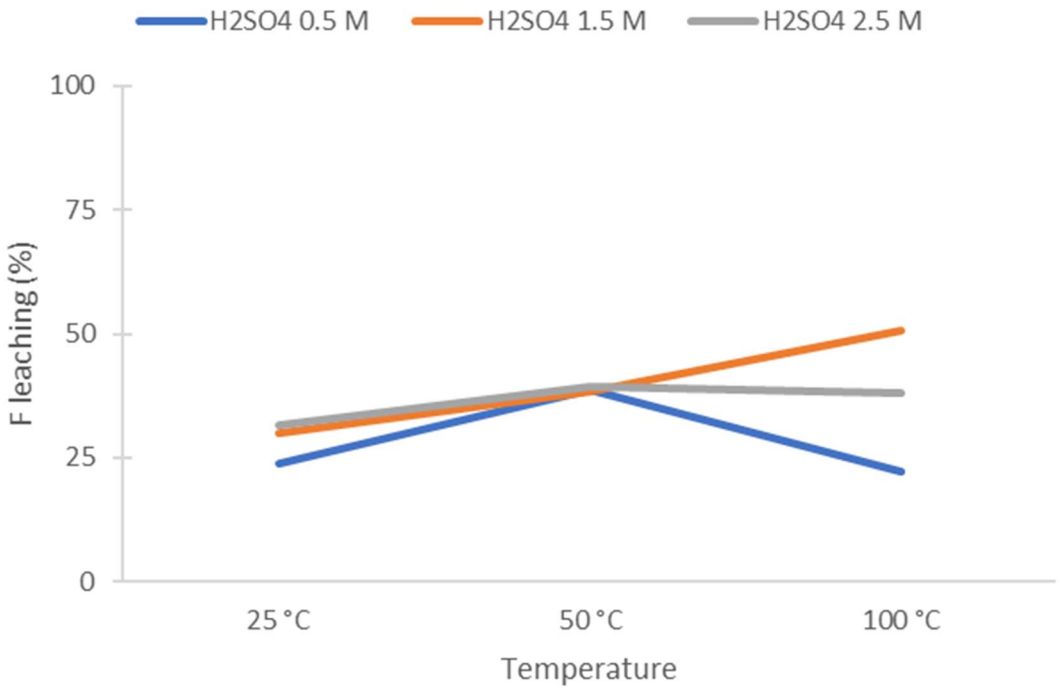


**Figure 5.11.a.-** Interaction [$H_2SO_4$] x Temperature for F leaching

Regarding the interaction between $H_2SO_4$ molarity and temperature, the optimum values for F leaching would be 1.5 M and 100 °C as the criterium was *the bigger the better*.

It is interesting that when employing 0.5 M $H_2SO_4$, if the temperature is increased from 50 to 100 °C, F leaching decreases. This fluoride behaviour was also reported by Lisbona et al, where, at similar pH conditions, F extraction from salt cake reached a maximum between 50 and 60 °C and then decreased at 90 °C.[17]

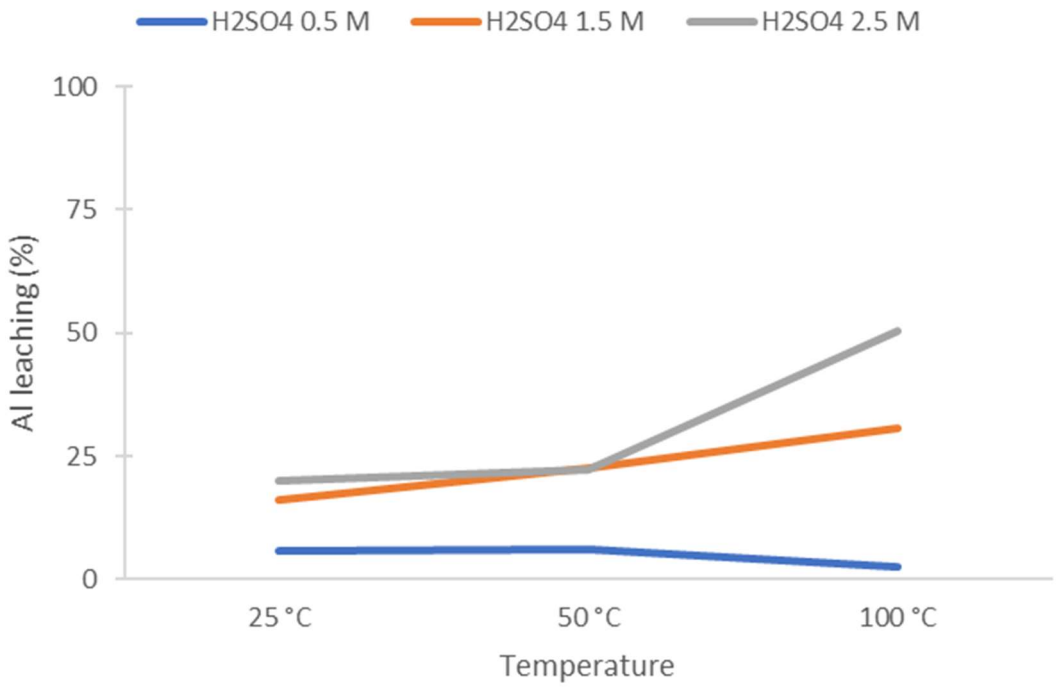


**Figure 5.11.b.-** Interaction [$H_2SO_4$] x Temperature for Al leaching

Regarding the interaction between $H_2SO_4$ molarity and temperature, the optimum values for Al leaching with *the smaller the better* criterium would be 0.5 M and any of the tested temperatures since there is no significant differences between them. In Table 5.9 the conclusions from Figures 5.10 and 5.11 are summarized:

**Table 5.9.-** Bests sets of conditions for F and Al leaching

| | Temperature (°C) | [$H_2SO_4$] (mol/L) |
|---|---|---|
| | Main effects | |
| F leaching | 50 | 1.5 |
| Al leaching | 25 | 0.5 |
| | Interaction | |
| F leaching | 100 | 1.5 |
| Al leaching | 25/50/100 | 0.5 |

The conditions that resulted in higher F leaching also resulted in higher Al leaching due to the high stability of $AlF_x$ complexes.[22–24] Therefore, the optimum conditions to achieve maximum F leaching were practically opposite to the conditions to obtain the

minimum Al leaching. Since a compromise is needed to achieve this PhD thesis scope, the criteria could not only be the ones derived from the Taguchi/ANOVA. The results shown in Table 5.8 are graphically represented in Figures 5.12.a and 5.12.b for an easier visualization and comparison.

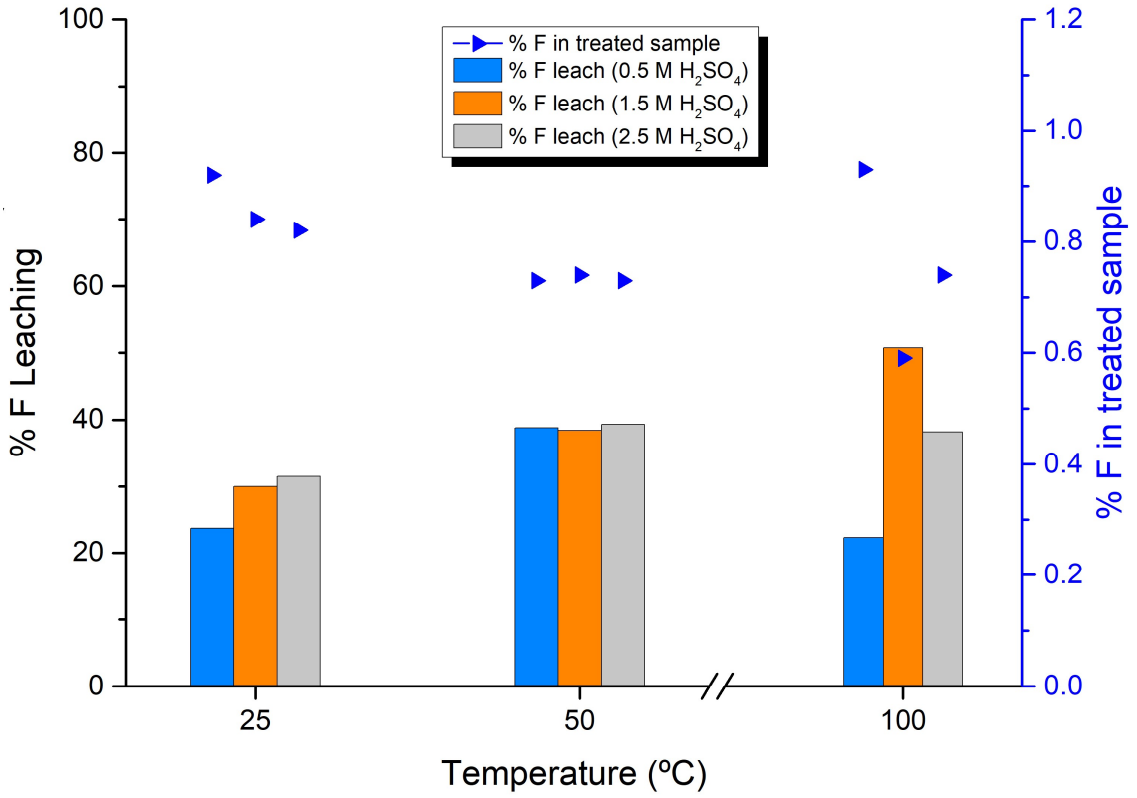


**Figure 5.12.a.-** F leaching results (%) (left axis) and F content (%) in leached sample (right axis). Right axis scale from 0 to 1.2 wt% F (original sample F content)

All the tested conditions leached sufficient fluoride to achieve a final fluoride content below 1 wt%. The set of conditions that resulted in the highest F leaching (50.7 %) were 100 °C and 1.5 M $H_2SO_4$, which also led to the third highest Al leaching (25.8 %). The second highest F leaching (39 %) was obtained at 50 °C and all of the tested molarities, and at 100 °C and 2.5 M. Although there was not a significant difference in F leaching between the mentioned conditions, Al leaching sharply increased when the temperature was increased from 50 to 100 °C (29.6 to 60.2 %), and when $H_2SO_4$ concentration was increased at 50 °C, from 6 % at 0.5 M to 30 % at 2.5 M.

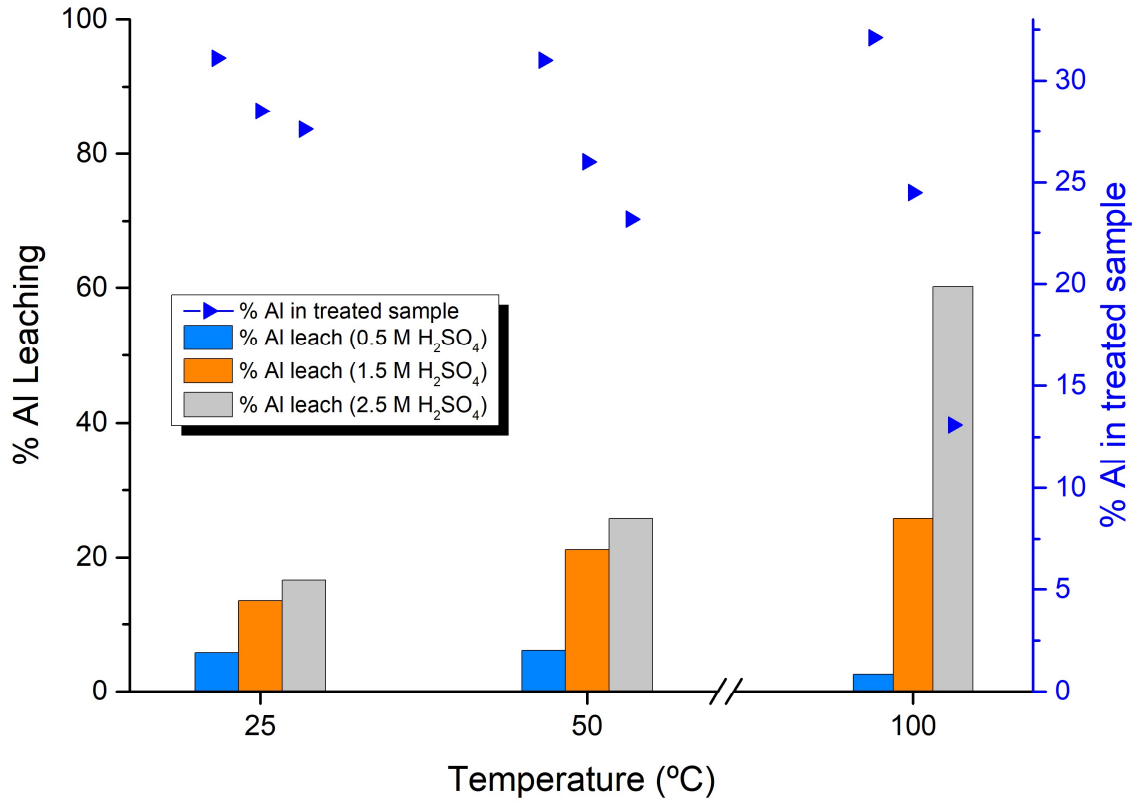


**Figure 5.12.b.-** Al leaching results (%) (left axis) and Al content (%) in leached sample (right axis). Right axis scale from 0 to 33.0 wt% Al (original sample Al content)

Taking into account all of the above, the selected conditions were 50 °C and 0.5 M. Once the process conditions were selected, the leaching evolution with time was studied in a series of experiments (Table 5.10) using the same sample as in the Taguchi experiments (SPC01). Each experiment was carried out twice to ensure repeatability, and reaction time was set to 0 when temperature reached 50 °C. Typically heating phase (15 – 20 min) was not considered in the reaction time.

**Table 5.10.-** Set of experiments to reduce reaction time

| Test | [$H_2SO_4$] (mol/L) | T (°C) | S/L (g/L) | t (min) |
|---|---|---|---|---|
| 1 | 0.5 | 50 | 250 | 90 |
| 2 | | | | 60 |
| 3 | | | | 30 |
| 4 | | | | 10 |

The results of this set of experiments are shown in Table 5.11 along with the mass balance error of each element and in Figures 5.13 and 5.14. In Figure 5.13 the leaching results of the studied elements (F, Al) *vs* reaction time is represented along with pH. As the leaching process is driven by the acid, it was hypothesized that the pH and leaching would

evolve symilarly. As it can be observed in Figure 5.13, the pH and fluoride extraction show analogous profiles. which could be highly convenient for industrial applications as the pH measurement is much easier than that of fluoride, and it could be carried out on-line. Thus, pH could be industrially used to determine the moment when the F leaching reaction reaches a plateau.

**Table 5.11.-** % leaching and mass balance error for time optimization tests

| | 10 min | 30 min | 60 min | 90 min |
|---|---|---|---|---|
| % $mass_{leach}$ | 12.6 | 13.2 | 12.0 | 13.6 |
| **$F_{leach}$** | 25.7 | 39.2 | 45.0 | 48.2 |
| $F_{MBe}$ | 1.4 | 5.5 | 9.9 | 10.6 |
| **$Al_{leach}$** | 7.1 | 9.8 | 6.2 | 7.6 |
| $Al_{MBe}$ | 1.5 | 4.0 | 0.4 | 1.2 |
| **$Ca_{leach}$** | 42.2 | 41.9 | 33.7 | 39.5 |
| $Ca_{MBe}$ | 19.5 | 22.8 | 14.2 | 20.1 |
| **$Mg_{leach}$** | 23.4 | 26.6 | 24.6 | 26.9 |
| $Mg_{MBe}$ | 5.0 | 7.2 | 11.4 | 10.4 |
| **$Fe_{leach}$** | 53.0 | 56.6 | 58.2 | 53.6 |
| $Fe_{MBe}$ | 9.1 | 1.7 | 1.7 | 10.5 |
| **$Si_{leach}$** | 29.8 | 23.1 | 18.3 | 23.2 |
| $Si_{MBe}$ | 6.4 | 0.3 | 3.2 | 2.4 |
| **$Na_{leach}$** | 52.8 | 54.9 | 56.0 | 62.0 |
| $Na_{MBe}$ | 12.7 | 11.9 | 14.6 | 11.8 |
| **$K_{leach}$** | 58.5 | 58.8 | 58.2 | 59.0 |
| $K_{MBe}$ | 2.9 | 2.4 | 0.5 | 3.3 |

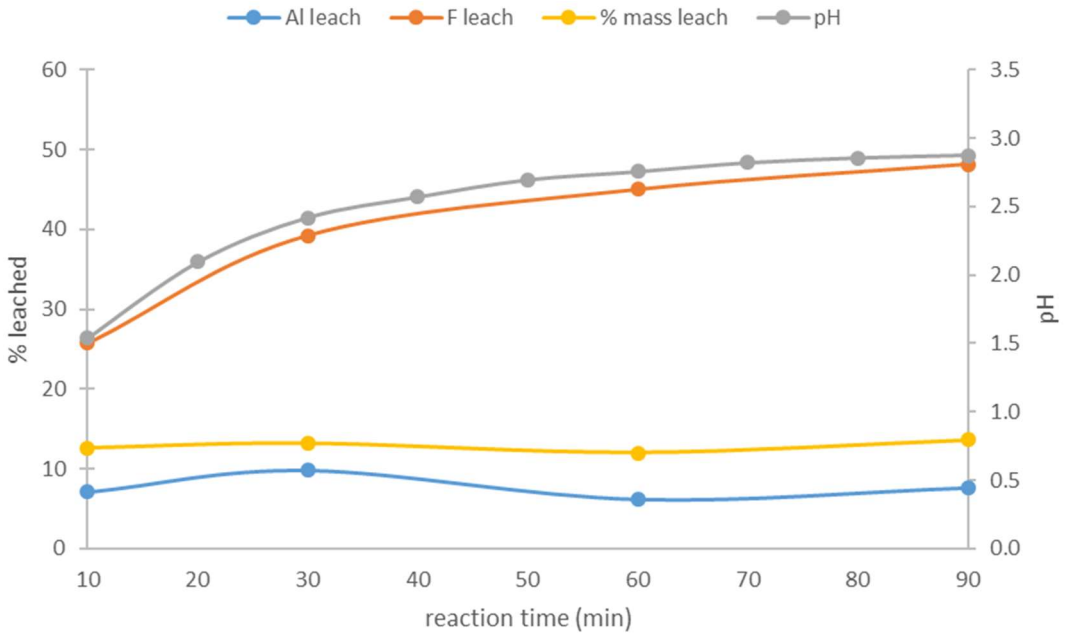


**Figure 5.13.-** Leaching of F and Al, and pH vs reaction time

According to the data, 90 % of total leaching would be accomplished at 49 min, and 95 % at 66 min. Thus, reaction time could be reduced in up to 45 % without losing a significant amount of F leaching.

In Figure 5.14 the leaching of the rest of Paval components is shown. Si appeared to precipitate for reaction times above 30 minutes, which could be attributed to the decreasing solubility of Quartz (Figure 5.16 and Table 5.12) as the solution pH increased.[25]

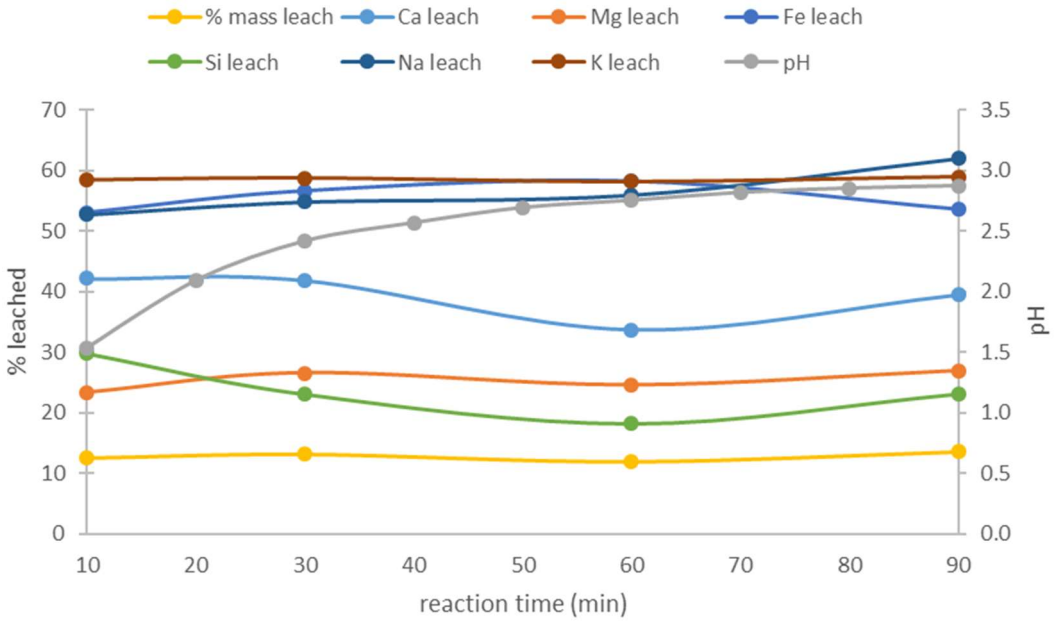


**Figure 5.14.-** Leaching of Ca, Fe, Mg, Si, Na, and K, and pH vs reaction time

In order to further understand the process, X-Ray Diffraction (XRD) and X-Ray Fluorescence (XRF) analyses were performed on the solid samples obtained from this last set of experiments (original SCP01 and treated for different amounts of time). In Figure 5.15 the diffraction profile of the original sample is presented and, in Figure 5.16, all diffractograms are overlapped.

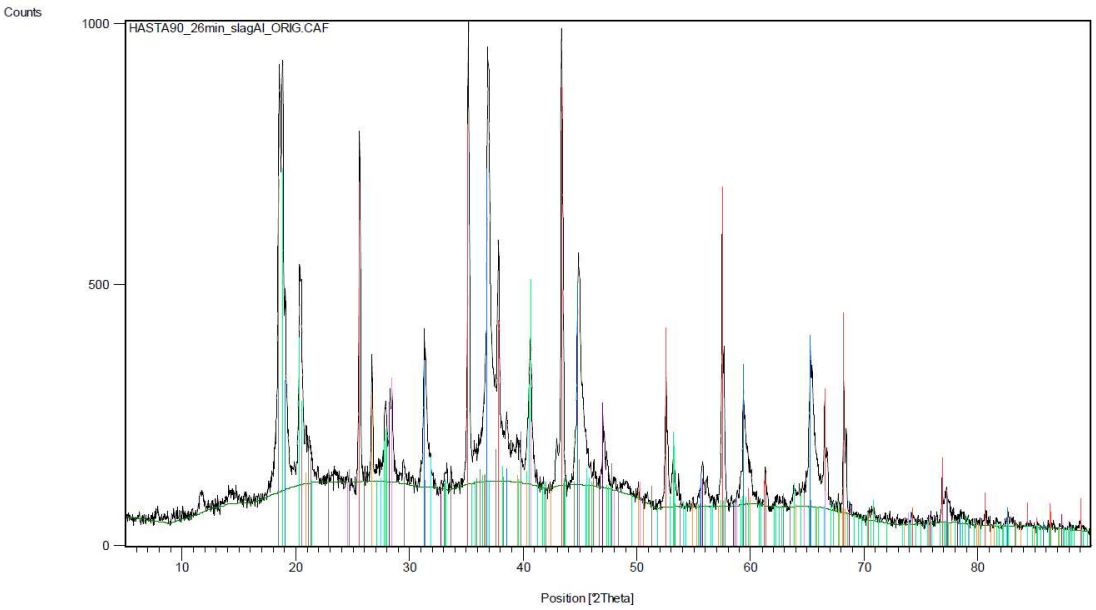


**Figure 5.15.-** XRD diffractogram of the original sample

Several phases were identified by XRD in the original sample. As the most abundant element in the sample was aluminum, Gibbsite ($Al(OH)_3$, lines in color green), Corundum ($\alpha$-$Al_2O_3$, lines in color red), and Magnesium Spinel ($MgAl_2O_4$, lines in color blue) were the most prominent phases. Although the signals of minor phases were partially covered by aluminum phases signals, it was possible to identify Quartz ($SiO_2$, lines in color orange), Fluorite ($CaF_2$, lines in color purple) as the only fluoride phase present in the sample, Halite (NaCl, lines in color light blue), and Sylvite (KCl, lines in color pink). In the untreated SCP01 sample Periclase (MgO) was also identified in 43° 2θ position.

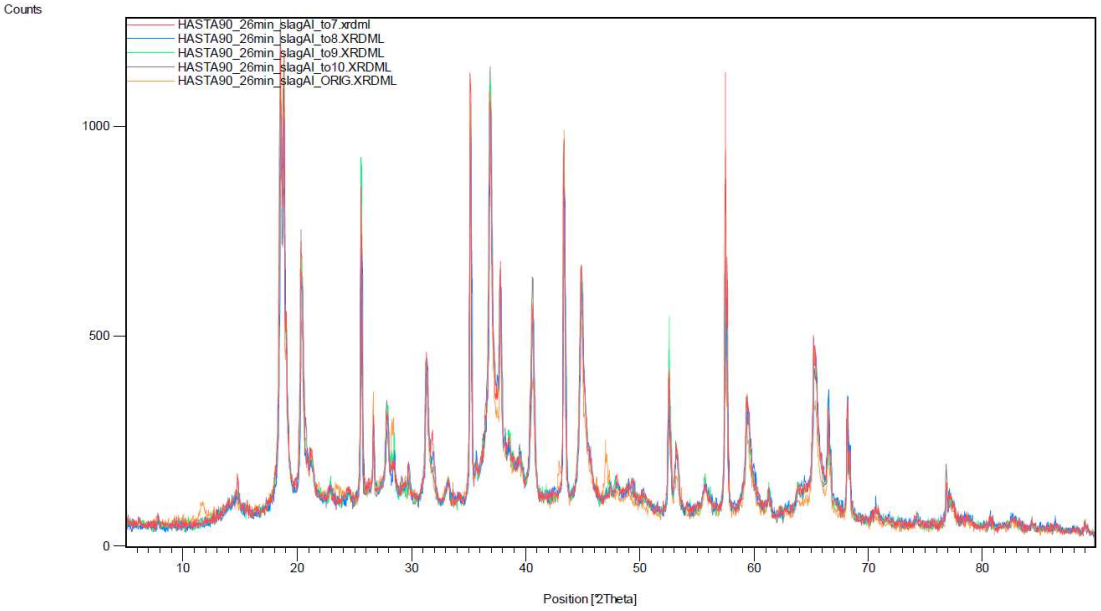


**Figure 5.16.-** All XRD superposed diffractograms

The same phases were identified in original and treated samples, and the leaching only affected the proportion of each phase in the samples. Due to the unique combination of phases present in the sample, by combining XRF and XRD analysis 95 % of the material phase composition could be deduced. In Figure 5.17 phase quantification in wt% of the original sample and sample treated for 60 min are represented. No MgO was detected in any of the treated samples, therefore it was leached by 0.5 M $H_2SO_4$ in less than 10 min at 50 °C, in good agreement with reported kinetic behavior of MgO dissolution in $H_2SO_4$.[26]

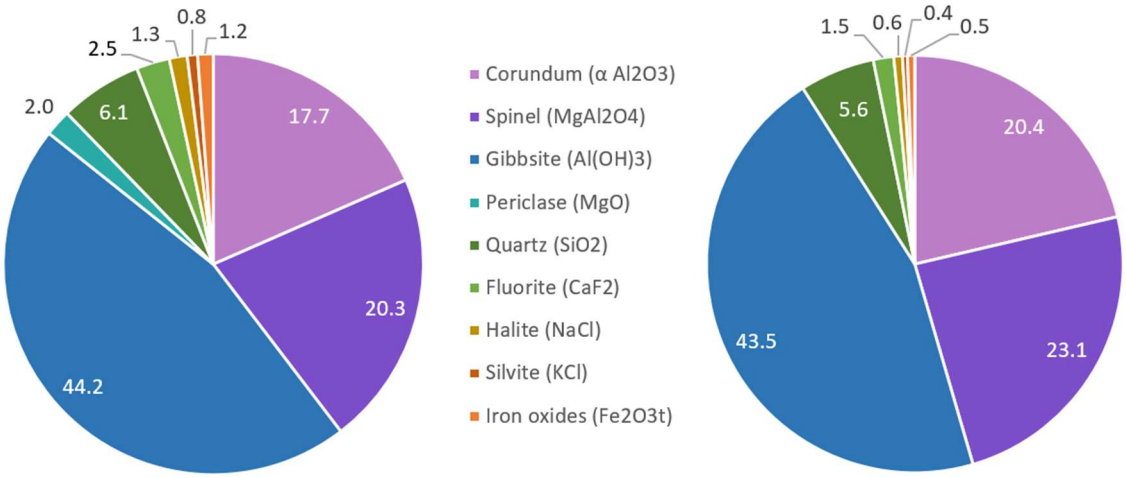


**Figure 5.17.-** Phase composition of original and treated SCP01

In Figure 5.18, the contribution of each phase to the leached material (12.0 %) with 0.5 M $H_2SO_4$, 50 °C, S/L 250 g/L, and 60 min reaction time is represented.

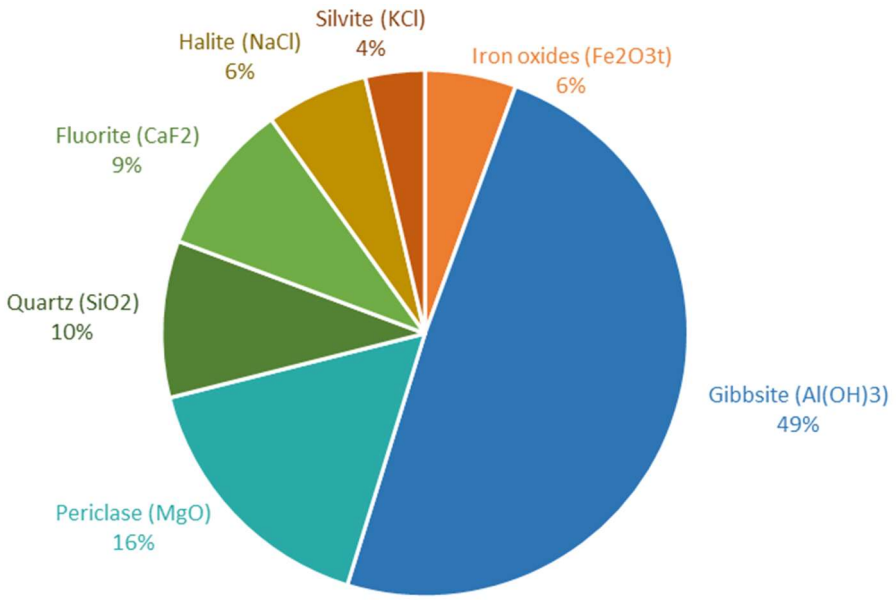


**Figure 5.18.-** Phase contribution to the leached material

Half of the leached material was $Al(OH)_3$, the most soluble aluminum phase present in Paval. This is thought to be the reason for the high velocity of Al leaching reaction (as observed in Figure 5.13 Al leaching reaches equilibrium in 10 minutes). 16 % of the leached material was MgO, and no $MgAl_2O_4$ was leached. $SiO_2$ was also leached and contributed to 10 % of the leached material, similarly to $CaF_2$ (9 %). Quartz leaching was possible due to the combination of highly acidic pH and the presence of fluoride in the solution. The remaining 16 % was accounted by NaCl (6 %), KCl (4 %), and $Fe_2O_3$ (6 %).

The obtained results can be extrapolated to other salt cake Paval samples. Salt Cake Paval is Befesa's main product, although they offer other types of Paval with different specifications, including F content, as a result of SPL additions. Therefore, the developed process was used to treat Paval samples with increasing amounts of SPL to study the sensitivity of the process to F content and determine the maximum value to guarantee a final product with a F content below 1 wt%.

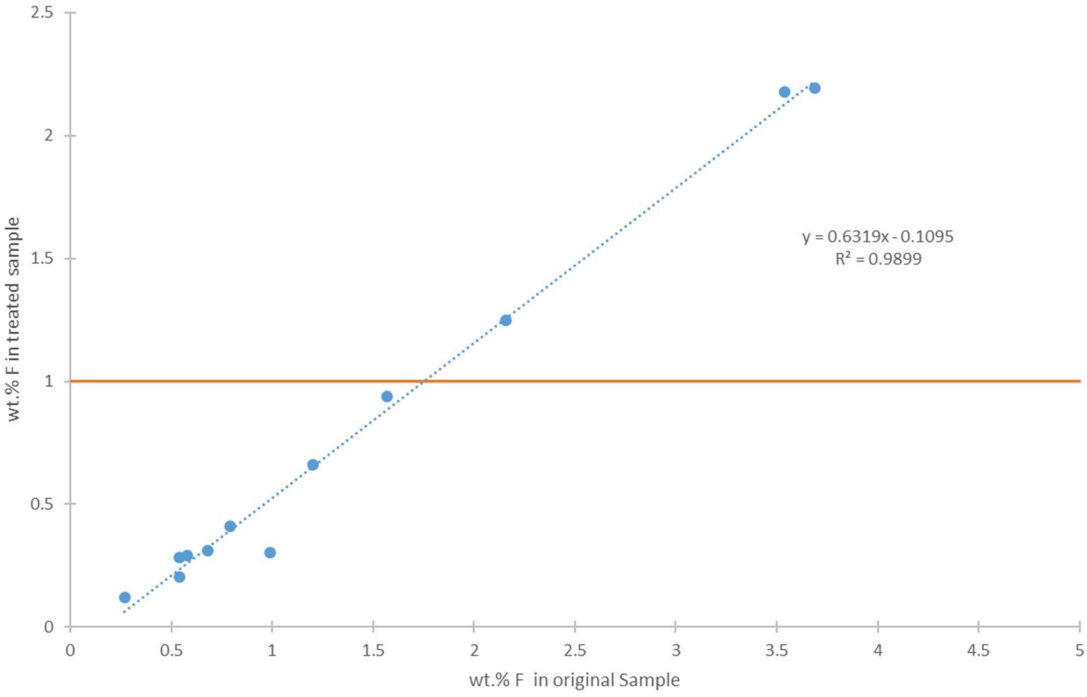


**Figure 5.19.-** Results of the treatment in samples with different fluoride content

From the tendency line obtained from the point cloud, Paval of similar characteristics containing up to 1.6 wt% F could be treated with this process to obtain a treated material containing less than 1.0 wt% F. If the phases present in the material were

significantly different the validity of the developed process should be carefully re-evaluated as the results are expected to be strongly dependent on the material phase composition.

The main objective of this PhD thesis, to reduce F content below 1 wt% in order to manufacture Bauxite based refractories, was achieved. Moreover, according to the elemental (XRF) and phase (XRD) composition analysis, Salt Cake Paval shares many similarities with Bauxite, the main source of Al. Therefore, the suitability of treated Paval as an alternative to Bauxite was studied.

## 5.4. Treated Paval as an alternative to Bauxite

Bauxite deposits are known to occur in at least 50 countries, with estimated world reserves of approximately 25 billion tonnes; and four countries (Australia, Guinea, Jamaica, and Brazil) account for 68 % of the world production. The current Bauxite reserve life index (ratio of known world reserves to the annual production in the same year) indicates adequate bauxite supply for about 180 years and is the same as it was in 1950. However, considering a 5 % annual growth rate, the currently known reserves will be exhausted within the next 20 years. Furthermore, it is important to note that mineral deposits may occur in regions with unfavorable economic or political conditions and new mineral deposit exploitation would require the construction of new production infrastructures and investments in transportation to the consuming locations. These facts make uncertain the future Bauxite availability and pricing, and thus it is interesting to explore alternative raw materials to substitute it.[1,27,28]

Approximately 85 – 90 % of the world Bauxite production is converted to alumina by the Bayer process for aluminum metal production, 10 % is utilized for nonmetal products, and the remaining 5 % for nonmetallurgical applications such as refractory, abrasive, and chemical industries.[27,28] As alumina production is the principal application of Bauxite, the use of treated Paval as feed for Bayer process would be highly promising. The Bayer process involves the digestion of crushed Bauxite in concentrated NaOH (3 – 7 M) at high temperatures (100 – 270 °C). The severity of the digestion depends on the aluminum form, being Gibbsite the most soluble phase, and on the present impurities . Once all available alumina is dissolved, the liquid is separated from an insoluble residue

known as red mud that contains the non soluble Bauxite components. Then, $Al(OH)_3$ is precipitated, washed and calcinated to obtain alumina.[28–30]

The digestion step is key to the process efficiency and thus, Bauxite purity is critical. Bauxite contains, in addition to hydrated alumina (in form of Gibbsite, Boehmite, and/or Diaspore), gangue minerals that have a negative effect on the process, as they increase the energy, caustic soda and flocculants required for the process.[1,27] Paval was already a good alternative, as a number of gangue compounds typically found in Bauxite ores, such as silicoaluminates, oxalates, sulfates, thiosulfates, and organic carbon, are not present in the Paval. Nonetheless, Paval still contains some gangue materials usually present in Bauxite such as iron oxides, quartz, chlorides and fluorides.[31] Luckily, they are either partially or totally leached in the process, making treated Paval a better feedstock than Bauxite for the Bayer process. Regarding the alumina content, it should be noted that many Bauxite ores are of poor quality (<40 % available alumina)[29] and while treated Salt Cake Paval contains aproximately 28 % of available alumina, it could be a good alternative to Bauxite in Europe due to its availability and local production.

## 5.5. Conclusions

The process to selectively leach fluoride from Salt Cake Paval was studied using the Design of Experiments methodology and discussed in this chapter.

Based on literature, the main variables for the fluoride leaching process are: the leaching agent (acid, base, and $Al^{+3}$) and its concentration, the reaction temperature, the solid to liquid ratio (S/L), the particle size and the contact time. The particle size was set below 1.00 mm, according to literature, to maximize exposure to the leaching media, and the S/L to 250 g/L as it was the most concentrated slurry which guarantees sufficient solid-liquid contact. Leaching time was set to 90 min to avoid kinetic limitations.

A preliminary leaching conditions screening showed that sufficient Al was leached from the raw material to ensure an efficient F removal. The leaching agents cited in the literature were tested and $H_2SO_4$ was selected as the most promising one as it showed high F removal selectivity and the possibility for F and Al leaching optimization.

A second screening was used to define the main variables affecting the leaching process, leading to a Design of Experiments focused on the 0.5-2.5 M $H_2SO_4$ concentration

and 25-100 °C temperature ranges. The ANOVA analysis of the results showed that reaction temperature, $H_2SO_4$ concentration and their interaction contributed to 95-100 % of the results variance, and the selected leaching conditions were 50 °C and 0.5 M. The reaction time study showed that it could be reduced from 90 to 59 min without losing a significant amount of F leaching. This process robustness was tested for other materials with higher F content and was valid for materials of similar characteristics containing up to 1.6 wt% F.

According to XRF and XRD results, Salt Cake Paval and Bauxite share many similarities in their elemental and phase compositions. As Bauxite availability and pricing is uncertain, treated Salt Cake Paval, with aproximately 28 % available alumina, and less impurities than untreated Paval could be a good alternative to Bauxite in Europe.

With the development of this process, the first objective of this PhD thesis was achieved. The hydrometallurgical treatment, however, produces a liquid residue, whose average composition is presented in Table 5.12. As it can be observed, sulfate ions are the main effluent component. They are one magnitude order higher that the $Cl^-$, Al, Mg, Fe and Na ions, and two orders of magnitude than that of $F^-$, Ca, Si, and K.

**Table 5.12 .-** Average composition (mg/L) of the liquid residue

| $SO_4^=$ | $Cl^-$ | $F^-$ | Al | Mg | Na | Fe | Ca | Si | K |
|---|---|---|---|---|---|---|---|---|---|
| 42200 | 876 | 1450 | 4475 | 3254 | 2031 | 1025 | 440 | 423 | 480 |

The most environmentally and economically friendly outcome for the effluent would be to be recycled into the hydrometallurgical process with minimal treatment. The recycling of the effluent with no prior treatment would translate into circuit problems due to the scaling nature of the effluent. In the next chapters, the purification and reutilization of this effluent will be studied in order to provide an integrated process with the minimum residue output.

## 5.6. Appendix

**Table 5.A.1.-** Sample elemental composition (wt%)

| | F | Al | Si | Fe | Ca | Mg | Na | K |
|---|---|---|---|---|---|---|---|---|
| SCP01 | 1.20 | 33.0 | 1.1 | 4.5 | 0.8 | 2.9 | 0.5 | 0.4 |
| SCP04 | 1.25 | 45.0 | 2.9 | 1.4 | 1.2 | 5.0 | 0.7 | 0.2 |
| SCP05 | 1.57 | 39.6 | 5.7 | 1.8 | 1.5 | 5.1 | 1.0 | 0.9 |
| SCP06 | 0.68 | 40.7 | 5.5 | 2.5 | 2.0 | 4.7 | 1.2 | 0.9 |
| SCP07 | 0.54 | 40.2 | 3.6 | 1.8 | 1.8 | 4.7 | 1.36 | 1.3 |
| SCP08 | 0.27 | 37.6 | 2.6 | 1.1 | 1.3 | 4.5 | 1.4 | 0.9 |
| SCP11 | 0.57 | 25.9 | 2.7 | 1.7 | 0.8 | 2.8 | 7.5 | 6.7 |
| MP01 | 2.16 | 36.9 | 3.3 | 1.4 | 1.0 | 4.6 | 1.2 | 0.5 |
| MP02 | 3.69 | 33.1 | 5.8 | 1.9 | 2.0 | 3.5 | 2.1 | 0.3 |
| MP03 | 3.54 | 34.5 | 5.5 | 1.7 | 1.8 | 3.6 | 1.8 | 0.3 |
| MP04 | 6.29 | 29.0 | 8.5 | 2.2 | 0.9 | 1.7 | 3.6 | 0.6 |
| SPLP01 | 15.3 | 21.1 | 15.8 | 3.2 | 2.1 | 0.0 | 12.8 | 0.8 |
| SPLP02 | 19.1 | 35.0 | 9.1 | 1.2 | 1.4 | 0.0 | 5.7 | 0.0 |

## 5.7. References


[1] M. Davies, P. Smith, W. J. Bruckard, J. T. Woodcock, *Miner. Eng.* **2008**, *21*, 605–612.
[2] W. J. Bruckard, J. T. Woodcock, **2007**, *20*, 1376–1390.
[3] J. F. Bush, *Reclaiming Spent Potlining*, **1989**, 4,889,695.
[4] G. C. Holywell, M. Kimmerle, R. T. Gilles, R. J. Grolman, *Recycling of Spent Pot Linings*, **1995**, 5,470,559.
[5] Z. N. Shi, W. Li, X. W. Hu, B. J. Ren, B. L. Gao, Z. W. Wang, *Trans. Nonferrous Met. Soc. China (English Ed.* **2012**, *22*, 222–227.
[6] Y. Li, H. Zhang, Z. Zhang, L. Shao, P. He, *J. Environ. Sci. (China)* **2015**, *31*, 21–29.
[7] D. F. Lisbona, C. Somerfield, K. M. Steel, *Ind. Eng. Chem. Res.* **2012**, *51*, 8366–8377.
[8] D. F. Lisbona, C. Somerfield, K. M. Steel, *Ind. Eng. Chem. Res.* **2012**, *51*, 12712–12722.
[9] J. F. Bush, *Halogen Recovery*, **1986**, 4,597,953.
[10] D. H. Jenkins, *Recovery of Aluminium and Fluoride Values from Spent Pot Lining*, **1994**, 5,352,419.
[11] H. Kaaber, M. Mollgaard, *Process for Recovering Aluminium and Fluorine from Fluorine Containing Waste Materials*, **1996**, 5,558,847.
[12] G. F. Gaydoski, J. F. Bush, *Aluminum-Fluorine Compound Manufacture*, **1985**, 4,508,689.
[13] K. Jomoto, T. C. Hughes, *Method of Extracting Fluorine from Minerals or Mineral Species*, **2001**, WO 95/01460.
[14] C. Torrisi, *Miner. Eng.* **2001**, *14*, 1637–1648.
[15] N. Antuñano, J. F. Cambra, P. L. Arias, *Hydrometallurgy* **2016**, *161*, 65–70.
[16] D. F. Lisbona, K. M. Steel, *Sep. Purif. Technol.* **2008**, *61*, 182–192.
[17] D. F. Lisbona, C. Somerfield, K. M. Steel, *Hydrometallurgy* **2013**, *134–135*, 132–143.
[18] D. F. Lisbona, K. M. Steel, *Miner. Met. Mater. Soc.* **2007**.
[19] M. Li, X. Zhang, Z. Liu, Y. Hu, M. Wang, J. Liu, J. Yang, *Hydrometallurgy* **2013**, DOI 10.1016/j.hydromet.2013.09.004.
[20] T. K. Pong, R. J. Adrien, J. Besida, T. A. O 'donnell, D. G. Wood, *Inst. Chem. Eng.* **2000**, *78*, DOI 10.1205/095758200530646.
[21] A. Al-Refaie, M.-H. Li, *J. Simul.* **2010**, *18*, 143–148.
[22] R. Bruce Martin, *Coord. Chem. Rev.* **1996**, *141*, 23–32.
[23] R. P. Agarwal, E. C. Moreno, *Talanta* **1971**, *18*, 873–880.
[24] M. Rietjens, *Anal. Chim. Acta* **1998**, DOI 10.1016/S0003-2670(98)00176-7.
[25] K. G. Knauss, T. J. Wolery, *Geochim. Cosmochim. Acta* **1988**, *52*, 43–53.
[26] D. D. Macdonald, D. Owen, *Can. J. Chem.* **2011**, *49*, 3375–3380.
[27] F. M. Meyer, *Nat. Resour. Res.* **2004**, *13*, 161–172.
[28] M. Authier-Martin, G. Forté, S. Ostap, J. See, *JOM* **2001**, 3–7.
[29] A. R. Hind, S. K. Bhargava, S. C. Grocott, **1999**, *146*, 359–374.
[30] G. Stopa, A. Carlos, B. De Araújo, S. Prasad, L. Gonzaga, S. Vasconcelos, J. Jaílson, N. Alves, R. Pereira, *Miner. Eng.* **2009**, *22*, 1130–1136.
[31] M. Wellington, F. Valcin, *Ind. Eng. Chem. Res.* **2007**, *46*, 5094–5099.

# Chapter 6

## Sulfate removal methodologies: A review

# Table of contents

## 6.1. Introduction

The main concerns of the waste stream in hand for purification, similar to Acid Mine Drainage (AMD), are the low pH, high sulfate concentration and dissolved metal contents. Therefore, analogously to AMD treatment, *(i)* acid neutralization, *(ii)* sulfate removal and *(iii)* metal removal are required. Currently, AMD is internationally considered among the most serious environmental problems, and consequently, it is the focus of a number of research initiatives. Thus, in the following subsections process details for the stablished sulfate removal methods (listed in Table 6.1) from AMD are described and its suitability for the effluent assessed. When selecting an appropriate effluent treatment, the following parameters should be considered: *(i)* composition of the effluent, *(ii)* specifications of the treated effluent, *(iii)* available infrastructure and space, and *(iv)* waste generation to ensure that additional environmental problems are not generated.[1–7]

**Table 6.1.-** Sulfate removal processes

| Precipitation | Membranes | Ion Exchange and Adsorption | Biological mechanisms |
|---|---|---|---|
| Gypsum | Reverse Osmosis | Sulf-IX™/GYP-CIX | Bioreactors |
| Barite | Electrical Dialysis Reversal | GYP-CIX hybrid | Constructed Wetlands |
| Ettringite | Nanofiltration | Adsorption | Alkalinity Producing Systems |
| | | | Permeable Reactive Barriers |

The sulfate removal methods will be described in the order stated in Table 6.1, as precipitation is typically used as either pretreatment or complement for most of the other purification methods. In Appendix 6.1 the main characteristics of the most relevant methods are summarized. When comparing costs, it should be noted that the tables were elaborated in 2002, cost estimates are time sensitive and have not been updated to present day costs, and that the estimated costs strongly depend on the specific process design, local market and labor costs.[1]

## 6.2. Sulfate removal by precipitation

Sulfate removal by precipitation consists on a chemical reaction that produces one of the following insoluble sulfate phases: *(i)* gypsum ($CaSO_4 \cdot 2H_2O$, $K_{sp} \sim 10^{-4}$), *(ii)* barite ($BaSO_4$, $K_{sp} \sim 10^{-10}$) or *(iii)* ettringite ($Ca_6Al_2(SO_4)_3(OH)_{12} \cdot 31H_2O$, $K_{sp} \sim 10^{-45}$).[8–10] The methods described in this section are based on the addition of chemicals to produce either of these phases (or various) to reduce the dissolved sulfate concentration.

The preferred bulk sulfate removal method, known as the High Density Sludge process, is gypsum precipitation *via* lime ($Ca(OH)_2$) addition. It is the simplest and most widely known in the mining industry, due to its high sulfate removal capacity and low cost. Moreover, lime also removes metals effectively by metal hydroxides precipitation, and reduces fluoride content to levels as low as 4 ppm by $CaF_2$ precipitation.[1,3–5,7,8,11–14] As limestone ($CaCO_3$) naturally occurs in a relatively pure state, it is more economical than lime. Therefore, it has been widely researched as a lime substitute for sulfate removal, and its chemical and economical feasibility proven.[15–18] Capitalizing on this economic advantage, an integrated limestone/lime process, capable of reducing sulfate concentration to 1094 mg/L, was recently developed. This process, described in Figure 6.1, also removes magnesium, fluoride and other metals, and consists of three steps: *(i)* Neutralization by limestone addition to achieve pH 6-8, resulting in $CO_2$ production and gypsum precipitation (1h). In this step, fluoride, iron and aluminum are reported to precipitate down to trace levels in solution,[16,17] *(ii)* lime addition to raise the pH to 12 for further gypsum precipitation along with $Mg(OH)_2$ and other possible hydroxides (4 h). *(iii)* pH adjustment with $CO_2$ from the first step with concurrent pure limestone precipitation ($K_{sp} \sim 10^{-8.43}$), which can be recycled into the first step of the process (0.5 h).[1,10,12,15–19]

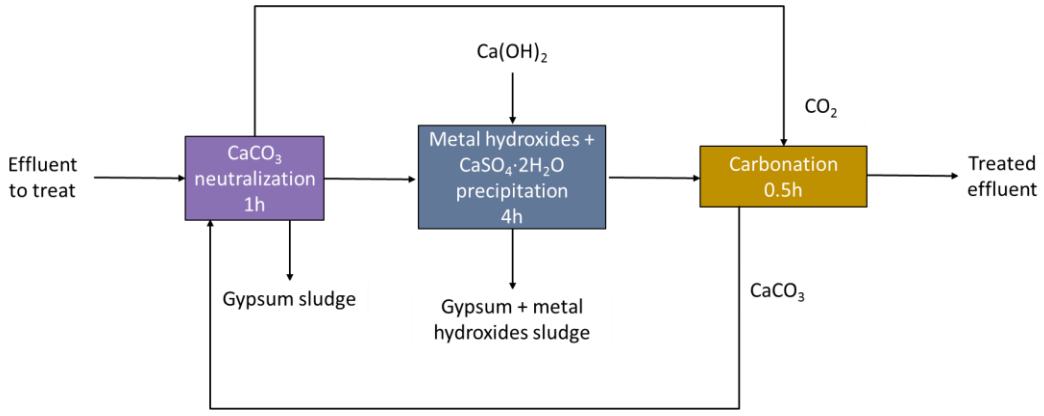


**Figure 6.1.-** Integrated limestone/lime process flow diagram (simplified)[1,19]

Limestone treatment is the most cost-effective treatment for neutralization of acid water to pH 7.2, and sulfate removal through gypsum precipitation down to 1900 mg/L levels can be achieved depending on the solution components. Then, by lime addition until pH 12, sulfate concentration can be decreased to 1100 mg/L. The settling rates of the sludges in the process steps were enhanced by adding a coagulant and/or a flocculant. The first and second steps were 74 % and 92 % faster respectively when using a flocculant polymer (3095), and the third step 100 % faster when using both a flocculant (3095) and a coagulant (PAC6). The reason to partially substitute lime with limestone is mainly economical, as the cost to neutralize 1 g/L of acidity is 69% lower using limestone than lime. The bulk of the solution would be neutralized to pH 6-8 with limestone and then lime would be added up to pH 12.4, thus achieving the highest costs savings.[1,10,12,15–19]

As shown to this point, sulfate removal by gypsum precipitation is limited by its solubility, which depends on the solution composition and ionic strength, and ranges from 1200 to 4000 mg/L. Hence, this process is often used as a pretreatment for waste streams with high sulfate concentrations. In order to achieve a sulfate concentration below gypsum solubility, barite and ettringite precipitation is used.

Sulfate removal by barite precipitation is highly efficient due to its high insolubility. The most commonly used Ba salts are $BaCl_2$,[4] $BaCO_3$,[20] $Ba(OH)_2$ and BaS,[2,21] which are expensive and toxic for the environment and thus, their use on an industrial scale needs a recovery plant to recycle them. When $BaCO_3$ is used, as it is also insoluble ($K_{sp}\sim10^{-8}$), limestone is usually added to soften the water and act as seed to promote barite

formation. In order to avoid limestone addition and reduce sludge disposal (essentially gypsum) and retention time, BaS is often employed.[2,22] However, metals in the solution tend to form metal sulfides, which are harmful for the downstream Ba recovery. In these cases, a previous lime step to precipitate the metals or a $H_2SO_4$ leaching step to oxidize metal sulfides is needed in order to maintain Ba recovery efficiencies. $Ba(OH)_2$ has been proposed for more neutral effluents where metals have been previously precipitated as metal hydroxides. This process eliminates the need for water treatment associated with $BaCO_3$ and BaS process, does not need long retention times and removes transition metals, Mg, and $NH_3$.[1–3]

An integrated BaS process was proposed in 2004 and consisted of *(i)* preliminary treatment with $Ca(OH)_2$, in which sulfate concentration decreased from 2650 to 1250 mg/L and Mg and metals were completely removed, *(ii)* sulfate removal below 200 mg/L by $BaSO_4$ precipitation *via* BaS addition, *(iii)* $H_2S$-stripping by $CO_2$ bubbling into the water, where $S^{2-}$ was lowered from 333 to 10 mg/L. Then the stripped $H_2S$ was absorbed into a $Fe^{3+}$ solution and converted to elemental sulfur, *(iv)* limestone crystallization, where limestone was precipitated due to $CO_2$ stripping with air and pH was increased from 5.7 to 7.2, and *(v)* BaS recovery by thermal reduction at 1050 °C with coal.[2]

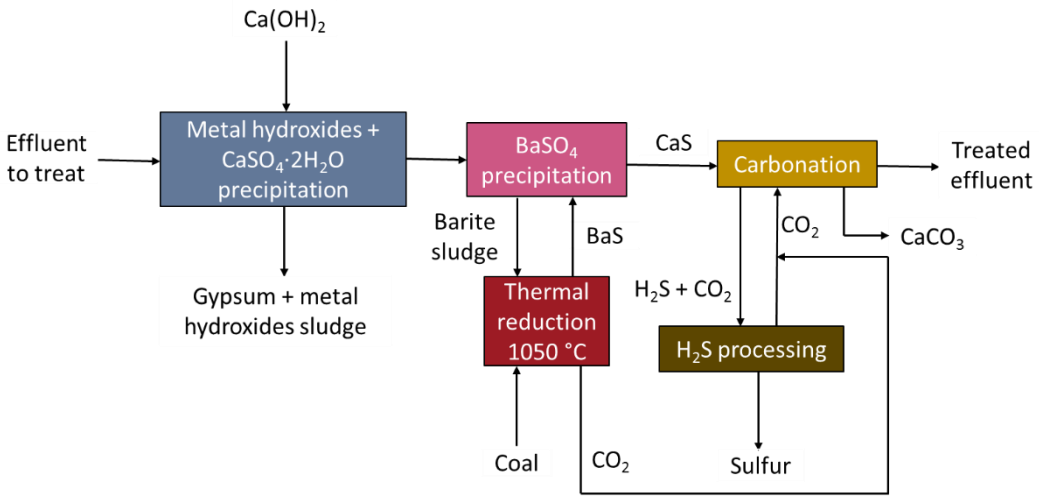


**Figure 6.2.-** Sulfate removal by BaS process flow diagram (simplified)[2]

Similar to the previous process, The Alkali Barium Calcium (ABC) Desalination Process uses Ba salts only after Gypsum precipitation by lime addition, minimizing thus

the Ba use. It consists of *(i)* neutralization, *(ii)* metal removal, *(iii)* gypsum precipitation and magnesium removal, *(iv)* carbonation, *(v)* final sulfate removal step by barite precipitation and *(vi)* $BaSO_4$ processing to recycle $BaCO_3$.[20,23]

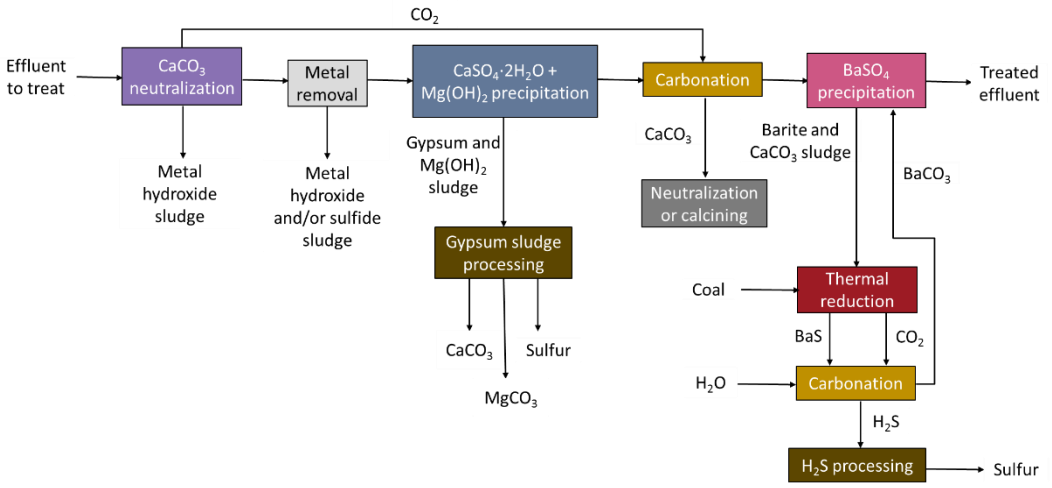


**Figure 6.3.-** ABC Desalination and barite sludge processing process flow diagram (simplified)[23]

Although $BaCO_3$ recycling reduces the costs and toxicity associated to Ba salts, the energy requirement for the ABC process would be relatively high due to the thermal reduction step required for $BaCO_3$ recycling. The MBA process is an enhancement on the ABC process where $Mg(OH)_2$ is also separated as a by-product.[6] Barium compounds are usually expensive and any residual $Ba^{2+}$ ions in solution generate a greater environmental concern than the original sulfate ions.[6,13] Where feasible to use, ettringite precipitation eliminates the use of hazardous barium compounds. There are several processes involving ettringite precipitation,[1,3–6,8,24–30] being the SAVMIN™ process the most widely known. It was firstly patented by Mintek in 1998, last actualized in 2017, and recently implemented in a 100 L/h demonstration plant for Sibanye-Stillwater, in South-Africa. In Figure 6.4 SAVMIN™ process flow diagram is presented:

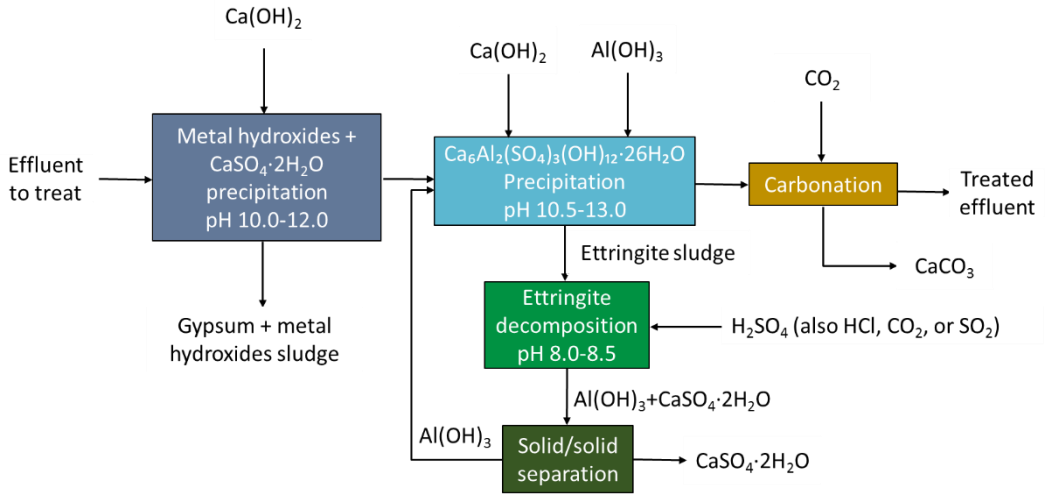


**Figure 6.4.-** SAVMIN™ Process flow diagram (simplified)[1,3,5,6,8,13,24,26–31]

The SAVMIN™ process consists of the following steps: *(i)* lime addition to rise the pH between 10.0 and 12.0, where dissolved metals precipitate as hydroxides and sulfates as gypsum, favored by seeding the solution with gypsum crystals. In previous patents (PCT/GB98/01610), this step was divided into 2 steps. First, pH was raised so only metals would precipitate as hydroxides, and secondly the solution was seeded with gypsum crystals to accelerate gypsum precipitation. The first step was removed in 2017 in order to simplify operation and lower costs *(ii)* ettringite precipitation by $Al(OH)_3$ and $Ca(OH)_2$ addition to the saturated gypsum solution, according the following reaction:

$$6\ Ca^{2+} + 3\ SO_4^{=} + 2\ Al(OH)_3 + 6\ OH^- + 26\ H_2O \leftrightarrow Ca_6Al_2(SO_4)_3(OH)_{12}{\cdot}26H_2O$$

As in this step $OH^-$ are consumed, NaOH or $Ca(OH)_2$ addition is required to maintain the solution pH between 10.0 to 13.0 for the reaction to proceed.[8,28,32] If the pH was higher than 13.0, $OH^-$ would compete with $SO_4^{=}$ which would not be removed from the solution. The formation of synthetic ettringite is reported to be a fast reaction by various researchers, reporting ettringite formation in 5 min and complete reaction at room temperature in 30 to 60 minutes. *(iii)* pH neutralization by carbonation, in which $CO_2$ addition precipitates relatively pure limestone or $Ca(HCO_3)_2$ that is removed by filtration. *(iv)* Ettringite decomposition and $Al(OH)_3$ recycling. The sludge from the third step is thickened, filtrated and put into contact with $H_2SO_4$ at a pH between 8.0 and 8.5 to decompose the ettringite into $Al(OH)_3$ (at lower pH $Al(OH)_x(SO_4)_y$ - type species are also precipitated) and gypsum according to the reaction:

$$Ca_6Al_2(SO_4)_3(OH)_{12}{\cdot}26H_2O + 3\ H_2SO_4 \leftrightarrow 6\ CaSO_4{\cdot}2H_2O\ (s) + 2\ Al(OH)_3\ (s) + 32\ H_2O$$

Then, 99.5 % of the precipitated $Al(OH)_3$ is recovered in a solid-solid separation unit, such as hydro-cyclone, where solids are separated by means of size exclusion. The separation is enhanced by seeding the solution with recycled gypsum, which promotes gypsum particle growth, increasing thus particle size differences between crystallized gypsum and amorphous $Al(OH)_3$ particles. The SAVMIN™ process can recover >95 % of the water, reduce the sulfate concentration to below 200 mg/L and the metals to trace levels. Moreover, despite not addressing monovalent ions, such as chlorides, and needing an average of 1.4 kg $Ca(OH)_2$ per treated $m^3$, and a relatively large number of solid/liquid separations, the $Al(OH)_3$ recovery step ensures that the process is highly cost-effective when compared to ion exchange and membrane separation techniques.[1,3,5,6,8,13,24,26–31]

The Cost-Effective Sulfate Removal (CESR) process, formerly known as the Walhalla process, is a variant of the SAVMIN™ process. The main differences between them is the use of a proprietary cement agent instead of $Al(OH)_3$ in CESR, and the recycling of ettringite in SAVMIN™. The CESR process consists of four steps, as shown in Figure 6.5: *(i)* Initial gypsum precipitation (40-60 min), *(ii)* precipitation of metals as hydroxides in a gypsum matrix (40-60 min), *(iii)* additional sulfate removal *via* ettringite precipitation (30-300 min), and *(iv)* pH reduction by carbonation.[1,3,4,25]

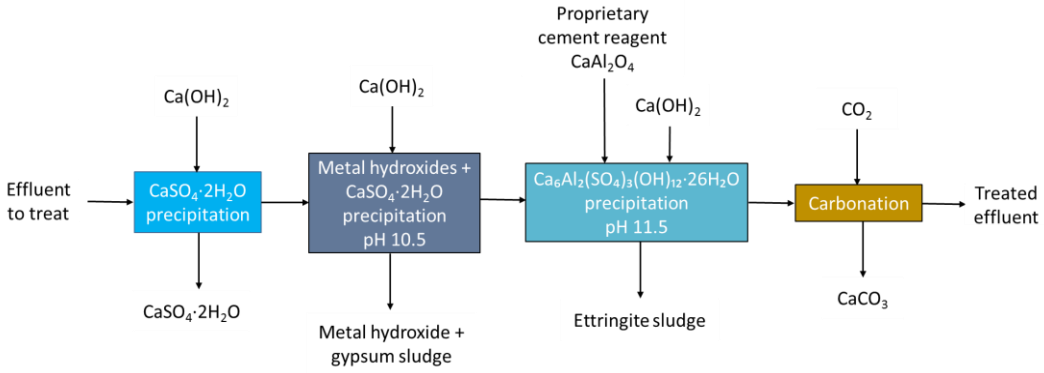


**Figure 6.5.-** CESR Process Flow Diagram (simplified)[1,3,4,25]

In the CESR process, *(i)* metal-free gypsum is precipitated by hydrated lime addition. For this step, the solubility characteristics of metals in the wastewater need to be carefully studied to prevent metal hydroxides precipitation, thus, minimizing the

volume of hazardous sludge. Gypsum sludge is removed by dewatering and filtration, and then, *(ii)* additional lime is added to raise the pH of the solution to 10.5, where dissolved metals precipitate as hydroxides. Removal of dissolved sulfate to concentrations below 100 mg/L is completed by *(iii)* raising the pH to 11.5 with lime, and adding a proprietary cement reagent (1.0 pound of reagent per pound of sulfate to be removed) to precipitate ettringite along with other contaminants like metals, nitrates, chlorides, fluorides, and boron. Gypsum interferes with the reaction of ettringite formation and, thus, it is completely removed before this step. Finally *(iv)* the pH is adjusted with $CO_2$ (g) to meet local discharge criteria and prevent scaling. Approximately 2 pounds of $CO_2$ are required and 4 pounds of limestone are produced per 1000 gallons of water with pH 8.5. After lowering the pH, water is clarified (resultant sludge is a mixture of gibbsite, limestone, and ettringite) and discharged. The CESR process is reported to reduce sulfate concentrations in industrial wastewaters below 100 mg/L.[1,3,4,25]

A variation of CESR and SAVMIN™ processes that uses $3CaO{\cdot}Al_2O_3$ (C3A) as aluminum source for ettringite precipitation was patented in 2012. By using C3A, aluminum sulfoaluminate is produced along with ettringite, and this mixture can be used as an enhancing component for cement production and/or as a neutralizer/coagulant in wastewater purification plants. This process includes a prior lime/limestone step if the sulfate concentration is above gypsum solubility, and it is able to remove sulfates to below 100 mg/L.[21]

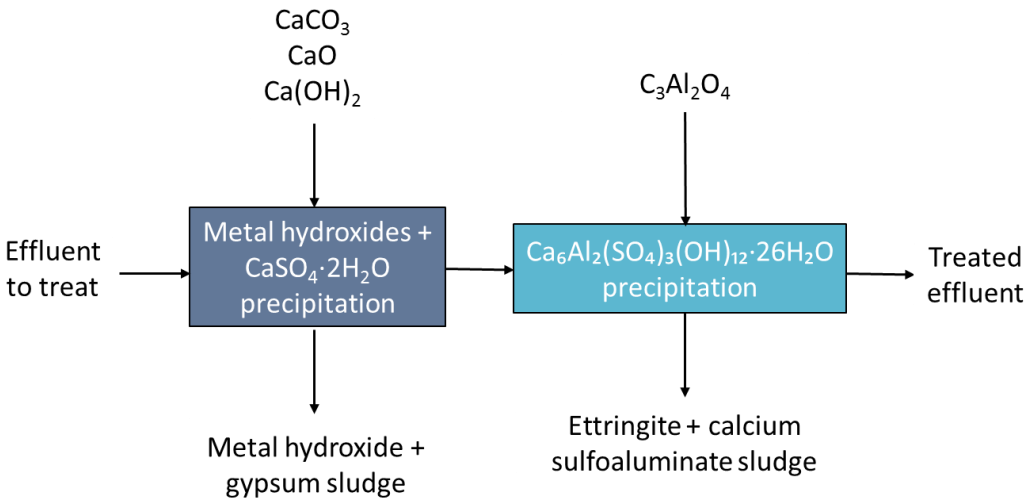


**Figure 6.6.-** 'C3A' Process Flow Diagram (simplified) [21]

The methods described so far have, to the best of our knowledge, not been implanted at industrial scale. The only commercially available ettringite precipitation process for sulfate removal below gypsum equilibrium concentrations is the LoSO$_4$™, operated by Veolia in South America.[6] In Figure 6.7 the LoSO$_4$™ Process Flow Diagram is shown.

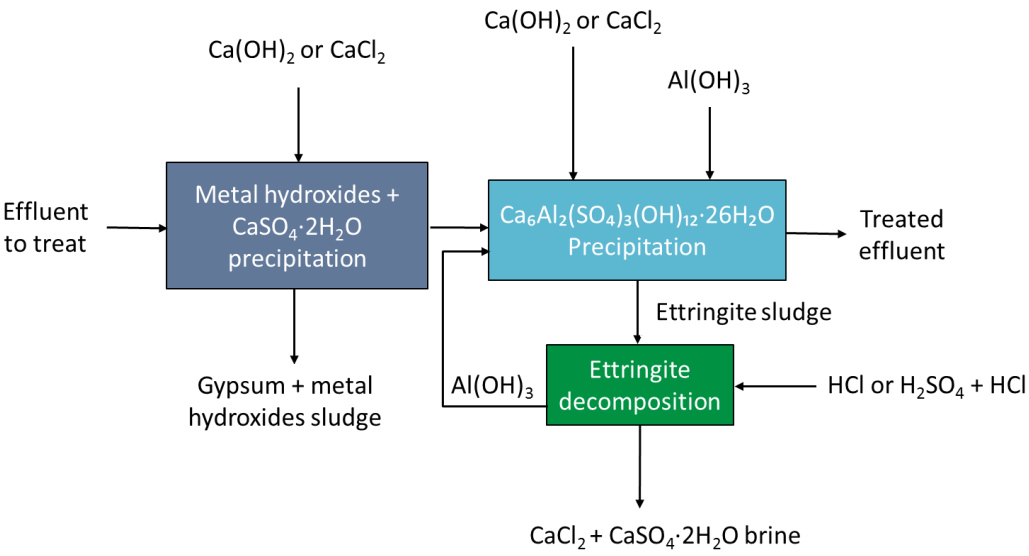


**Figure 6.7.-** LoSO$_4$™ Process Flow Diagram (simplified)[5,6,33]

Similarly to the aforementioned precipitation processes, in the LoSO$_4$™ one, first sulfates are precipitated as gypsum *via* lime or calcium chloride addition, and secondly ettringite is precipitated *via* lime or calcium chloride and $Al(OH)_3$ addition. More than 95 % of $Al(OH)_3$ is recovered and reused by disaggregating ettringite with either HCl or

a mixture of HCl and $H_2SO_4$. The $CaCl_2$ produced by ettringite decomposition increases gypsum solubility, and together with large amounts of water, solid gypsum formation is avoided, precipitating only $Al(OH)_3$. Nonetheless, this method of recycling ettringite introduces chloride ions into the product water, which creates a concentrated brine residue, thus complicating the system.[5,6,33]

As seen in SAVMIN and $LoSO_4$, there is an economical motivation to recover $Al(OH)_3$ in order to reduce reagent consumption. An alternative ettringite recycling method without external acid addition patented in 2015 is described in Figure 6.8. It harnesses the typically low pH of the effluent to decompose ettringite while neutralizing it and precipitating gypsum. Then, $Al(OH)_3$ and gypsum are separated by a hydro-cyclone. The remaining sulfates would be removed by gypsum and ettringite sequential precipitation.[33]

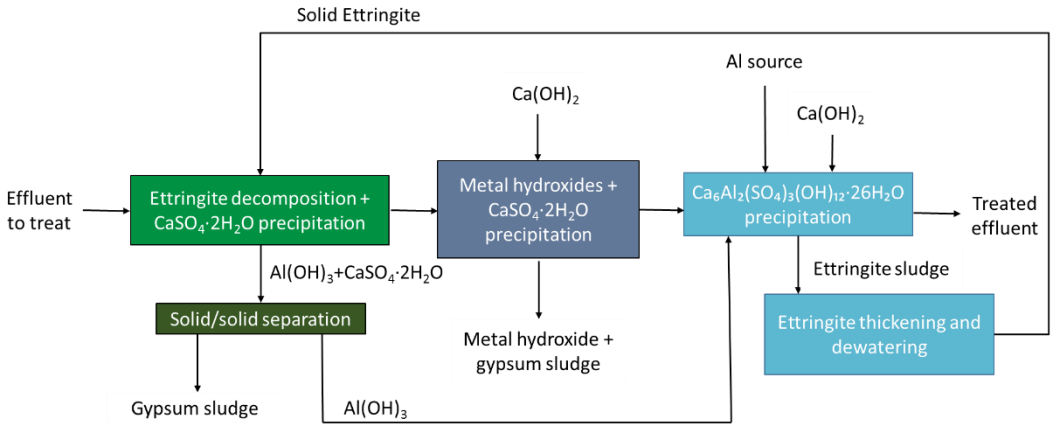


**Figure 6.8.-** Patented process for simultaneous ettringite decomposition and sulfate removal Process Flow Diagram (simplified) [21]

Although none of the ettringite based processes directly address monovalent ions, metals, nitrates, chlorides, fluorides and boron have been reported to partially coprecipitate with ettringite,[1] and ettringite has been reported to be a suitable adsorbent for $Na^+$, $Cl^-$ and $NO_3^-$ ions.[25,34]

## 6.3. Sulfate removal by membranes

Membrane based separation techniques use semi-permeable materials that allow some species through (permeate) while others are retained in the feed effluent (retenate). The corrosive and scaling nature of the typical AMD effluents would damage and/or block the membrane materials and, therefore, a pre-neutralization step is required to remove the bulk of the sulfates and metals from solution prior to its final purification. Membranes are used either to concentrate (Reverse Osmosis (RO)) or to purify (Electrodialysis (ED)). As described in Figure 6.9, in ED an electric potential drives the dissolved ions through a semi-permeable membrane (pore size 1-2 nm), leaving behind the purified effluent. In RO, on the other hand, high-pressure pumps, overcoming the osmotic pressure which can range from 17 to 80 bar, force the effluent through a semi-permeable membrane (pore size 0.1-5000 nm) which selectively excludes ions.[1,20]

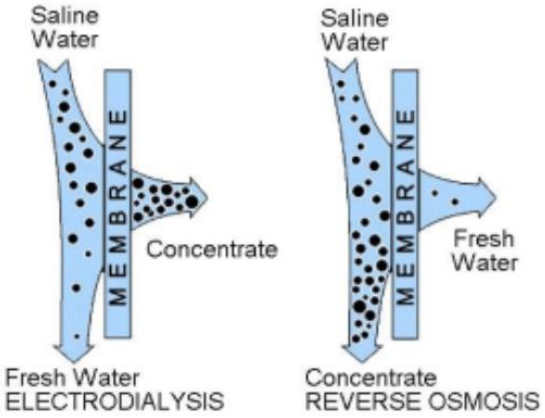


**Figure 6.9.-** Mechanism of membranes in ED and RO[1]

A RO process usually consists of four stages, *(i)* a pre-treatment: usually pH adjustment, filtration to remove suspended solids and mineral precipitation for dissolved metals (especially Al and Fe) to prevent membrane fouling, and chlorination to prevent microbial growth. *(ii)* High-pressure pumping (the most energy-demanding step), *(iii)* separation in the membrane assembly, and *(iv)* post-treatment, which consists on adjusting the pH, alkalinity, hardness and even $H_2S$ removal from the treated effluent. The brine discharge flow, and therefore the brine salinity, determines the feed water recovery and required operating pressure. When water is low in Ca (<100 mg/L) and $SO_4^=$ (<700 mg/L), conventional RO is suitable, although at higher concentrations,

maximum water recovery is reduced to 80 % and modified methods like Slurry Precipitation and Recycle Reverse Osmosis (SPARRO), and High Recovery Precipitating Reverse Osmosis (HiPRO) are more adequate.[1,3,20]

Both SPARRO and HiPRO actively promote gypsum precipitation prior to membrane treatment in order to reduce membrane walls corrosion and fouling by salt precipitation. SPARRO, formerly known as Seeded Reverse Osmosis (SRO) and then redeveloped and patented as SPARRO, seeds the effluent with gypsum crystals (3-10 % slurry) by recycling the waste sludge to prevent mineral precipitation on the membranes (scaling). A SPARRO process capable of reducing sulfate concentration from 6639 mg/L to 152 at 95 % water recovery was reported, however, it required a high energy consumption and suffers from poor seeding control, which resulted in failing and fouling of membranes, salt rejection and low membrane lives.[1,3,5,20,35–37]

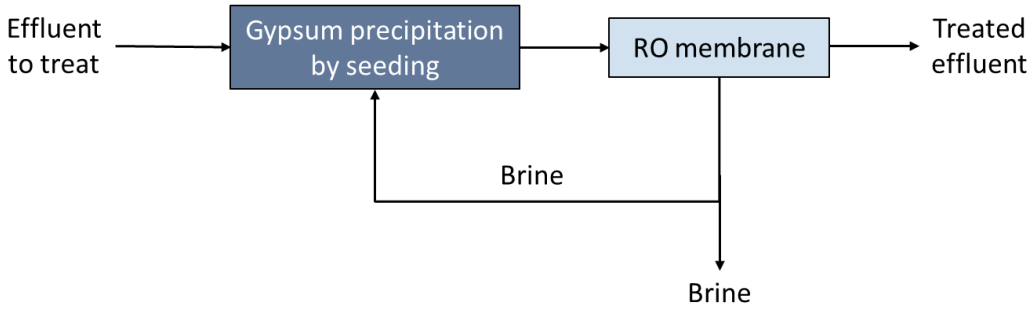


**Figure 6.10.-** SPARRO process flow diagram (simplified)[1,3,5,20,35,36]

HiPRO is the most recently developed process that combines precipitation and membrane technology, with a plant operating at full capacity since 2007. It achieves ultra-high water recoveries (>97 %) and potable water quality. On the other hand, it requires relatively high maintenance due to scaling, and produces a brine (<3 % of the feed) and solid waste (calcium and metal sulfates) that need to be managed.[1,3,5,20,36]

Electrodialysis (ED) is a membrane separation process based on ions migration through ion-selective membranes by an electrical field, moving through only dissolved salts, as illustrated in Figure 6.11. Anions are attracted to the positive electrode and can only pass through the anion-selective membrane, and *vice versa* with cations. By a proper arrangement of the ion-selective membranes and electrodes, the ions are trapped in the concentrate stream flow while the water molecules remain in the product

stream flow. Each pair of membranes is called a cell, the basic ED unit consists of several hundred cells connected with electrodes in a so-called membrane stack. The electrical dialysis reversal process (EDR) operates on the same principle as ED, with the particularity that, at regular intervals, electrodes polarity is reversed and the product and concentrate stream flows switch positions, highly enhancing the process by self-regenerating the membranes. The principal advantage of EDR compared to ED is that the cells are periodically cleaned and deposits on the membranes minimized. Moreover, EDR requires less chemical pretreatment than ED to prevent membrane fouling and is also able to treat a feed water with higher concentrations of suspended solids than RO. A pilot plant at the Beatrix gold mine in South Africa achieved in 1990 80 % salt recovery and 84% water recycling for an effluent high in Fe, Mn, Na, Cl and sulfates.[1,3,38,39]

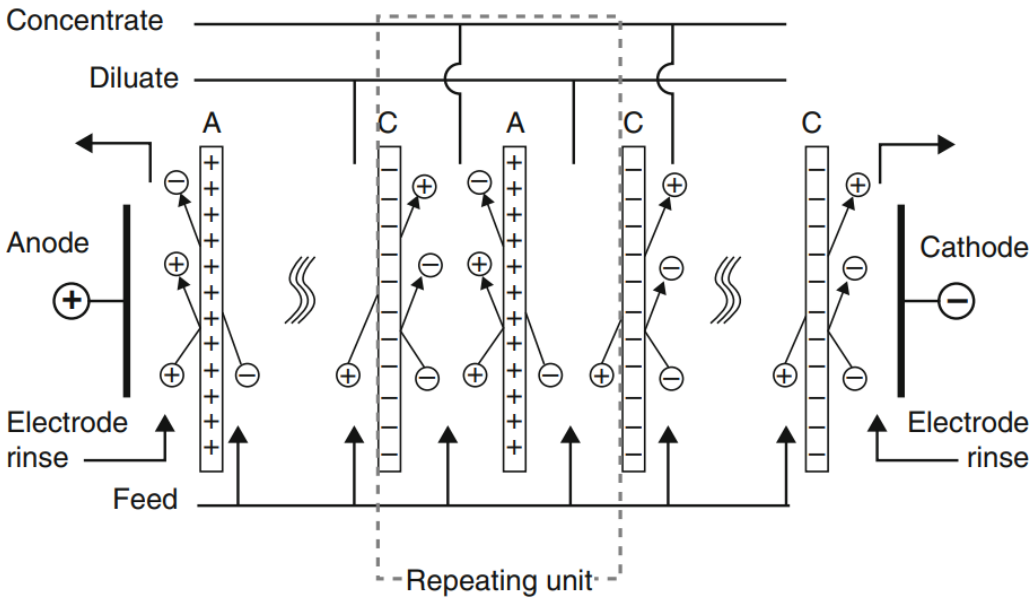


**Figure 6.11.-** ED principles[39]

Examples of membrane technologies applied to the treatment of mine waters comprise RO and ED with the predominance of the former. Both processes also require stream pretreatment to prevent fouling and microbial growth. The process recovers 65 % of the feed water, and the remaining 35 %, high in sulfates, is treated with lime. This process consisted on *(i)* metals precipitation with lime, *(ii)* manganese removal, *(iii)* ultrafiltration of suspended and colloidal solids, *(iv)* desalination by either RO or nanofiltration.[13]

Nanofiltration (NF) is another membrane process that operates at pressures higher than micro or ultrafiltration but lower than RO. NF membranes, also known as loose RO membranes have a high removal efficiency for divalent (and trivalent) ions like sulfates, and lower removal selectivities for monovalent ions like nitrates and chlorides, which tend to pass the membrane. The reject stream usually comprises between 10 and 40 % of the original flow, although in operation, a sulfate brine is often precipitated and the sludge is dewatered and concentrated, enhancing water recovery. For example, a NF process to remove sulfates from aqueous waste streams with recycle was patented where the generated reject stream was between 1 and 5 % of the feed effluent.[4,12,40]

Although membrane-base processes cannot directly treat scaling effluents (sulfate concentrations higher than gypsum equilibrium), they are efficient for effluents high in non-scaling ions, like $Na^+$ or $Cl^-$. Therefore, RO is suitable for sulfate removal when monovalent contaminants must also be removed. Membrane-base processes need a high investment, maintenance and operation costs, in addition to a tendency to suffer from a number of blinding and fouling mechanisms that can result in frequent shut-downs for cleaning and in a short operating life for the membranes themselves. All the membrane approaches to sulfate treatment produce brine as a waste product, whose composition vary depending on the effluent and, accordingly, its disposal.[1,4,5,12,20,21,33,35]

## 6.4. Sulfate removal by ion exchange and adsorption

Similarly, to membranes, ion exchange resins are well suited to the removal of dissolved sulfate close to gypsum saturation. Ion exchange resins are composed of a high concentration of polar groups (acid or basic) included in a synthetic polymer matrix, with a fixed radical and a mobile ion (replacement ion). The mobile ion is exchanged for the target ions from the solution, which are of equal electric charge. Several processes have been proposed, being the the Sulf-IX™ process by BioteQ (formerly GYP-CYX) devised to remove calcium and sulfate, the best documented. The Sulf-IX™ process consists of three steps, as described in Figure 6.12.

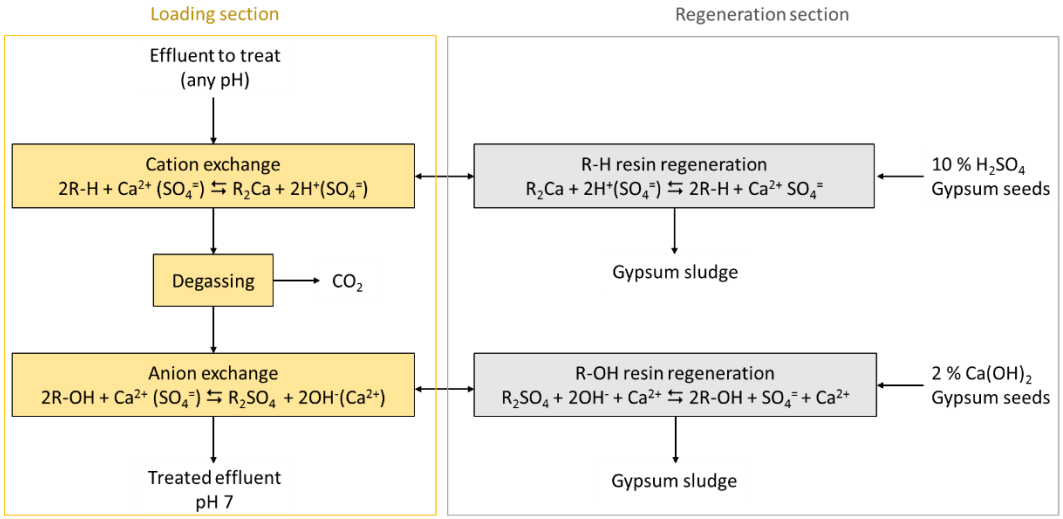


**Figure 6.12.-** Sulf-IX™ Process Flow Diagram (adapted)[1,3,4,13,21]

The effluent is *(i)* pumped multiple times through a strong acid cation resin (R-H) where cations are exchanged for $H^+$. This resin is regenerated by leaching cations with 10 % $H_2SO_4$ and then seeded with gypsum crystals for precipitation. The regenerated resin is rinsed with treated effluent and returned to the cation exchange section. *(ii)* After cation exchange, the effluent is pumped to a degassing tower where carbonate alkalinity is removed, and finally is (*iii*) pumped multiple times through a weak base anion resin (R-OH) where anions are exchanged for $OH^-$. Similarly to the cation resin, the anion resin is regenerated by leaching anions with a 2 % lime solution seeded with gypsum crystals to precipitate gypsum. The solution is reused thanks to continuous precipitation of gypsum in both regenerations, which together with $CO_2$ from the degassing stage are the only waste products of this process. The treated effluent is low in anions and has a neutral pH. The number of contact stages depends on the initial composition of the effluent and its required purification, being able to achieve a reduction in sulfates from 4500 to <50 ppm with water recoveries up to 90 %. The first commercial plant using Sulf-IX™ has been operating in Arizona since 2011 with a capacity of 600 $m^3$/day. [1,3–5,13,21]

A variation of the GYP-CIX process, known as GYP-CIX hybrid, was designed for effluents with high concentrations of Ca and $SO_4^=$, consisting on a combined process of precipitation and ion-exchange, as described in Figure 6.13.

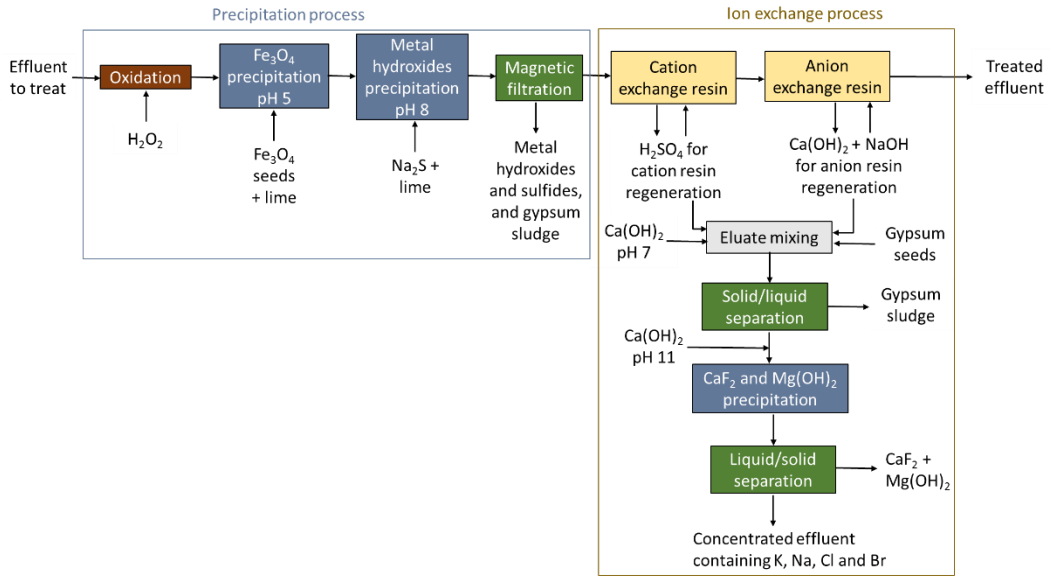


**Figure 6.13.-** GYP-CIX Process Flow Diagram (adapted)[1]

In the precipitation part of the process, the effluent $SO_4^=$ concentration is reduced from 6 to 3 g/L by *(i)* oxidation with $H_2O_2$ to ensure Fe and Mn maximum oxidation, *(ii)* seeding with $Fe_3O_4$ (0.5 g/L) and pH raising to 5 by lime addition to prevent $H_2S$ (g) formation in the next process step, *(iii)* $Na_2S$ and lime addition to pH 8, where metal sulfides and hydroxides precipitate, and *(iv)* magnetically filtration. The ion-exchange part of the process is very similar to the Sulf-IX™ process with only slight differences in the regeneration of resin, where sulfates are reduced below 50 mg/L.[1]

The main advantage of ion exchange resins is that it is possible to recover their original exchange capacity through regeneration.[21] In order to further reduce costs, ion exchangers manufactured from low-cost materials are under research. For example, a strong basic anion exchanger (RS-AE) highly selective to sulfates was obtained by treating rice straw with epichlorohydrin (carcinogen) and trimethylamine, and it removed up to 74.76 mg $SO_4^=$/g RS-AE.[41] Similarly, the adsorption on different low-cost materials has been reported to reduce sulfate concentrations in aqueous solutions. The sulfate adsorption on fine powdered limestone (<0.045 mm) was reported to fit Langmuir isotherm with a maximum uptake of 23.7 mg $SO_4^=$/g limestone. In approximately 10 h, the limestone reduced sulfate concentrations from 588.0 to 100 mg/L in a stirred reactor.[13] The sugarcane bagasse cellulose modified with zirconium oxychloride was reported to retain 4 mg $SO_4^=$/g cellulose.[42] These low-cost propositions

are still far from being a competitive alternative to commercial resins and adsorbents for sulfate removal at large scale.

## 6.5. Sulfate removal by biological systems

As in the case of the membrane and ion exchange technologies, pure biological sulfate removal systems are generally suited only for low sulfate effluents (< 1 g/L), and can accept higher sulfate concentrations when supplemented with a chemical precipitation pretreatment. Biological systems rely on sulfur reducing bacteria (SRB), which consume sulfates as oxidants for their metabolism. In order to produce energy for metabolic activity, microbes facilitate electron transference from organic reduced substrates (*i.e.* organic matter, $H_2$, and CO) to oxidized species (*i.e.* $O_2$ or $SO_4^=$). Biological sulfate removal systems reduce $SO_4^=$ to $HS^-$, and then $HS^-$ is removed as elemental S *via* sulfur bacteria oxidation, precipitation as metal sulfides, or $H_2S$ (g) stripping. The SRB based sulfate treatments are limited by the presence of $H_2S$, toxic for SRB, dissolved metals, and substrate depletion by other anaerobic bacteria.

Biochemical reactors (BCR) are engineered treatment systems that use an organic substrate to drive microbial and chemical reactions to reduce the concentration of sulfates, metals and acidity. Passive bioreactors are BCR that can operate for months at a time without any external energy, chemical input, and human intervention, *e.g.* constructed wetlands, alkalinity producing systems, and permeable reactive barriers. Among the developed active BCR (mixed, packed bed, fluidized bed, sludge blanket and gas-lift), the most significant designs for AMD treatment are (*i*) a continuous, fluidized bed reactor where the generated $H_2S$ is stripped with an inert gas and used in a separate reactor to precipitate metals as sulfides, and (*ii*) the THIOPAQ™ process, developed by the PAQUES company (Netherlands) with the first commercial plant built in 1992. It consists on a first anaerobic step where the effluent is put in contact with SRB in the presence of a hydrogen source, typically $H_2$ or $CH_3COOH$, and a second aerobic step where sulfides are oxidized to elemental sulfur. The main advantages claimed by THIOPAQ™ process are low $H_2S$ concentrations, most of the $H_2S$ is dissolved in water rather than in the gas phase, is carried out at ambient temperature, and its flow rates

can be varied. However, it needs a source of carbon and hydrogen such as synthesis gas in large-scale applications and therefore, the cost of a reformer to produce it needs to be taken into account. [1,3–5,21,43–45]

Recently, an anaerobic packed bed reactor bioprocess based on a microbial sulfate-reducing halotolerant consortium and low-cost organic substrates was designed. It was reported to admit up to 3602 ppm $SO_4^=$, 1400 ppm Cu, 27.9 ppm Fe, 20.4 ppm Zn and 0.6 ppm Ni with pH 2.95. The first steps of this process, designed to remove metals, toxic for SRB, are lime addition to pH 6.3 and a bio sorption step. The SRB biofilm is created in 9 days and afterwards, sulfates and trace metals removing from the effluent to industrial water standards is started.[45]

A pilot plant based on bacteria immobilized on wood chips was commissioned at Sibanye-Stillwater (Johannesburg, South Africa) which removed >95 % of the sulfates, leaving the treated effluent with 200-600 ppm $SO_4^=$ and the metal content was reduced to trace levels. The process produced less amount of solid waste than the conventional chemical precipitation methods.[5]

As mentioned before, there are three developed passive biological processes, described in Figure 6.14. The selection of a suitable passive treatment depends on the water chemistry, flow rate, local topography and site characteristics. Constructed Wetlands can be free water surface (FWS) and subsurface flow (SF), being FWS most of the natural wetlands and the more appropriate for sulfate removal. FWS are generally shallow basins with a subsurface barrier that prevents leaking, where the waste stream flows over a vegetated surface. For acidic effluents, anaerobic wetlands are used, where sulfate removal is carried out by sulfate reduction and alkalinity is achieved by dissolving limestone. The presence of other oxidants can affect sulfate reduction in wetlands and has been suggested as a potential explanation for low rates of sulfate reduction for AMD. Compared to active BCR, sulfate reduction rates in wetlands are very low.

Together with wetlands, alkalinity-producing systems are the main passive treatment systems for acid rock drainage. They can be either Anoxic Limestone Drains (ALD) or Vertical Flow Systems (VFS). ALD are buried limestone cells or trenches capped with clay, which in addition of preventing atmospheric exposure, create an environment

high in $CO_2$ and low in $O_2$. This increases lime dissolution and prevents iron hydroxide precipitation that could inhibit lime dissolution and clog the drain. The effluent is then discharged into a settling pond to increase the pH by degassing and promote metal precipitation. VFS are a combination of ALD and anaerobic wetlands, consisting in three layers. The first layer has 1-3 m of water. The second (below), 0.2-0.3 m of organic compost, and then 0.5-1 m of limestone. As in ALD, the effluent is discharged into an aerobic pond to increase the pH by degassing and precipitate metals. The retention times for sulfate removal by ALD vary from 23 to 51 h, and by VFS from 4 to 90 h.

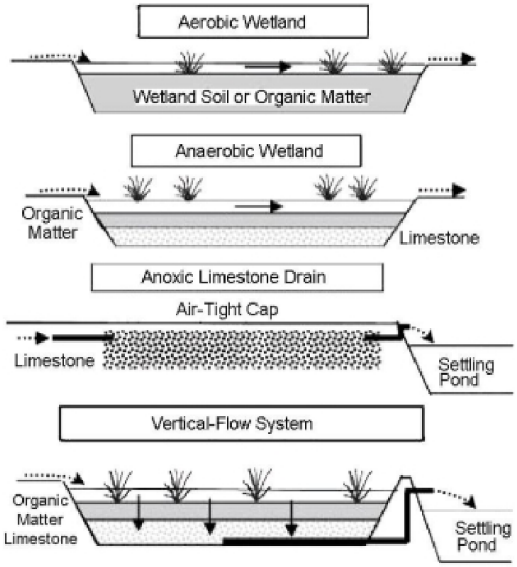


**6.14.-** Passive biological treatments for sulfate removal[1]

The last main passive biological treatment for sulfate removal are Permeable Reactive Barriers (PRB), which are reactive zones in an aquifer, created through the addition of a reactive material designed to either immobilize or degrade the contaminants. The most common reactive materials are zero-iron to reduce metal contaminants and precipitate oxyanions; limestone to precipitate metal hydroxides and sulfates, and organic matter as substrate. The reduction of $SO_4^{=}$ to $HS^-$ enhances metal sulfide precipitation, provided sufficient concentrations of trace metals are available to remove the sulfide to low values, although no PRBs have been constructed for sulfate treatment specifically to the best of our knowledge. As in the mentioned passive treatments, sulfate removal rate is very slow, about 14 mg/L per day.

When there is a natural occurrence of SRB, *in situ* sulfate reduction (ISSR, developed by Arcadis) is an interesting system, as it combines the biological sulfate reduction with the remediation hydrogeology approaches. A carbon source (lactate) is injected to catalyze sulfate reduction by *in situ* SRB, and the sulfur is then removed as metal sulfides and or elemental sulfur. ISSR's advantages are the suitability of many low-cost carbon sources (molasses, sewage sludge, sawdust and manure, among other wastes from various industries), the low potential for process disruptions, and the low effort to operate. However, the generated precipitate needs to be managed, the final water quality can be suboptimal, the distribution of the carbon source in the subsurface can be uneven, and the possible rebound effect after treatment. [1,3–5,21,43–45]

Passive systems maintain a large working inventory and operate slowly but require low maintenance and operational input and use natural materials such as woodchips, gravel, manure and compost substrate. In contrast, active treatments proceed rapidly, requires a smaller inventory but frequent maintenance and monitoring, external sources of chemicals, energy and labor and incurs in higher capital costs for infrastructure development.

## 6.6. Conclusions

In order to select the most appropriate effluent treatment, the following parameters were considered: *(i)* composition of the effluent in hand, *(ii)* specifications of the treated effluent, *(iii)* infrastructure and available space, and *(iv)* waste generation to ensure that additional environmental problems are not generated.

The effluent generated in the previous chapter of this thesis has low pH (2-3), high sulfate concentration (~ 40 g/L), dissolved metals and fluoride. The main concern is thus, decreasing sulfate concentration. For that, gypsum precipitation through lime and limestone addition is selected, as it is the preferred bulk sulfate removal in the mine industry due to its simplicity and low-cost. Although its main drawback is the generated sludge, it can be dewatered and concentrated to lower the volume and recover water. However, after a gypsum precipitation based process, between 1500 and 4000 mg/L of sulfates remain in the stream, depending on composition and ionic strength.[4,8,12,13]

At this point, other sulfate removal alternatives need to be considered to further decrease sulfate concentration so that the purified effluent can be reused in the system or discharged (in the hundreds of mg/L range).

Among the chemical precipitation processes, SAVMIN is the preferred treatment as it can decrease sulfate concentrations to very low levels (10 mg/L) while recycling the produced ettringite and avoiding the use of harmful Ba salts.

Membrane-based processes, although being commercially available and having achieved acceptance for sulfate removal, need a high initial investment, maintenance and operation costs, in addition to a tendency to suffer from fouling that can result in frequent shut downs and in a short operating life for the membranes. All the membrane approaches to sulfate treatment produce brine as a waste product, which adds a new environmental problem.

Despite the intrinsic discontinuous nature of the ion exchange technologies, a system can be designed to operate continuously, and the resins can be regenerated. However, the membranes need to be periodically replaced and the regeneration requires a regeneration unit, where gypsum sludge is produced.

Although passive biological methods are very economical and require low operating and maintenance costs, they are the most sensitive and the slowest of the studied processes. Active biological methods have higher sulfate removal rates, but the associated costs do not compensate for this effluent.

Taking all into account, in the next chapter, a SAVMIN™ approach will be studied for the purification of the effluent, including gypsum and ettringite precipitation.

## 6.7. Appendix 6.1

**Summary of case studies on chemical treatment processes with mineral precipitation**

| | Limstone/Lime | BaS | SAVMIN | CESR |
|---|---|---|---|---|
| | 2001 | 1990 | 1999-2001 | 2001 ? |
| **Pretreatment** | no | no | no | no |
| **Feed water** | $SO_4$: 3,000 mg/L | $SO_4$: 27,500 mg/L | $SO_4$: 649 mg/L | $SO_4$: 29,100 mg/L |
| **Product water** | $SO_4$: 1,219 mg/L | $SO_4$: 190 mg/L | $SO_4$: 69 mg/L | $SO_4$: 190 mg/L |
| **Brine production** | no | no | no | no |
| **Sludge production** | low-moderate | low-moderate | moderate-high | high-very high |
| **Monitoring** | moderate-high | high | high | high |
| **Maintenance** | low | low | low | low |
| **Capital cost**[1] | unknown (low) | USD 0.48 M per $10^3$ $m^3$/day ($\Delta$ $SO_4$: 2,000 mg/L) | USD 0.31 M per $10^3$ $m^3$/day | unknown |
| **Operating costs**[1] | USD 0.10 / $m^3$ | USD 0.36 / $m^3$ ($\Delta$ $SO_4$: 2,000 mg/L) | USD 0.17 / $m^3$ | USD 0.79 / $m^3$ ($\Delta$ $SO_4$: 1,500 mg/L) |
| **Advantages** | - also trace metal removal<br>- very cheap | - low levels of sulphate<br>- recycling of expensive BaS | - low levels of sulphate<br>- recycling of ettringite<br>- also trace metal removal | - low levels of sulphate<br>- also trace metal removal |
| **Disadvantages** | - limited sulphate removal<br>- production of sludges | - little trace metal removal<br>- production of sludges | - production of sludges | - production of sludges |
| **Improvements** | - recycling of sludges | - recycling of sludges | - recycling of sludges | - recycling of sludges |

[1] Assuming South African R 1 = USD 0.104 or R 9.62 = USD 1.00 (Nov. 2002)

**Summary of case studies on treatment processes using membranes and ion-exchange**

| | RO | SPARRO | EDR | GYP-CIX |
|---|---|---|---|---|
| | 2001 | 1992-1994 | 2001 | 2001 |
| **Pretreatment** | yes | yes | yes | no |
| **Feed water** | $SO_4$: 4,920 mg/L | $SO_4$: 6,639 mg/L | $SO_4$: 4,178 mg/L | $SO_4$: 4,472 mg/L |
| **Product water** | $SO_4$: 113 mg/L | $SO_4$: 152 mg/L | $SO_4$: 246 mg/L | $SO_4$: <240 mg/L |
| **Brine production** | yes | yes | yes | yes |
| **Sludge production** | low | low | low | low-moderate |
| **Monitoring** | low-moderate | low-moderate | low-moderate | low |
| **Maintenance** | high | high | high | moderate |
| **Capital cost** | USD 0.44-0.53 M[1] per $10^3$ $m^3$/day | USD 0.52 M[2] per $10^3$ $m^3$/day | USD 0.56-0.67 M[1] per $10^3$ $m^3$/day | USD 0.33-0.37 M[1] per $10^3$ $m^3$/day |
| **Operating costs** | USD 0.88 / $m^3$ | USD 0.22[2] / $m^3$ | USD 0.48 / $m^3$ | USD 0.60 / $m^3$ |
| **Advantages** | - drinking water quality | - drinking water quality<br>- improved membrane life | - drinking water quality | - drinking water quality |
| **Disadvantages** | - scaling problems<br>- short membrane life | - short membrane life | - scaling problems<br>- short membrane life | - production of sludges |
| **Improvements** | - not suitable for scaling waters | - membrane life | - not suitable for scaling waters | - recycling of sludges |

[1] Calculated from capital costs for plants with feed of 45-80 $10^3$ $m^3$/day (worst-case scenario Grootvlei mine water)
[2] Costs based on 1992 prices (S.A.), conversion used: South African R 1 = USD 0.104 or R 9.62 = USD 1.00 (Nov. 2002)

**Summary of case studies on treatment processes using biological sulphate removal**

| | Bioreactor | Constructed Wetland | Alk. Producing Systems | Permeable Reactive Barrier |
|---|---|---|---|---|
| | 2001 | 1993/1999 | 1999 | 1999-2002 |
| **Pretreatment** | yes | yes | yes | no |
| **Feed water** | $SO_4$: 8,342 mg/L | $SO_4$: 1,700 mg/L | $SO_4$: 3,034 mg/L | $SO_4$: 2,500-5,200 mg/L |
| **Product water** | $SO_4$: 198 mg/L | $SO_4$: 1540 mg/L | $SO_4$: 1,352 mg/L | $SO_4$: 840 mg/L |
| **Sludge production** | low-moderate | no | no | no |
| **Monitoring** | moderate-high | low | low | low |
| **Maintenance** | moderate | low | low | low |
| **$SO_4$ reduction rate** | 12-30 g/L,day | 0.3-197 mg/L,day | 0 mg/L,day | max. 10.5-15.3 mg/L,day |
| **Capital cost** | USD 0.24 M[1] per $10^3$ $m^3$/day ($\Delta$ $SO_4$: 2,000 mg/L) | unknown (low) | unknown (low) | USD 65,000 |
| **Operating costs** | USD 0.27[1] / $m^3$ ($\Delta$ $SO_4$: 2,000 mg/L) | unknown (low) | unknown (low) | USD 30,000 / yr |
| **Advantages** | - also trace metal removal<br>- recycling of $H_2S$ and $CO_2$ | - also trace metal removal<br>- passive treatment | - gypsum precipitation<br>- also (trace) metal removal | - passive treatment<br>- also trace metal removal |
| **Disadvantages** | - cost of C + energy source<br>- production of sludge | - little sulphate reduction | - no sulphate reduction ? | - long-term performance ? |
| **Improvements** | - recycling of sludge<br>- cheap C + energy source | - specific design requird | - specific design requird | - alternative reactive media |

[1] Costs based on 1992 prices (S.A.), conversion used: South African R 1 = USD 0.104 or R 9.62 = USD 1.00 (Nov. 2002)

## 6.8. References


[1] International network for acid prevention, *Treatment of Sulphate in Mine Effluents*, **2003**.

[2] J. P. Maree, P. Hlabela, R. Nengovhela, A. J. Geldenhuys, N. Mbhele, T. Nevhulaudzi, F. B. Waanders, *Mine Water Environ.* **2004**, *23*, 195–203.

[3] R. . Bowell, in *IMWA Preceedings*, **2004**, pp. 329–342.

[4] M. Reinsel, "Sulfate Removal Technologies: A Review," can be found under https://www.wateronline.com/doc/sulfate-removal-technologies-a-review-0001, **2015**.

[5] R. Naidoo, K. Preez, Y. Govender-ragubeer, in *IMWA*, **2018**, pp. 215–220.

[6] AECOM, *Direct Potable Reuse Feasibility Study Report*, **2017**.

[7] M. Arnold, M. Gericke, R. Muhlbauer, in *IMWA 2016*, **2016**, pp. 1–4.

[8] S. Tait, W. P. Clarke, J. Keller, D. J. Batstone, *Water Res.* **2009**, DOI 10.1016/j.watres.2008.11.008.

[9] C. J. Warren, E. J. Reardon, *Cem. Concr. Res.* **1994**, *24*, 1515–1524.

[10] F. Visconti, J. M. De Paz, J. L. Rubio, *Eur. J. Soil Sci.* **2010**, *61*, 255–270.

[11] M. M. Emamjomeh, M. Sivakumar, A. S. Varyani, *Desalination* **2011**, *275*, 102–106.

[12] K. Sathrugnan, L. A. Reyes, *Sulfate Removal from Aqueous Waste Streams with Recycle*, **2012**, WO 2012/109313.

[13] A. M. Silva, R. M. F. Lima, V. A. Leão, *J. Hazard. Mater.* **2012**, *221–222*, 45–55.

[14] H. Davies, P. Weber, P. Lindsay, D. Craw, B. Peake, J. Pope, *Appl. Geochemistry* **2011**, *26*, 2121–2133.

[15] J. P. Maree, G. J. Van Tonder, P. Millard, T. C. Erasmus, *Water Sci. Technol.* **1996**, *34*, 141–149.

[16] J. P. Maree, P. Du Plessis, C. J. Van der Walt, *Water Sci. Technol.* **1992**, *26*, 345–355.

[17] J. P. Maree, P. Du Plessis, *Water Sci. Technol.* **1994**, *29*, 285–296.

[18] J. P. Maree, M. De Beer, W. F. Strydom, A. M. Christie, *IMWA Proc. 1998* **1998**, 12.

[19] P. Geldenhuys, A.J., Maree, J.P., de Beer, M., Hlabela, *J. South African Inst. Min. Metall.* **2003**, 345–354.

[20] H. Swanepoel, Sulphate Removal from Industrial Effluents through Barium Sulphate Precipitation, North-West University, **2011**.

[21] J. Arellano Ortiz, *METHOD FOR TREATING SULPHATE-LADEN WASTE AND FOR RECYCLING THE RESULTING SLUDGE*, **2015**, EP 2 955 161 A1.

[22] D. J. Bosman, J. A. Clayton, J. P. Maree, C. J. L. Adlem, *Int. J. Mine Water* **1990**, *9*, 149–163.

[23] M. De Beer, J. P. Maree, J. Wilsenach, S. Motaung, L. Bolgo, V. Radebe, in *Mine Water Innov. Think.*, Sidney, **2010**, pp. 4–5.

[24] V. S. Ramachandra, Z. Chun-Mei, *Mater. Struct.* **1986**, *19*, 437–444.

[25] M. A. Reinsel, *J. Am. Soc. Min. Reclam.* **1999**, *1999*, 546–550.

[26] M. Kotze, Z. Hendriette, *Improved Effluent Treatment Process for Sulphate Removal*, **2017**, CA 2993284.

[27] J. . Smit, in *Int. Symp. Mine, Water Environ. 21st Century*, Seville, Spain, **1999**.

[28] D. Damidot, U. A. Birnin-Yauri, F. P. Glasser, *Adv. Cem. Res.* **1994**, *7*, 129–134.

[29] D. J. Hassett, G. J. McCarthy, P. Kumarathasan, D. Pflughoeft-Hassett, *Mater. Res. Bull.* **1990**, *25*, 1347–1354.

[30] C. Hall, P. Barnes, A. D. Billimore, A. C. Jupe, X. Turrillas, *J. Chem. Soc. - Faraday Trans.* **1996**, *92*, 2125–2129.

[31] P. J. Usinowicz, B. F. Monzyk, L. Carlton, *Proc. Water Environ. Fed.* **2014**, *2006*, 139–153.

[32] D. Guimarães, V. de A. Oliveira, V. A. Leão, *J. Therm. Anal. Calorim.* **2016**, *124*, 1679–1689.

[33] P. Richard George, *PROCESS FOR THE TREATMENT OF HIGH SULPHATE WATERS*, **2015**, WO 2015/162540 A1.

[34] D. Hou, T. Li, Q. Han, J. Zhang, *Comput. Mater. Sci.* **2018**, *153*, 479–492.

[35] W. Pulles, G. J. G. Juby, R. W. Busby, *Water Sci. Technol.* **1992**, *25*, 177–192.

[36] D. G. Randall, J. Nathoo, A. E. Lewis, *Desalination* **2011**, *266*, 256–262.

[37] A. Drak, R. Zaken Porat, in *IWC 16-Reserve RO*, **2017**.

[38] M. Tedesco, H. V. M. Hamelers, P. M. Biesheuvel, *J. Memb. Sci.* **2018**, *565*, 480–487.

[39] A. Brunetti, R. Di Felice, *Encyclopedia of Membranes*, **2016**.

[40] M. Mullett, R. Fornarelli, D. Ralph, *Membranes (Basel).* **2014**, *4*, 163–180.

[41] W. Cao, Z. Dang, X. Q. Zhou, X. Y. Yi, P. X. Wu, N. W. Zhu, G. N. Lu, *Carbohydr. Polym.* **2011**, *85*, 571–577.
[42] D. R. Mulinari, M. L. C. P. da Silva, *Carbohydr. Polym.* **2008**, *74*, 617–620.
[43] A. H. Kaksonen, P. D. Franzmann, J. A. Puhakka, *Biodegradation* **2003**, *14*, 207–217.
[44] J. Shayegan, F. Ghavipanjeh, P. Mirjafari, *Process Biochem.* **2005**, *40*, 2305–2310.
[45] C. Hurtado, P. Viedma, D. Cotoras, *Hydrometallurgy* **2018**, *180*, 72–77.

# Chapter 7

Effluent purification

# Table of contents

## 7.1. Introduction

The hydrometallurgical treatment developed in Chapter 5 of this PhD thesis produces an effluent (see its elemental composition in Table 7.1.). The ideal destination of this stream would be its directly recycle into the hydrometallurgical process. This option, however, is impracticable due to the scaling nature of this untreated effluent (henceforth, UT effluent, Table 7.1), as only a few hours after filtration a precipitate appears in the samples. At industrial scale, the effluent would need to be treated as soon as possible to avoid scaling problems in the circuit.

**Table 7.1.-** Hydrometallurgical process effluent average composition (mg/L) and pH

| | $SO_4^{=}$ | $Cl^-$ | $F^-$ | Al | Mg | Na | Fe | Ca | Si | K | pH |
|---|---|---|---|---|---|---|---|---|---|---|---|
| UT | 42200 | 876 | 1450 | 4475 | 3254 | 1025 | 2031 | 440 | 423 | 480 | 2.5 |

In this chapter, the effluent purification for safe reutilization is studied in order to provide an integrated process with the minimum wastes output. As stated in Chapter 6, a SAVMIN™ approach was selected, and in this chapter its process parameters are tailored to achieve the optimum effluent purification for its recycling.

## 7.2. Integrated process

As described in Chapter 6, SAVMIN™ consists of three steps. First, lime ($Ca(OH)_2$) is added to remove sulfates and metals as gypsum ($CaSO_4 \cdot 2H_2O$) and hydroxides ($Me(OH)_x$) respectively. Second, lime ($Ca(OH)_2$) and aluminum hydroxide ($Al(OH)_3$) are added to precipitate ettringite ($Ca_6Al_2(SO_4)_3(OH)_{12} \cdot 26H_2O$), and finally $CO_2$ is added to neutralize the pH and precipitate $CaCO_3$. In this chapter, the first two steps of SAVMIN™ process were tested to determine the achievable purification levels for our effluent. Additionally, partial substitution of lime ($Ca(OH)_2$) with limestone ($CaCO_3$) was studied as a potential economic improvement of the process.

Material stream recycling reduces raw material consumption and, consequently, wastes output, resulting in a more efficient process. Therefore, effluents with different

purification levels were assessed to be reintroduced as feed water for the hydrometallurgical process leaching solution.

### 7.2.1. Gypsum precipitation

As stated in the previous chapter, the most used method for bulk sulfate removal is gypsum precipitation by lime addition. Metal hydroxides and calcium fluoride also precipitate because of the high pH and $Ca^{2+}$ concentration in the solution respectively. The reactions that take place in this process are:

$$SO_4^{=} + Ca^{2+} + 2H_2O \rightleftharpoons CaSO_4 \cdot 2H_2O\ (\downarrow)$$

$$Me^{x+} + xOH^- \rightleftharpoons Me(OH)_x\ (\downarrow)$$

$$2F^- + Ca^{2+} \rightleftharpoons CaF_2\ (\downarrow)$$

*Where *Me*, in this case can be Al, Mg and Fe.

Room temperature (25 °C) was selected, as gypsum solubility increases with higher temperatures,[1,2] and cooling the amount of effluent involved in the process would be disproportionately expensive at industrial scale. Solid lime was added to avoid increasing the effluent volume which would translate in lower sulfate removal efficiencies, as lime is slightly soluble in water (1.85 g/L at 25 °C).[3]

Gypsum precipitation was tested by adding different Ca excess, being 0 % stoichiometric proportions, and 100 % twice the stoichiometric quantity, based on sulfate concentration. For this calculation, the Ca already present in the solution was not computed due to its low concentration. Then gypsum precipitation equilibrium is reported to require from several minutes up to 5 h;[2,4] therefore, 24 h reaction time was used to ensure equilibrium conditions. The tests were carried out with 0.5 M $H_2SO_4$, and the UT effluent, as impurities in the solution could affect gypsum solubility,[4] as observed in Figure 7.1. While the variation of the Ca excess did not significantly alter sulfate removal from 0.5 M $H_2SO_4$, it greatly affected sulfate removal from the UT effluent. With up to a 20 % Ca excess, the sulfate equilibrium concentrations remained constant at approximately 3300 mg/L, dropped to 1800 mg/L at 50 % Ca excess, and rose again to 2400 mg/L at 100 % Ca excess. In view of these results, 50 % Ca excess was selected for

the gypsum precipitation by lime addition (GP process) as it provided the lowest final sulfate concentration.

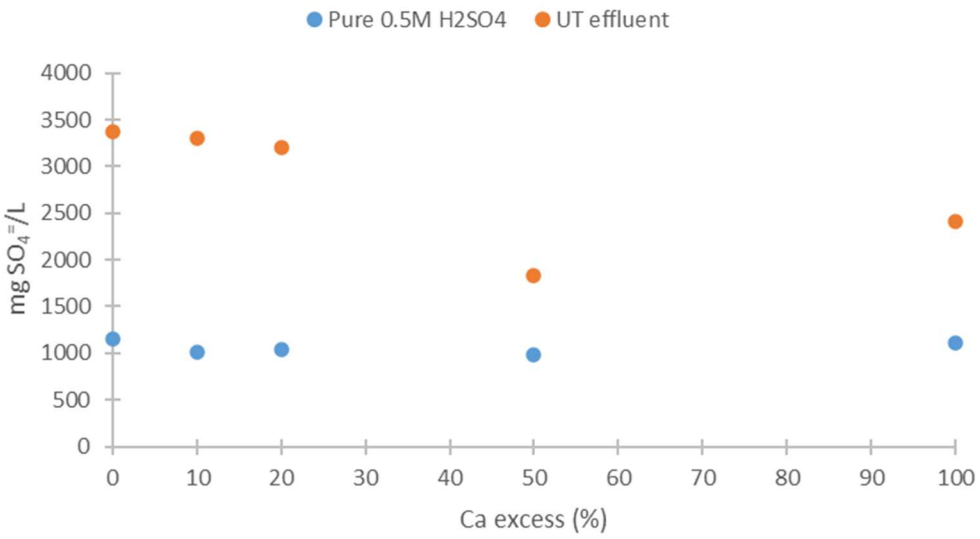


**Figure 7.1.-** Gypsum precipitation by lime addition (24 h)

Once the Ca excess was determined, the time evolution of the reaction was monitored by measuring the conductivity and pH, to determine the required time for the precipitation. As shown in Figure 7.2, in the first 3 minutes after the lime addition to the solution, a sharp decrease in conductivity was observed (from 63.9 to 6.2 mS/cm), followed by a slight increase (from 6.2 to 9.3 in 57 minutes). The pH showed an analogous behavior, as it increased sharply at first (from 2.5 to 10.3 in the first 3 minutes of reaction), followed by a slow increase (from 10.3 to 12.6 in 57 minutes). These data evidence a high reaction rate and thus, 30 minutes reaction time was selected for the GP process as a conservative reaction time.

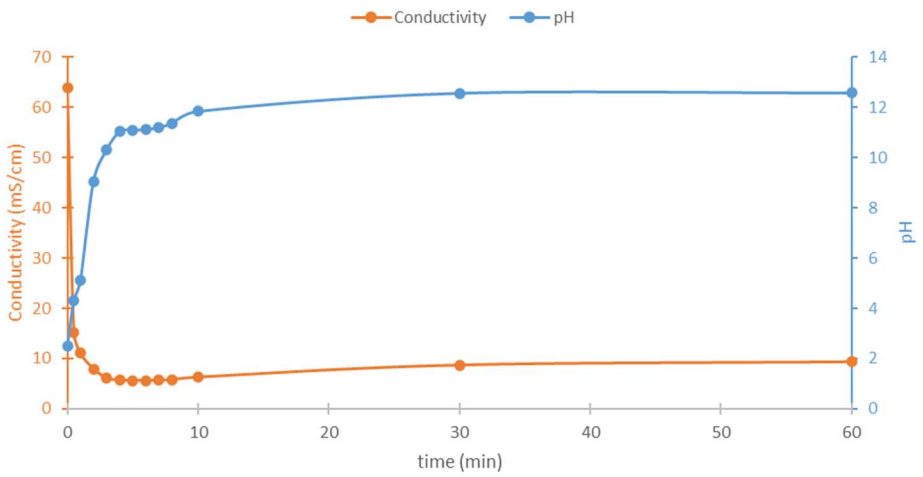


**Figure 7.2.-** Conductivity and pH *vs.* time in GP process

The solid obtained in the GP process was analyzed by X-Ray Diffraction (XRD) technique (Figure 7.3), where the identified phases were gypsum ($CaSO_4 \cdot 2H_2O$, in red), ettringite ($Ca_6Al_2(SO_4)_3(OH)_{12} \cdot 26H_2O$, in blue), and small amounts of basanite ($CaSO_4 \cdot 0.5H_2O$, in green). The presence of basanite was expected as the solid was dried overnight in an oven at 105 °C, and gypsum dehydration starts at temperatures below 100 °C, as seen in Figure 7.A.1, in the appendix.

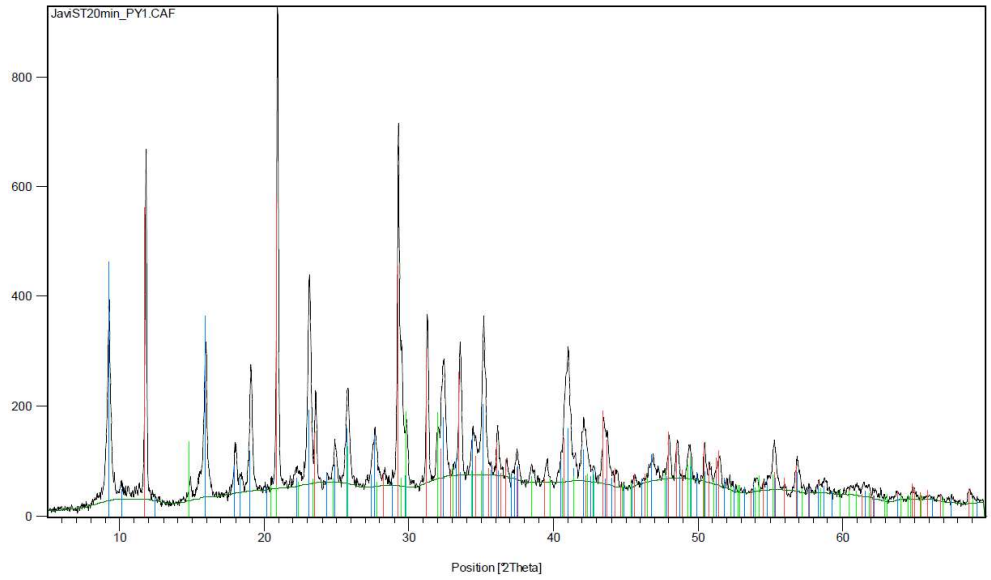


**Figure 7.3.-** XRD diffractogram of the solid obtained in GP process

In the GP process, in addition to sulfate compounds, metal hydroxides, calcium fluoride and silica were removed to trace levels as shown in Table 7.2. These phases were not identified in the XRD diffractogram due to their low concentrations compared to the sulfate phases ones.

**Table 7.2.-** Average composition (mg/L) of UT and GP effluent

| | $SO_4^=$ | $Cl^-$ | $F^-$ | Al | Mg | Na | Fe | Ca | Si | K | pH |
|---|---|---|---|---|---|---|---|---|---|---|---|
| UT effluent | 42200 | 876 | 1450 | 4475 | 3254 | 1025 | 2031 | 440 | 423 | 541 | 2.5 |
| GP effluent | 1748 | 872 | <0.1 | <0.1 | <0.1 | 1185 | <0.1 | 648 | <0.1 | 557 | 12.4 |

As metal removal was part of this chapter's scope, it is interesting to understand the metal hydroxide precipitation mechanisms that take place in GP process. Thus, lime was added to achieve different pH values, promoting the formation of different compounds, and then the obtained effluent was analyzed. As shown in Figure 7.4, by rising the pH from 2.5 (UT effluent) to 5.0, *(i)* Al precipitates as $Al(OH)_3$ because this hydroxide is highly insoluble from mildly acidic pH to mildly basic pH (Figure 7.A.2, in the

appendix), *(ii)* fluoride precipitates as $CaF_2$, because this salt is highly insoluble in a wide pH range[5], *(iii)* Fe precipitates as $Fe(OH)_3$, as its minimum solubility pH is 3.5-4.0 (the minimum solubility of $Fe(OH)_2$ is at pH 9.5), and *(iv)* Si precipitates as $SiO_2$, because Si ions were only soluble as long as there was fluoride available to form a soluble complex ($SiF_6^=$).[6,7] At pH 7.0, Fe is completely removed from the solution, and Mg is partially precipitated as $Mg(OH)_2$, which is soluble at acidic and neutral pH, and insoluble at pH 9 and higher. At pH 9 only trace amounts of Mg remained in the solution, and this metal was completely removed at pH 12.4. At this pH, $Al(OH)_3$ is partially solubilized, and $Al^{3+}$ appears precipitated as ettringite,[4,8,9] the only aluminum phase detected in the XRD diffractogram of the GP precipitate (Figure 7.3).

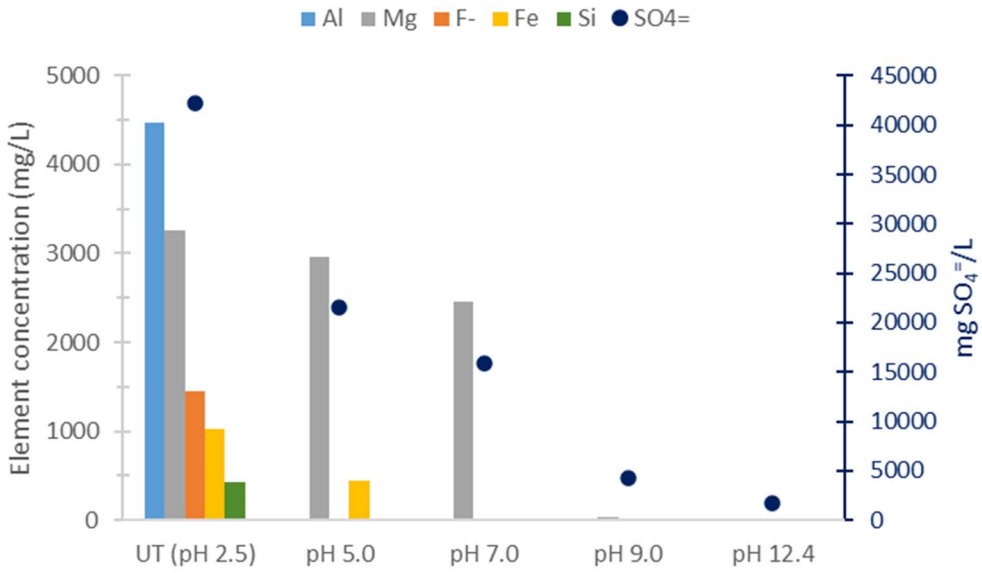


**Figure 7.4.-** Element concentration in effluent *vs.* pH

The designed GP process removes 95 % of the sulfates from the solution by increasing the pH of the solution to 12.4, requiring a 51 g/L lime dosage. The GP process economics could be improved by partially replacing lime with limestone, as limestone is reported to be the most cost-effective treatment for neutralization of acid water to pH 7.2.[10] To asses this alternative process, first the approximate amount of limestone necessary to achieve neutral pH was determined by adding limestone to the effluent while monitoring the pH of the solution (Figure 7.5). The pH increased from 2.5 to 6.5 when adding 52 g/L lime dosage. From this point, the pH showed an asymptotic behavior, requiring additional 80 g/L to increase the pH by only 0.5 points, and additional 123 g/L to further increase it by 0.3 points.

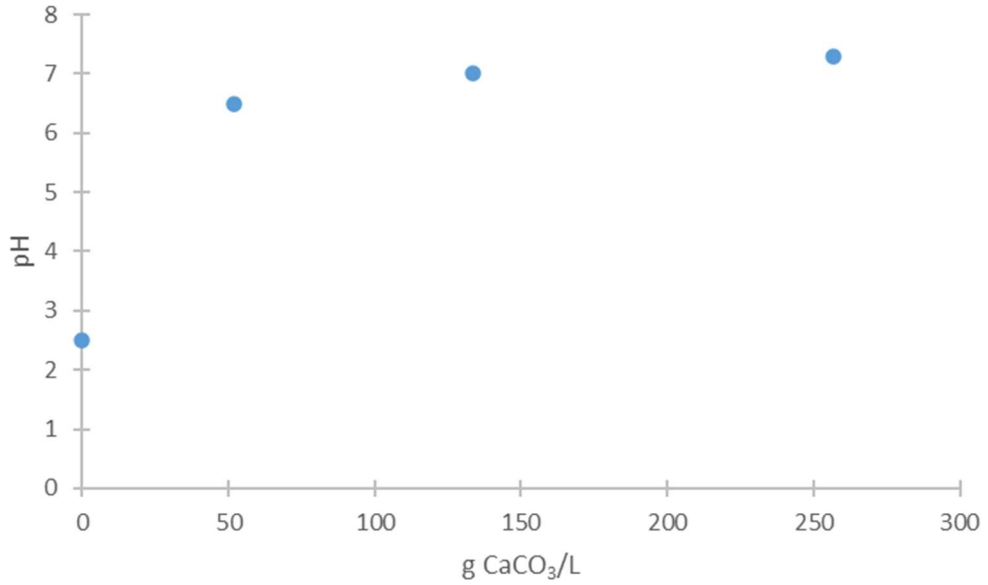


**Figure 7.5.-** Limestone dosage for different pH

Once the limestone dosage was established at 52 g/L, equivalent to a 20 % Ca excess, the evolution of the precipitation was monitored by measuring the conductivity and the pH of the solution. This gypsum precipitation process using limestone until neutral pH was named GP' in order to differentiate it from the gypsum precipitation process in one step with lime (GP process). Figure 7.6 shows that, in the first 2 minutes after the limestone addition, the conductivity sharply decreased (from 63.9 to 12.6 mS/cm), and then stabilized at 11 mS/cm.

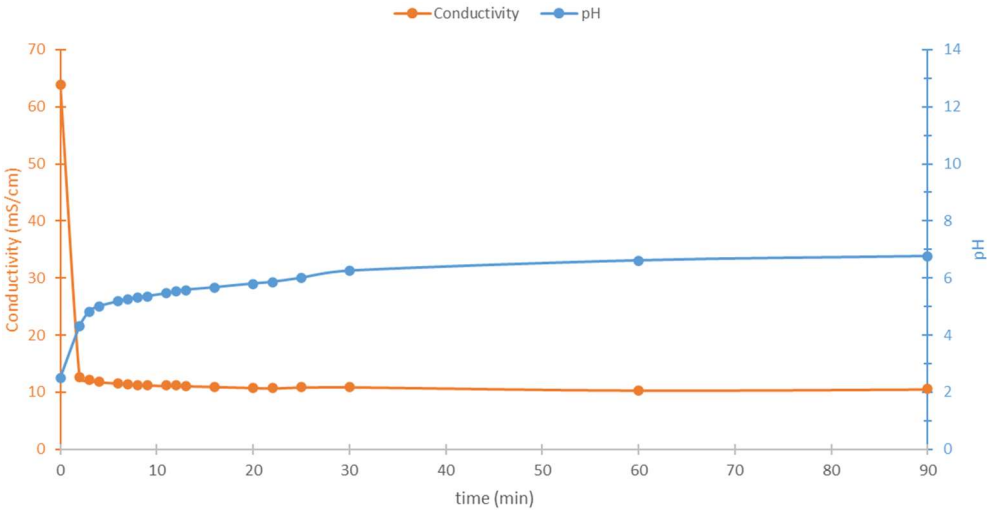


**Figure 7.6.-** Conductivity and pH *vs.* time in GP' process

The pH sharply increased at first (from 2.5 to 4.8 in the first 3 minutes of reaction), continued to increase at lower rate (from 4.8 to 6.9 in 27 minutes) and stabilized at 6.9.

These data evidence that the reaction was completed in 30 minutes and, thus, it was selected for the GP' treatment. In this process, 80 % of the sulfates were removed from the effluent, and the $F^-$, Al, Fe, and Si down to trace levels (Table 7.3). The NaKCl salts remained soluble, as in the GP process, and Mg was partially removed, in agreement with the previous metal precipitation *vs.* pH study.

**Table 7.3.-** Average composition (mg/L) of the UT, GP and GP' effluent

| | $SO_4^=$ | $Cl^-$ | $F^-$ | Al | Mg | Na | Fe | Ca | Si | K | pH |
|---|---|---|---|---|---|---|---|---|---|---|---|
| UT effluent | 42200 | 876 | 1450 | 4475 | 3254 | 1025 | 2031 | 440 | 423 | 541 | 2.5 |
| GP effluent | 1748 | 872 | <0.1 | <0.1 | <0.1 | 1185 | <0.1 | 648 | <0.1 | 557 | 12.4 |
| GP' effluent | 8174 | 877 | <0.1 | <0.1 | 2271 | 865 | <0.1 | 416 | <0.1 | 516 | 6.9 |

The GP' precipitate XRD diffractogram (Figure 7.7) was very similar to the GP precipitate, where gypsum ($CaSO_4 \cdot 2H_2O$, in red), calcite ($CaCO_3$, in blue), and small amounts of basanite ($CaSO_4 \cdot 0.5H_2O$, in green) were the identified phases. As in the GP precipitate, the main phases concealed other minority ones, *i.e.* metal hydroxides, silica and calcium fluoride. The absence of ettringite peaks, however, agrees with the previously proposed hypothesis, in which ettringite precipitates at higher pH, where aluminum hydroxide is dissolved again and this high pH favors ettringite formation.[4,8,9]

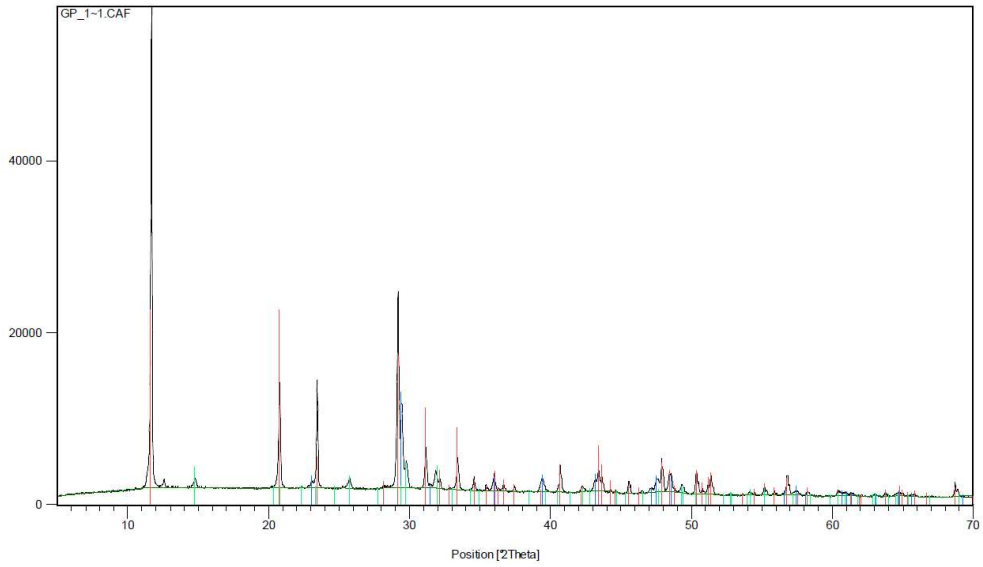


**Figure 7.7.-** XRD diffractogram of the solid obtained in GP' process

The GP' process removed sulfates from 42200 to 8174 mg/L by using limestone instead of lime. Once the pH is neutral, lime is the best reactant to remove sulfates from the solution down to gypsum equilibrium concentrations. This step was named GP'' in order to distinguish it from the previous lime-only addition process GP. As stated before,

the effluent composition strongly affects sulfate removal results and, thus, it was necessary to test different lime excesses for GP''. The tested lime amounts (Figure 7.8) showed a linear behavior between the lime dosage and the sulfate removal which can be attributed to the less complex nature of the GP' effluent compared to the UT effluent. The pH was stable at 12.3 for Ca excesses below 20 % and then it presented an exponential behavior, reaching pH 13.0 for a 50 % Ca excess. At a 30 % Ca excess the obtained pH and effluent composition (Table 7.A.1 in the appendix) were equivalent to the GP treatment, and thus this percentage was selected to better compare both processes (GP and GP'+GP'').

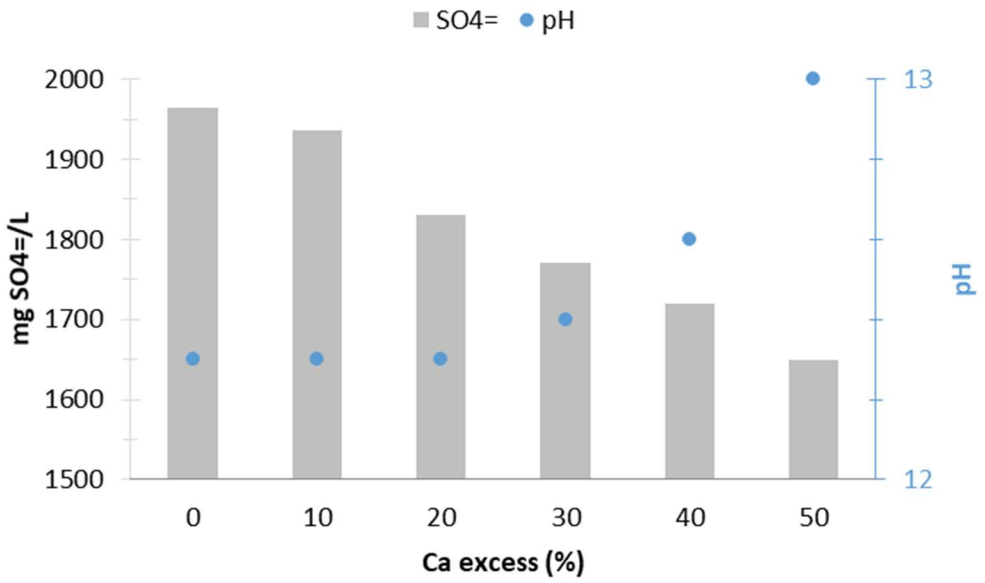


**Figure 7.8.-** Sulfate concentration and pH *vs.* Ca excess in GP''

The GP'' process evolution was monitored by measuring conductivity and pH, to determine the required time for the precipitation. As shown in Figure 7.9, the pH sharply increased from 6.9 to 10.8 in the first 0.5 minutes of reaction and remained stable afterwards. The conductivity, on the other hand, increased from 10 to 16 mS/cm in the first 3 minutes, decreased to 13.6 in the next 10 minutes, and stabilized at 13.7. Despite the sulfate removal, the final conductivity was higher than the initial, probably due to the lime excess. The XRD diffractogram of the solid obtained in GP'' (Figure 7.A.3 in the appendix) was similar to those obtained from GP and GP' with the particularity that, in addition to the previously identified phases, brucite ($Mg(OH)_2$, in grey) was detected due to its higher proportion than in the GP and GP' precipitates.

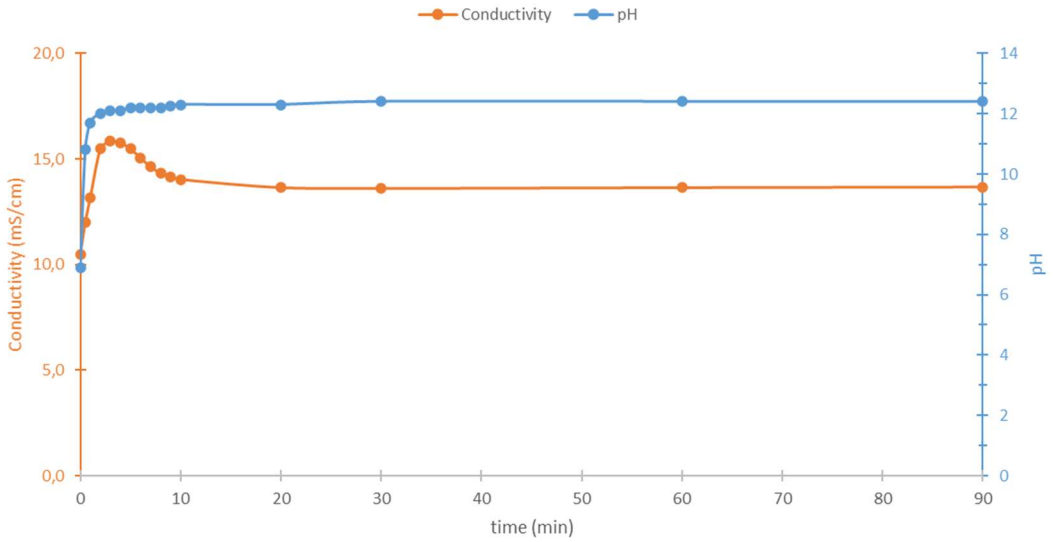


**Figure 7.9.-** GP'' pH and conductivity (mS/cm) evolution in time

In the combined process GP'+GP'', 52 g/L of limestone and 8.5 g/L of lime substituted the 51 g/L of lime needed in the GP, as shown in Figure 7.10. According to the literature, the use of limestone is 70 % more economic than lime, making the GP'+GP'' relative reactant cost approximately 50 % of that of GP. Moreover, the partial substitution of lime with limestone resulted in a 10 % lower sludge production, expressed in dry basis.

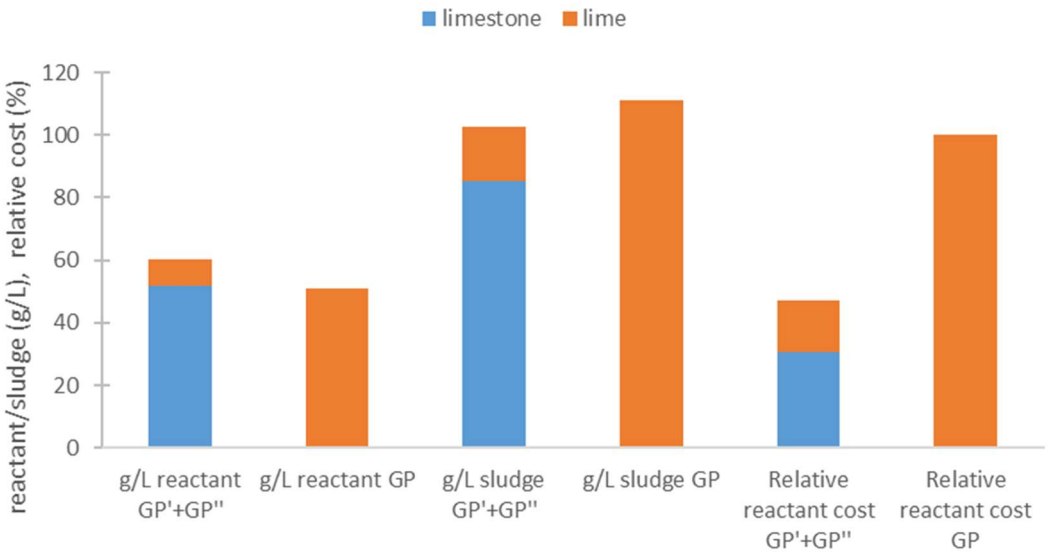


**Figure 7.10.-** Reactant dosage, produced dry sludge and relative reactant costs in GP'+GP'' and GP processes

According to the reactant relative costs and produced sludge amounts, the combined limestone/lime process was considered the optimum alternative to remove sulfates from the effluent.

### 7.2.2. Ettringite precipitation

The second step in the SAVMIN™ process is the ettringite precipitation by adding aluminum hydroxide and lime and maintaining the solution pH between pH 10.0 and 13.0, where sulfate concentration is reduced from the gypsum equilibrium concentration (approximately 1700 mg/L in GP/GP'' effluent) to below 200 mg/L.[7,11]

$$6\,Ca^{2+} + 3\,SO_4^{=} + 2\,Al^{3+} + 12\,OH^- + 26\,H_2O \rightleftharpoons Ca_6Al_2(SO_4)_3(OH)_{12}\cdot 26H_2O(\downarrow)$$

The GP effluent was used for the ettringite precipitation tests because it is equivalent to the GP'' effluent and easier to prepare at lab scale. The tests were carried out with 0, 20 and 50 % Ca and Al excess in relation to sulfates, disregarding the dissolved Ca in the GP effluent. The pH and conductivity did not vary in 20 h, producing the effluents shown in Figure 7.11:

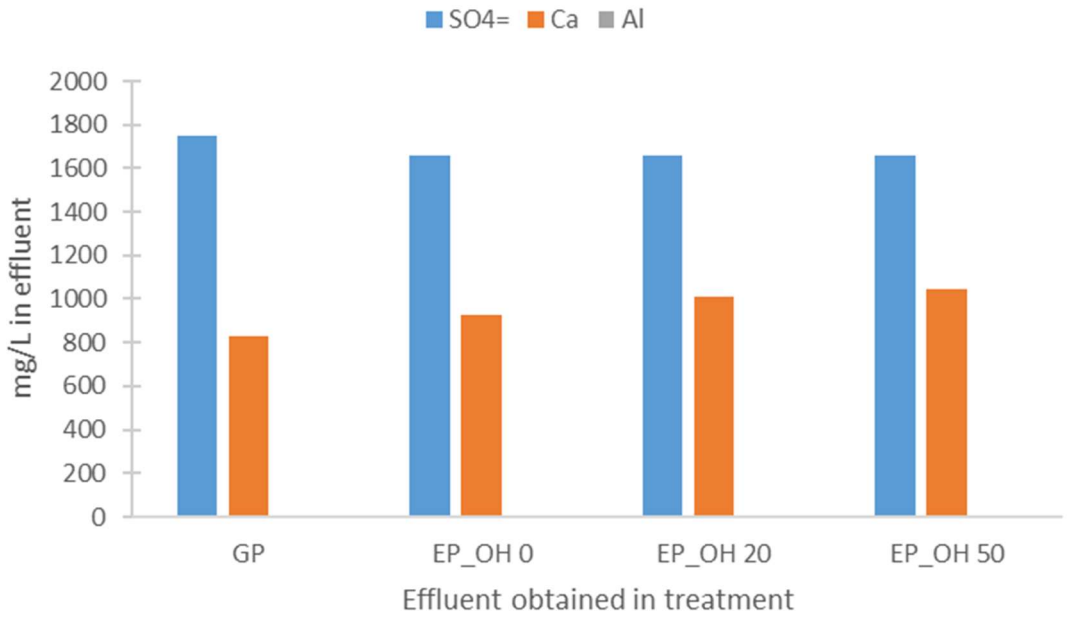


**Figure 7.11.-** Composition of the effluents obtained in GP and EP processes

After 20 h contact time the sulfate concentration only decreased by 5.6 %, regardless the Ca and Al excess. This fact, together with the marginal Al and Ca increase in concentration suggests that none of the reactants was dissolved, and therefore only trace amounts of ettringite could be formed. This fact was confirmed by the XRD analysis (Figure 7.12) of the solid obtained in the EP_OH 0 treatment, in which calcite ($CaCO_3$, in red), gibbsite ($Al(OH)_3$, in blue), portlandite ($Ca(OH)_2$, in green) and a small amount of ettringite ($Ca_6Al_2(SO_4)_3(OH)_{12}\cdot 26H_2O$, in grey) were the identified phases. Calcite presence

is common in ettringite synthesis, because of the high reactivity between calcium and carbonate ions, which probably come from atmospheric $CO_2$ dissolution in the high pH liquid.[12]

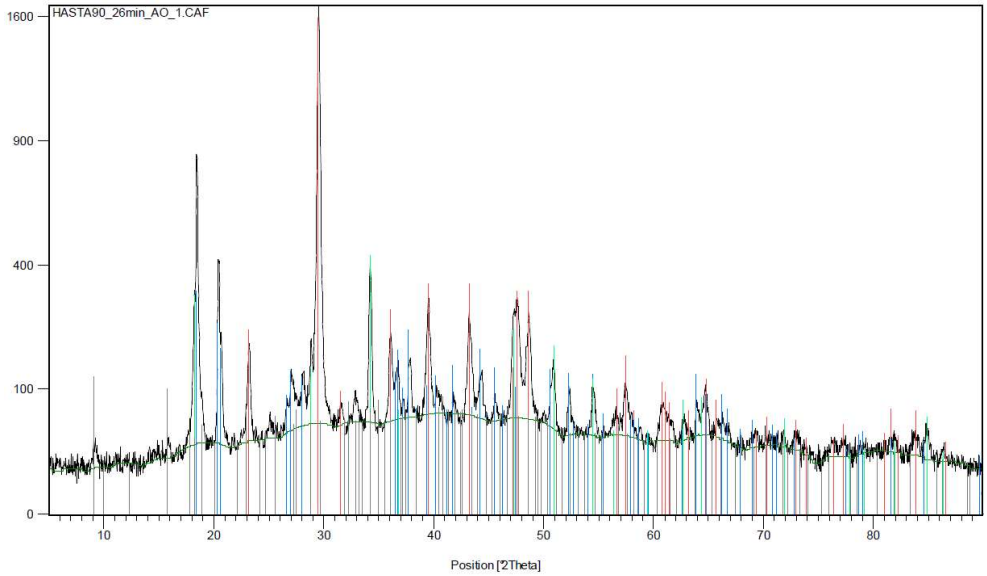


**Figure 7.12.-** XRD diffractogram of the precipitate from EP_OH 0

The low ettringite formation obtained in the previous tests was attributed to the low aluminum hydroxide solubility, and therefore more soluble Al sources were tested to confirm this hypothesis. Among the soluble aluminum salts, aluminum chloride and nitrate were selected which, opposite to the aluminum hydroxide, maintain the pH in the ettringite formation range because of the Lewis acid nature of $Al^{3+}$. Thus, aluminum chloride (EP_Cl 0) and nitrate (EP_$NO_3$ 0) were tested as Al sources, together with lime, at stoichiometric proportions and along 1 h reaction time, achieving sulfate concentrations down to 50 mg/L in both cases. These results confirmed that the low aluminum hydroxide solubility prevented ettringite formation. Additionally, it was found that, unlike in gypsum precipitation, no calcium or aluminum excess was required to aid the reaction, due to the extremely low solubility of ettringite ($K_{sp}\sim10^{-45}$).[13] The sulfate, calcium and aluminum contents in the GP effluent and after ettringite precipitation (EP_Cl 0 and EP_$NO_3$ 0 effluents) are presented in Figure 7.13, showing that aluminum was quantitatively dissolved and reacted, as no aluminum was detected in the final solutions. The calcium concentration slightly decreased from the inicial GP concentration, indicating that along with ettringite, other aluminum-free calcium phases were precipitated, *e.g.* calcite or gypsum. Although both salts produced extensive sulfate removals, $AlCl_3$ was

selected for the ettringite precipitation (EP) process to avoid adding new ions (nitrates) into the effluent.

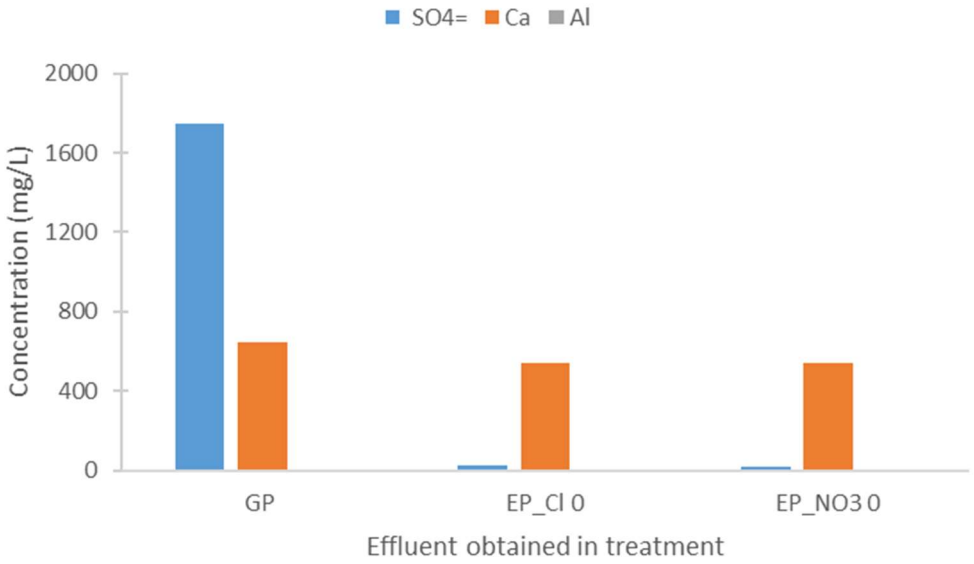


**Figure 7.13.-** Composition of the effluents obtained in GP and EP processes

With the selected aluminum source and excess, the reaction was monitored by measuring pH and conductivity (Figure 7.14) to determine the evolution of the ettringite precipitation, which is reported to require 30 to 60 minutes at room temperature.

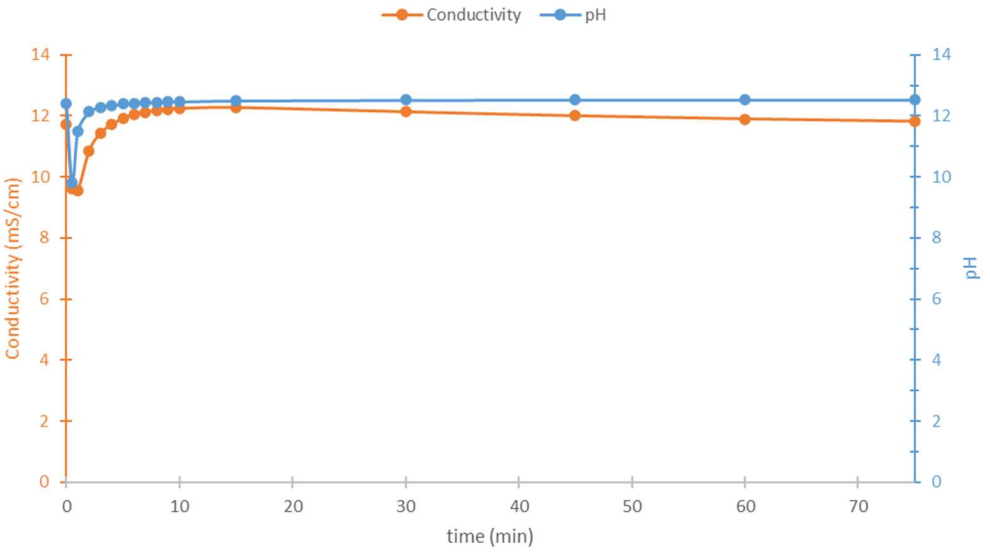


**Figure 7.14.-** EP pH and conductivity (mS/cm) evolution in time

The conductivity and pH showed a similar behavior, decreasing abruptly in the first 0.5 minutes, recovering the initial value in the following 4 minutes and stabilizing at their

original values afterwards. According to these data and the reported literature values, 30 minutes were selected as a conservative reaction time for ettringite precipitation (EP).

The solid obtained in the EP process was analyzed by XRD (Figure 7.15), where the presence of calcite ($CaCO_3$, in red) and basanite ($CaSO_4 \cdot 0.5\ H_2O$, in blue) was confirmed, and only small amounts of ettringite ($Ca_6Al_2(SO_4)_3(OH)_{12} \cdot 26H_2O$, in grey) were detected. This last result was unexpected considering the observed high sulfate removal. The elevated background indicates the presence of unidentified amorphous phases which most probably contain the aluminum removed from the solution (Figure 7.13).

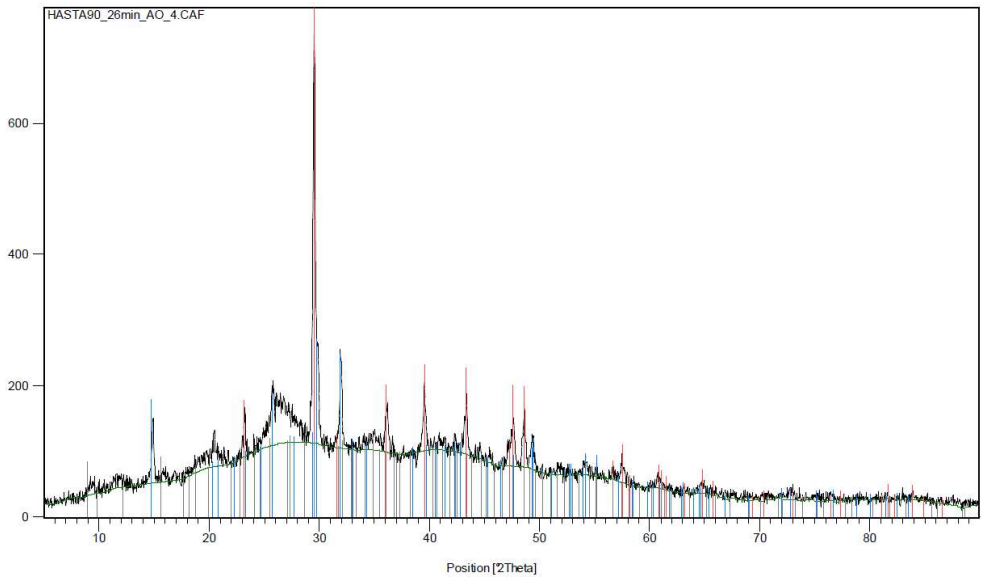


**Figure 7.15.-** XRD difractogram of the precipitate from EP

The presence of calcite, coming from atmospheric $CO_2$, suggested a possible relationship between the $CO_2$ presence and the absence of significant amounts of ettringite in the precipitate. It has been experimentally demonstrated that calcium aluminate phases in the presence of carbonates lead to different hydrates compared to carbonate-free system.[8,14–16] Moreover, the carbonate concentration in equilibrium with atmospheric $CO_2$ ($3 \cdot 10^{-3}$ mol $CO_3^=$/L in GP effluent) is enough to decompose ettringite into calcite, gypsum and alumina gel,[17,18] as it is frequently higher than the ettringite stability limit reported in literature ($8.39 \cdot 10^{-6}$ mol $CO_3^=$/L).[8] Although basanite and calcite, detected in the EP solid by XRD, are products typically obtained in ettringite decomposition by carbonate presence,[14] these phases are soluble in the solution

conditions. The final sulfate concentration, therefore, suggested that ettringite decomposition occurred once the solid had been separated from the solution.

Thermal decomposition of ettringite, as it only affects the obtained solid, was a better explanation for the low amounts of ettringite found in the precipitate, which was dried overnight at 105 °C. Ettringite is reported to be generally stable up to 110 °C, and its thermal decomposition to occur suddenly at temperatures between 110 and 125 °C, in which basanite, anhydrite and calcium aluminate monosulfate ($Ca_4[Al(OH)_6]_2SO_4 \cdot 8H_2O$) are formed.[19–23] The ambient moisture was also reported to impact ettringite decomposition, decreasing its thermal decomposition temperature to 93 °C under drying conditions.[24] Additionally metaettringite, a product from ettringite decomposition, is typically formed at temperature ranges between 50 and 100 °C as a consequence of reducing water vapor pressure below 100 mm Hg.[22]

To confirm this thermal decomposition, the EP solid was dried in a desiccator at room temperature and then analyzed by XRD (Figure 7.16) where ettringite ($Ca_6Al_2(SO_4)_3(OH)_{12} \cdot 26H_2O$, in red) was found to be the main phase, accompanied with small amounts of calcite ($CaCO_3$, in blue).

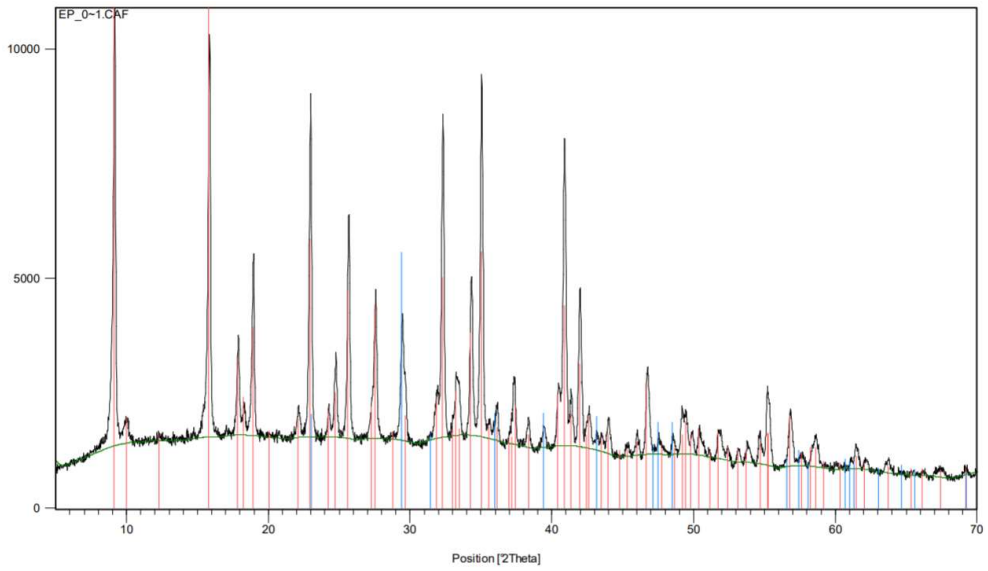


**Figure 7.16.-** XRD precipitate from EP dried in dessicator

Consequently, ettringite thermal decomposition needs to be taken into account if the crystal structure plays an important role in its application, which will be discussed in section 7.3 of this chapter.

### 7.2.3. Effluent recyclability

The scope of this chapter is to purify the effluent to be recycled into the hydrometallurgical process to reduce the volume of produced residues while avoiding scaling problems in the circuit. In the previous sections of this chapter, three effluents suitable to be recycled into the hydrometallurgical process were produced:

**Table 7.5.-** Average chemical composition (mg/L) and pH of GP and EP effluents

| | $SO_4^=$ | $Cl^-$ | $F^-$ | Al | Mg | Na | Fe | Ca | Si | K | pH |
|---|---|---|---|---|---|---|---|---|---|---|---|
| GP’ | 8174 | 879 | <0.1 | <0.1 | 2271 | 865 | <0.1 | 416 | <0.1 | 516 | 6.9 |
| GP’’ | 1770 | 876 | <0.1 | <0.1 | <0.1 | 1200 | <0.1 | 1025 | <0.1 | 560 | 12.4 |
| EP | 70 | 2320 | <0.1 | <0.1 | <0.1 | 1244 | <0.1 | 541 | <0.1 | 405 | 12.3 |

The dissolved solids, in addition to potential scaling problems, need to be heated and pumped through the circuit, which results in an unnecessary energy consumption. Therefore, to select the most appropriate effluent to recycle into the hydrometallurgical process, the incremental improvement of each process shall be considered versus its processing cost. Although multiple parameters affect the economic evaluation (reactor vessel volumes and construction materials, multiple reactant storage, dosing and procurement systems, and number of separation steps among others) only reactant cost was considered.

According to a lab-scale reactant supplier (Sigma Aldrich), anhydrous aluminum chloride is 10 % more expensive than lime. As shown in Figure 7.17, the GP’’ process, which reduces sulfates from 8174 to 1748 mg/L and total dissolved solids from 13.1 to 5.2 g/L by lime addition, entails an additional 54 % reactant cost. To further remove sulfates to trace levels, reactant cost would increase an additional 17 % (80 % from GP’), but the dissolved solids amount would only decrease from 5.2 to 4.6 g/L, due to the chlorides added in the aluminum salt. The GP’’ process significantly improved the effluent (79 % sulfate removal and 60 % less dissolved solids) compared to the additional reactant costs (54 %). On the other hand, the EP process required 17 % additional reactant costs and resulted in an effluent with similar pH and total dissolved solids. Thus, the recycling tests were carried out using the GP’’ effluent, as a balanced option between the cost and the effluent purification level.

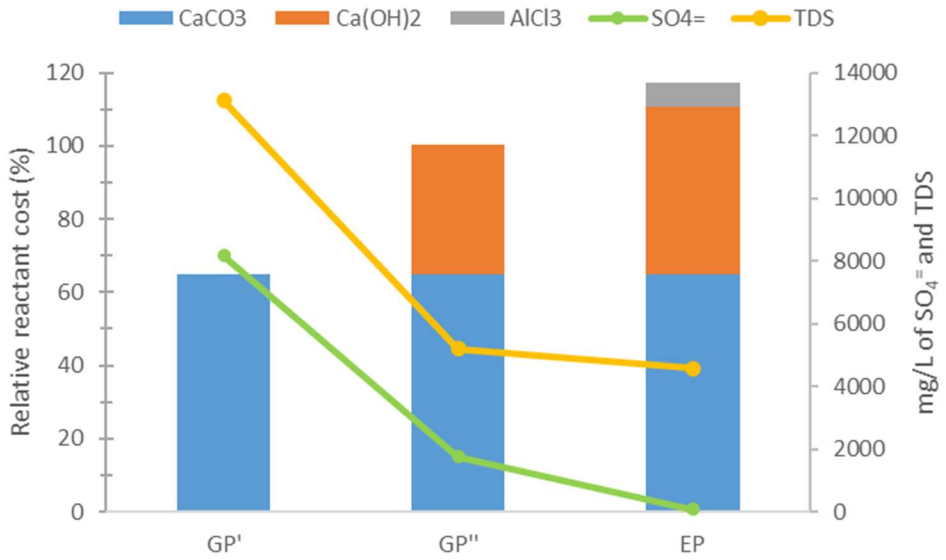


**Figure 7.17.-** Relative reactant cost (%) and mg/L of total dissolved solids and $SO_4^=$

As the pH of the GP'' effluent was 12.4, fresh 98 % $H_2SO_4$ addition was necessary in order to recover the acidity required for the hydrometallurgical process; *i.e.* the effluent is the solvent to make the leaching solution with fresh acid, not the leaching agent itself. When preparing different 0.5 M $H_2SO_4$ solutions, no noticeable differences in the required fresh acid amount were observed between using milliQ water and GP'' effluent as solvent, probably due to the volumes used in the laboratory tests (500-100 mL).

The test where the GP'' effluent was mixed with 98 % $H_2SO_4$ and used to leach Paval sample SCP01 was named 'Reuse 1' and its leaching results were identical to those obtained using fresh 0.5 M $H_2SO_4$, as shown in Figure 7.18:

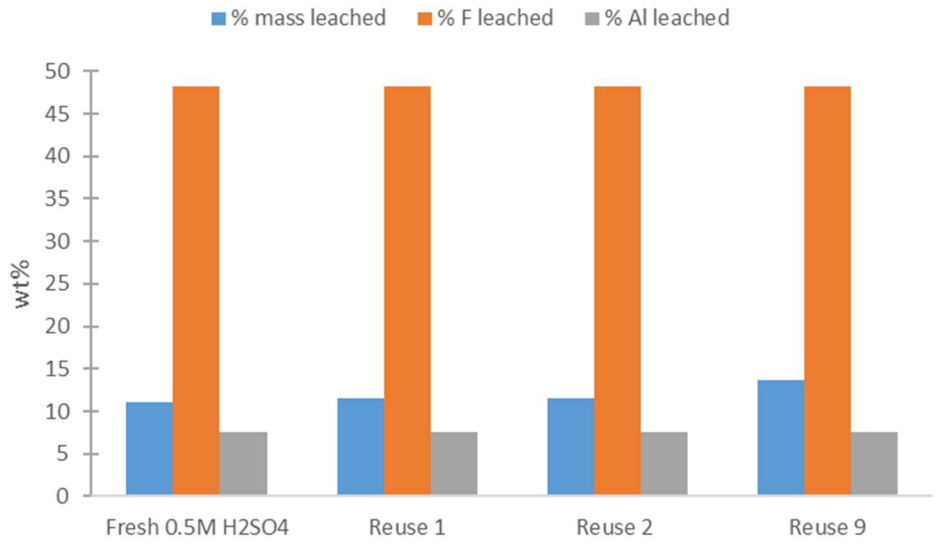


**Figure 7.18.-** Effluent reutilization tests leaching results

The GP effluent from Reuse 1 test (GP 01 effluent) was again mixed with 98 % $H_2SO_4$ and used to leach Paval sample SCP01. This test was named 'Reuse 2', and the leaching results were again identical. In view of the good results for the first two reuses, a synthetic effluent with the chemical composition of an effluent reused 9 times and treated with limestone and lime (GP'' 09 effluent) was prepared and used to leach Paval sample SCP01 obtaining identical results.

To determine the effect of the GP'' reuse on the final solid product composition, the SCP01 Paval sample treated with fresh 0.5 M $H_2SO_4$, and the solids from reutilization 9 were analyzed by XRF and XRD, obtaining the results shown in Figure 7.19:

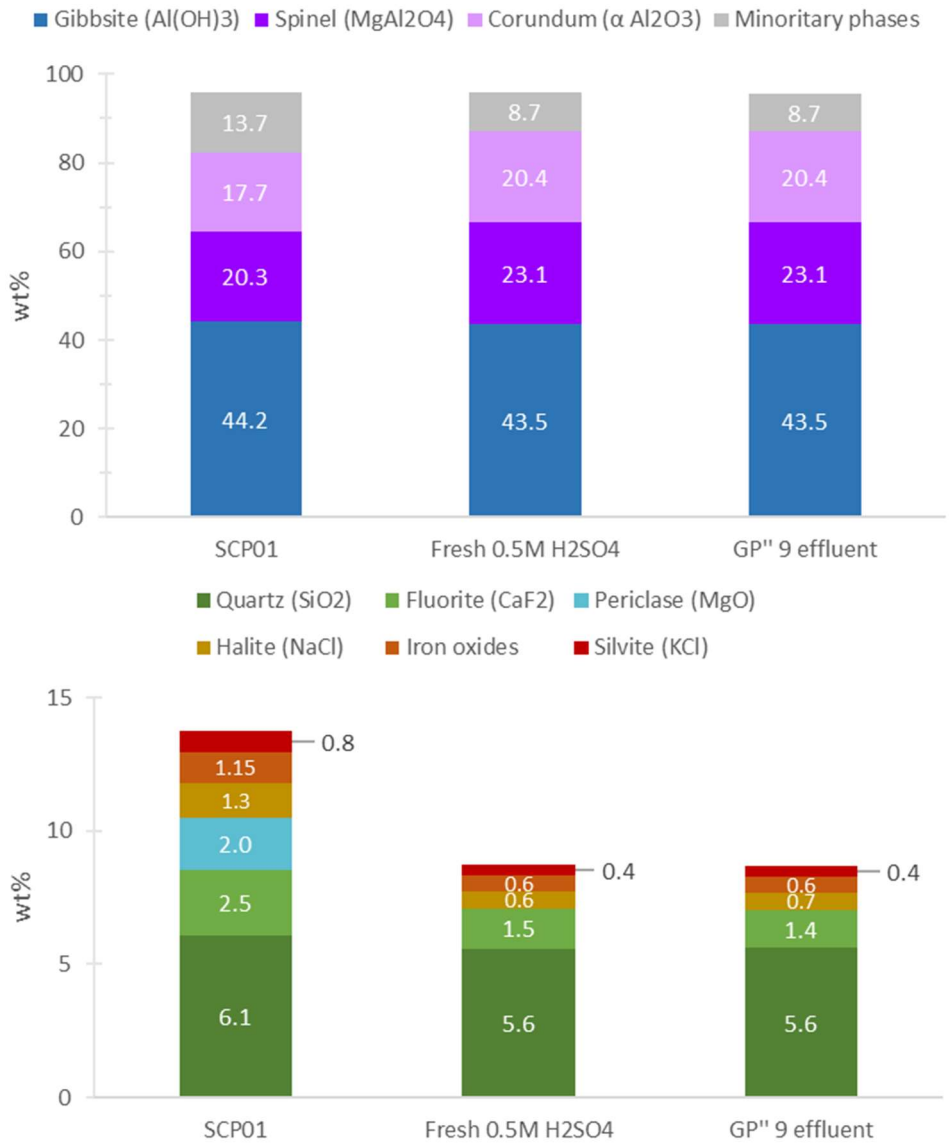


**Figure 7.19.-** Main (up) and minoritary (down) phase composition of SCP01 untreated and treated with fresh and reused effluent

In good agreement with the leaching results shown in Figure 7.18, the treated SCP01 with Reuse 9 had an identical phase composition to that of the obtained when fresh 0.5 M $H_2SO_4$ was used. 50 % of fluoride, 7.5 % of the aluminum (only from the gibbsite phase) along with 27 % Mg, 23 % Si, 54 % Fe, 40 % Ca, 62 % Na and 59 % K were leached. This implies that SCP01 was not contaminated with the elements from GP'', *i.e.* sulfates and other salts and that reutilization of the effluent is chemically viable for at least 9 recycles. The XRD diffractogram of the GP'' 9 (Figure 7.A.4 in the appendix) was also equivalent to the GP'' precipitate, *i.e.* the identified phases were gypsum ($CaSO_4{\cdot}2H_2O$, in red), ettringite ($Ca_6Al_2(SO_4)_3(OH)_{12}{\cdot}26H_2O$, in blue), and basanite ($CaSO_4{\cdot}0.5H_2O$, in green).

Regarding the produced effluents in the hydrometallurgical process, it was noticed that the concentrations of Na, K and Cl proportionally increased with the number of reuses (Figure 7.20) as these elements do not take part in gypsum precipitation.

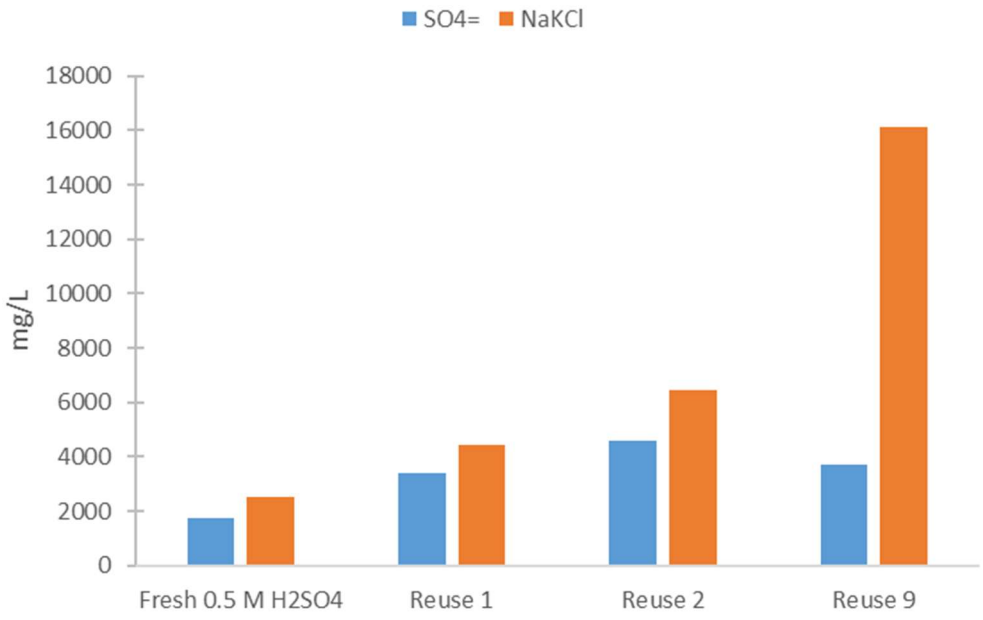


**Figure 7.20.-** Sulfate and NaKCl concentration (mg/L) *vs.* number of reuses

While calcium concentration remained constant with the number of reuses, chloride, sodium and potassium accumulated in the system due to their high solubilities. The accumulation of these elements, in addition to the higher ion strength, influences gypsum thermodynamic equilibrium,[25] ($K_{sp} = 10^{-4.62}$ in aqueous solutions at 25 °C) which is defined by the following equation: [26,27]

$$SO_4^{=} + Ca^{2+} + 2H_2O \rightleftharpoons CaSO_4 \cdot 2H_2O\ (\downarrow)$$

$$K_{sp}(T) = (m_{Ca^{2+}}\gamma_{Ca^{2+}}) \cdot \left(m_{SO_4^{=}}\gamma_{SO_4^{=}}\right) \cdot \alpha_{H_2O}^{n} \approx (m_{Ca^{2+}})(m_{SO_4^{=}})(\gamma_{CaSO_4})^2(\alpha_{H_2O})^2$$

Where *m* is the molal concentration of each ion, *γ* the activity coefficient, *α* the water activity and *n* depend on the hydration state of gypsum, being either 0 (anhydrite), 0.5 (hemihydrate) or 2 (dihydrate). As gypsum formation occurs in an aqueous media, only the dihydrate is formed (*n*=2). Since $K_{sp}$ is constant at a fixed temperature, if any of the variables is changed, the remaining variables will change to balance the equation. On the one hand, when increasing the ionic strength of the solution, the activity coefficient ($\gamma_{CaSO_4}$) decreases and, after passing a minimal point, $\gamma_{CaSO_4}$ increases.[25] On the other hand, Na ion concentration was reported to increase $\gamma_{CaSO_4}$,[25,28] which would result in a gypsum solubility decrease, while K and Cl were reported to largely increase gypsum solubility first, and decrease smoothly afterwards.[2,25,26,29–31] These relationships highlight the complexity of the system that should be carefully considered to optimally design the effluent reutilization.

In view of the intricate interactions between the NaKCl and gypsum solubility, its influence on the ettringite solubility was confirmed by carrying out an EP test to the GP'' 9 effluent (Figure 7.21), which showed a 100 % sulfate concentration increase for a 635 % higher NaKCl concentration.

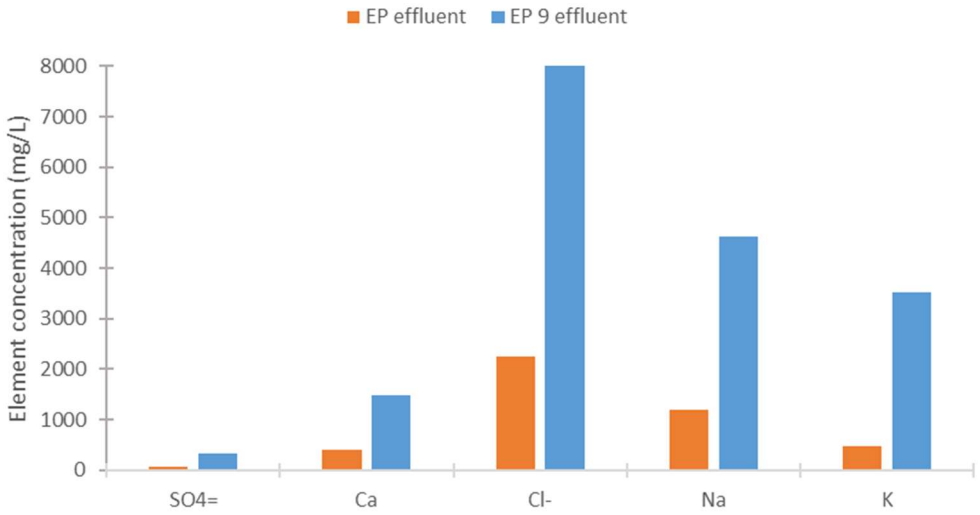


**Figure 7.21.-** Concentration of $SO_4^{=}$, Ca, Cl, Na and K in EP and EP 9 effluents

Despite the higher NaKCl concentration in the effluent, the phase composition of the obtained precipitate (Figure 7.A.5 in the appendix) was found to be equivalent to the

solid obtained in EP. Considering all of the above factors, the number of viable reuses could depend on the allowable sulfate concentration in the EP treated effluent.

## 7.3. Process byproducts applications

In the above-proposed processes for effluent purification several byproducts were produced and, in this section, their possible applications are discussed.

The main byproduct by volume is the EP effluent, accounting for approximately 3.5 L of effluent per kg of treated Paval if no GP'' reuses are carried out. The effluent amount would ideally decrease linearly with the number of reuses, down to 0.4 L per kg of treated Paval with 9 reuses, with increasing salt concentrations as shown in Table 7.6:

**Table 7.6.-** Composition of EP effluent with none and 9 reuses

| | $SO_4^=$ | $Cl^-$ | Ca | Na | K | pH | mS/cm |
|---|---|---|---|---|---|---|---|
| direct use | 70 | 2320 | 541 | 1244 | 405 | 12.3 | 11.8 |
| 9 recycles | 200 | 9635 | 1482 | 4631 | 3532 | 12.3 | 16.3 |

Although the NaKCl accumulation does not affect fluoride selective leaching, this additional material in the process would require higher energy inputs than the fresh leaching agent for pumping, filtering and heating among others. Therefore, a balance shall be considered between the increasing energy demand of the process due to the reuses and the reduction in effluent byproduct generation and treating costs.

The pH of the EP effluent is 12.3 and it contains high NaKCl concentrations and is saturated in lime. Following the SAVMIN™ approach, $CO_2$ released in the GP' process from limestone decomposition, could be used to neutralize this effluent and recover $CaCO_3$ to be reused in the process. This effluent could be suitable to enter the Salt Slag processing as feed water for salt slag treating, where the NaKCl present in the effluent would be recovered and used in the secondary aluminum production.

In the GP'+GP'' processes 100 g gypsum /L of effluent are produced, or 400 g gypsum/kg treated Paval. It is difficult to evaluate if this parameter would be affected by the effluent reuses because *(i)* gypsum solubility increases in the GP'+GP''

process with the reuse NaKCl salt accumulation and *(ii)* the leaching agent to be treated contains increasing sulfate concentrations due, again, to the increase gypsum solubility.

Gypsum can be used as a sulfate source for commercial cements such as Portland,[19] to neutralize red muds from the Bayer process prior to their landfill disposal,[32] as desilication agent for Bauxite and Bayer liquors,[31,33,34] for the production of functional building material that stores solar energy,[35] and for contaminated soil recovery and mineral processing.[2] Moreover, if the precipitate is heated above 100 °C, anhydrite ($CaSO_4$) is obtained instead of gypsum, which is industrially used as binder for screed mortars, floor screed applications, cement production, aerated block production, fertilizer production and the inerting industry among others.[36]

Finally, 8 g of ettringite are produced per liter of EP effluent. In the case when no effluent reuse is carried out, this translates into 30 g of ettringite per Paval kg. This figure would decrease with the effluent reuses but, considering the effect of the NaKCl accumulation on the ettringite solubility, the decrease is not expected to be linear.

As described in Chapter 6, aluminum hydroxide and gypsum can be obtained from the ettringite decomposition by acid attack.[4,7,8,11,15,19,37–44] Additionally, ettringite can be used as the main cementing compound in a number of calcium aluminate and gypsum based formulations,[19] as well as sorbent for arsenate.[12,45] However, arsenate was found to be removed more efficiently by coprecipitating with ettringite by substituting $SO_4^=$ in its structure. This is possible because ettringite's complex crystal structure is able to include many other ionic components within the crystal lattice, a characteristic that could be exploited to immobilize hazardous chemicals from external effluents, providing an additional source of income.

The ettringite structure enables, on one hand, the replacement of sulfate with oxyanions of similar structure and radius, such as $CrO_4^=$,[47,51–53] $AsO_4^-$,[43,47,51–53] $VO_4^-$, $SeO_4^=$,[47,51–53] $B(OH)_4^-$, $BO_3^=$, $SO_3^=$, $CO_3^=$, $IO_3^-$,[3] $MoO_4^=$,[43,46,48–50,52,53] $BrO_3^-$ and $NO_3^-$.[52] On the other hand, divalent and trivalent cations such as $Ni^{2+/3+}$, $Co^{3+}$, $Ti^{3+}$,[46] $Cr^{3+}$,$Pb^{2+}$, $Zn^{2+}$,[43,47,54,55] $Cu^{2+/3+}$, $Cd^{2+}$, $Fe^{2+/3+}$,[47] $Sr^{2+}$,[56] $Ba^{2+}$,$Hg^{2+}$,[46,56] $Mn^{2+/3+}$, $U^{3+}$,[57] Ga and Ge[3] can substitute $Ca^{2+}$ and $Al^{3+}$ in the estructure. This potential line needs to consider the

possibility that ettringite may become a hazardous waste when certain compounds are incorporated in its structure.

## 7.4. Conclusions

In this chapter, the reutilization of the hydrometallurgical effluent was studied to provide an integrated process with low material input and minimum residue output. In order to achieve this goal, a purification step of the original effluent was required due to the scaling nature of the untreated liquid stream. For this purification, a SAVMIN™ approach was used, tailoring the reactants and their dosage for this particular process. The block diagram of the designed integrated process is shown in Figure 7.22.

The SAVMIN™ first step is the bulk sulfate and metal removal, as gypsum and hydroxides respectively, by lime addition. With a 51 g/L lime dosage (GP), sulfate concentration in the UT effluent decreased from 42200 to 1748 mg/L, the metals were removed to trace levels, and the pH increased from 2.5 to 12.4 in 30 minutes. This process economics was improved by partial substitution of lime with limestone which, according to literature, is 70 % more economic. This limestone/lime process (GP'+GP'') produced an equivalent effluent with a 42 g/L limestone and 8.5 g/L lime dosage in approximately 50 minutes, while reducing sludge production by 10 % and reactant costs by 50 %.

The SAVMIN™ second step is sulfate removal as ettringite, by lime and aluminum hydroxide addition at a pH between 10.0 and 13.0. The low solubility of aluminum hydroxide was found to prevent ettringite formation, and by changing the aluminum source to aluminum chloride, sulfate concentration decreased from 1748 to 70 mg/L in 30 minutes using a 2.5 g/L lime and 1.1 g/L aluminum chloride dosage. This step process (EP) required 17 % additional reactant costs and resulted in an effluent with trace sulfate concentrations, and similar pH and total dissolved solids (NaKCl and $Ca(OH)_2$).

Recycling tests were carried out using the GP'' effluent, as a balanced option between the effluent purification level and its reactant costs. GP'' effluent was found to be successfully reused for at least 9 recycles, regardless of the NaKCl and sulfate accumulation in the stream. Similarly, the sulfate concentration of GP'' 9 effluent was

decreased to 140 mg/L by EP process, obtaining an effluent high in NaKCl and lime. This effluent would be suitable to enter the Salt Slag processing after a possible carbonation step to neutralize its pH and recover limestone for the GP' process.

In addition to the EP effluent, gypsum/anhydrite and ettringite were produced in the effluent purification processes. Gypsum and anhydrite have several applications, such as cement industry, Bayer red muds neutralization, screed mortar applications, contaminated soil recovery or mineral processing. Ettringite could be used as cementing compound, as sorbent, and dissolved by acid attack to produce aluminum hydroxide and gypsum. Alternatively, the complex crystal structure of ettringite makes it an interesting solid to immobilize hazardous chemicals from external effluents, providing an additional source of income.

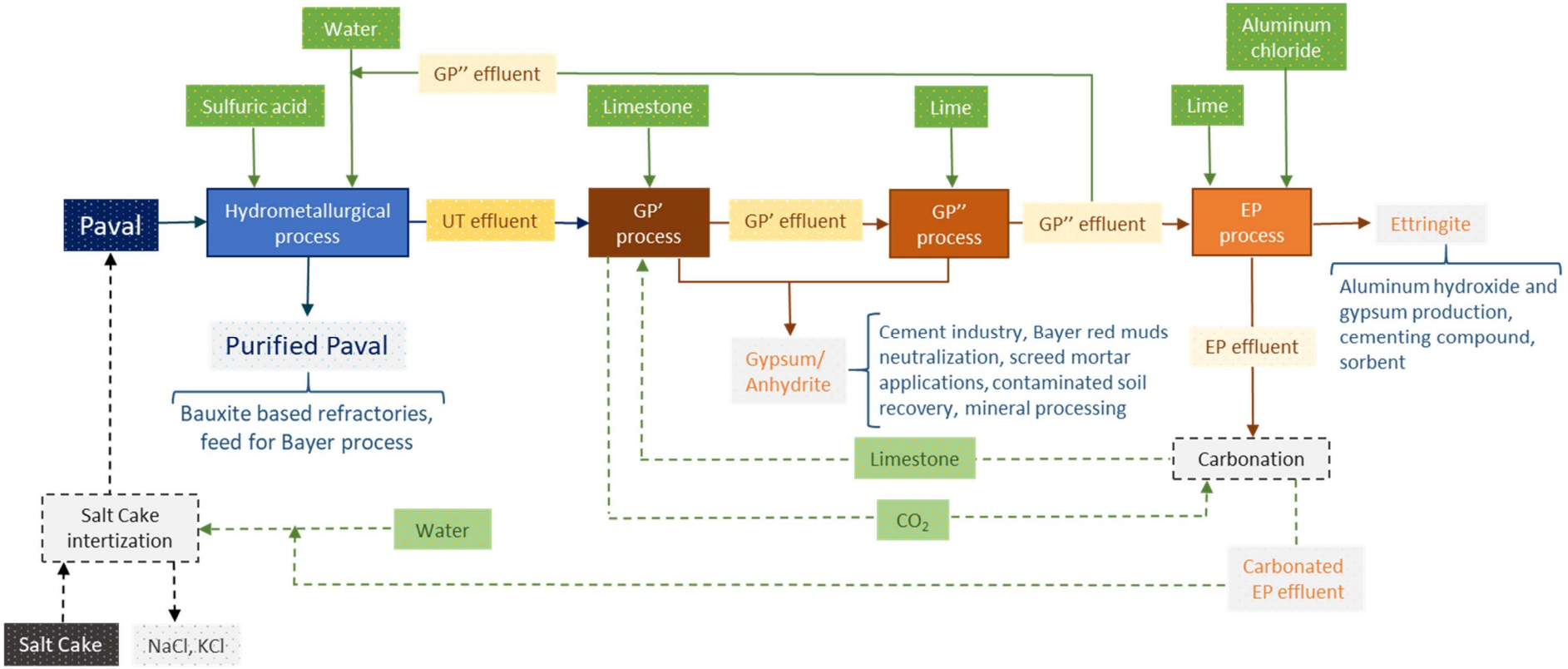


Hydrometallurgical process: 4 L of 0.5 M $H_2SO_4$ per kg of SC Paval at 50 °C for 60 minutes
GP': Gypsum precipitation process by 52.0 g/L limestone dosage addition at room temperature for 30 minutes
GP'': Gypsum precipitation process by 8.5 g/L lime dosage addition at room temperature for 20 minutes
EP: Ettringite precipitation process by 2.5 g/L lime and 1.1 g/L aluminum chloride dosage addition at room temperature for 30 minutes
---: Discontinuous lines are the theoretical proposals

**Figure 7.22.-** Integrated process block diagram

## 7.5. Appendix

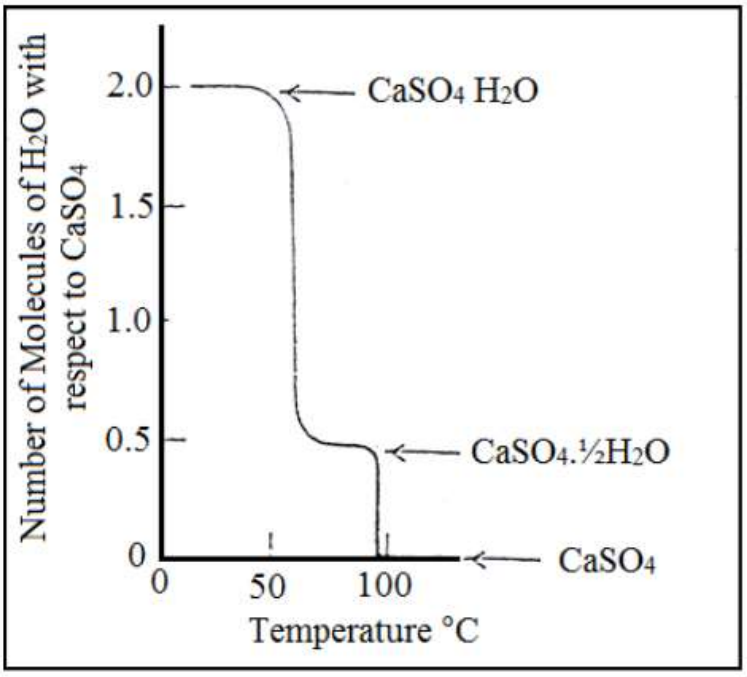


**Figure 7.A.1.-** Gypsum dehydration with temperature[58]

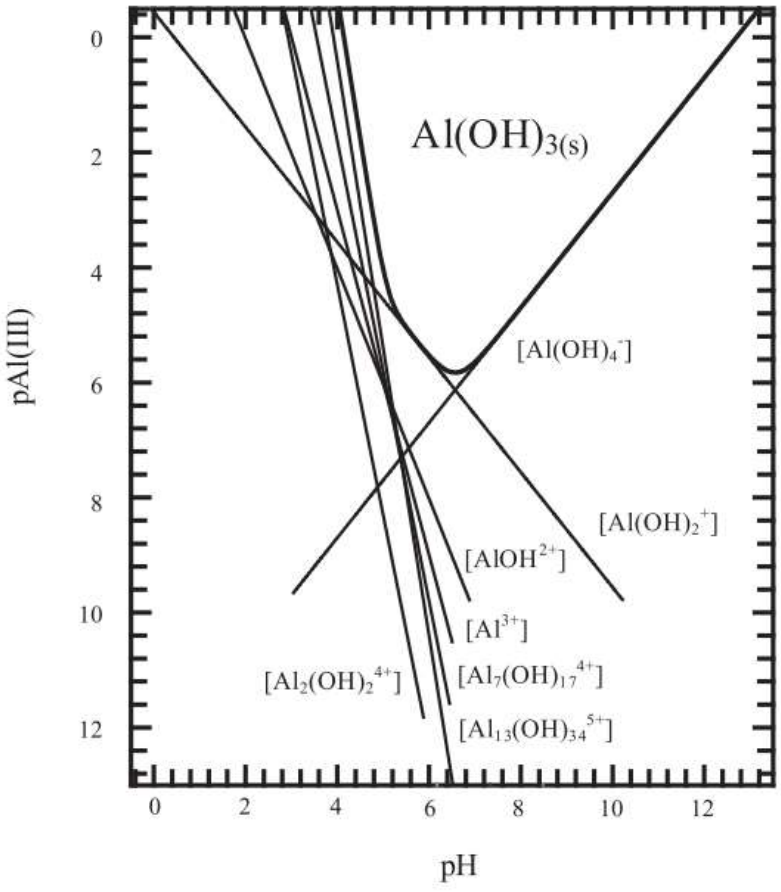

**Figure 7.A.2**.- Aluminum hydroxide solubility and dissolved phases vs. pH[59]

**Table 7.A.1.-** Average composition (mg/L) of the UT, GP, GP' and GP'' effluent

| | $SO_4^=$ | $Cl^-$ | $F^-$ | Al | Mg | Na | Fe | Ca | Si | K | pH |
|---|---|---|---|---|---|---|---|---|---|---|---|
| UT effluent | 42200 | 876 | 1450 | 4475 | 3254 | 1025 | 2031 | 440 | 423 | 541 | 2.5 |
| GP effluent | 1748 | 872 | <0.1 | <0.1 | <0.1 | 1185 | <0.1 | 831 | <0.1 | 557 | 12.4 |
| GP' effluent | 8174 | 877 | <0.1 | <0.1 | 2271 | 865 | <0.1 | 416 | <0.1 | 516 | 6.9 |
| GP'' effluent | 1770 | 876 | <0.1 | <0.1 | <0.1 | 1200 | <0.1 | 1025 | <0.1 | 560 | 12.4 |

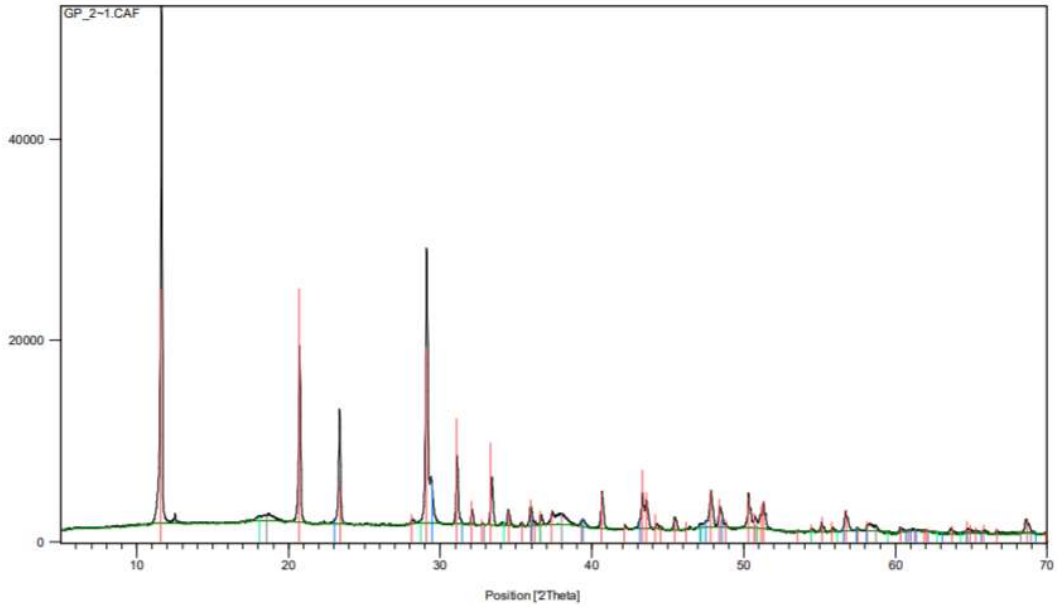


**Figure 7.A.3.-** XRD diffractogram of the solid obtained in GP'' process

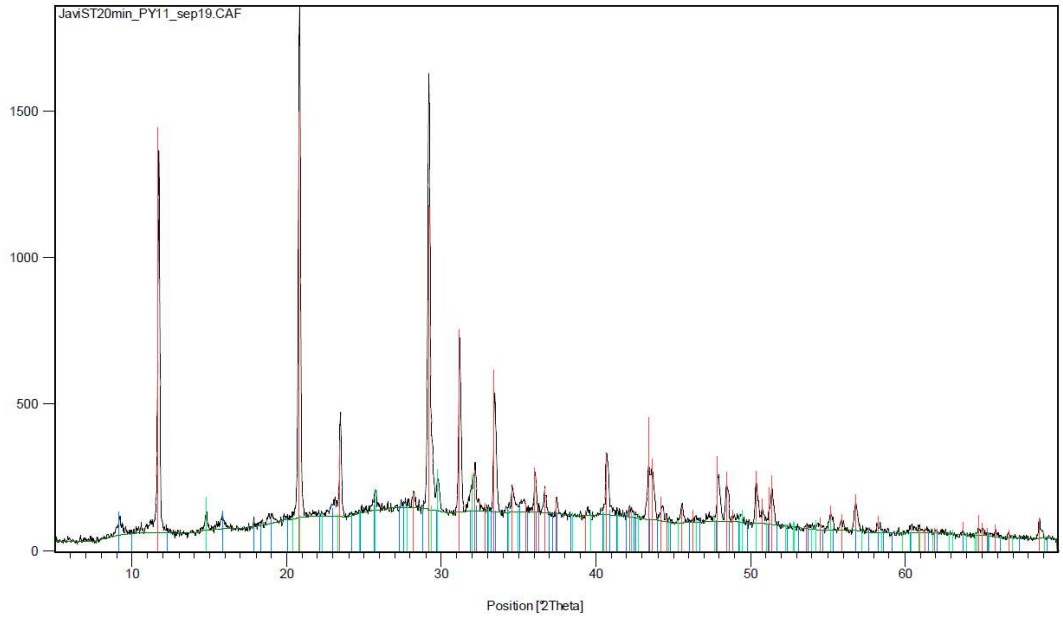


**Figure 7.A.4.-** XRD diffractogram of the solid obtained in GP 9 process

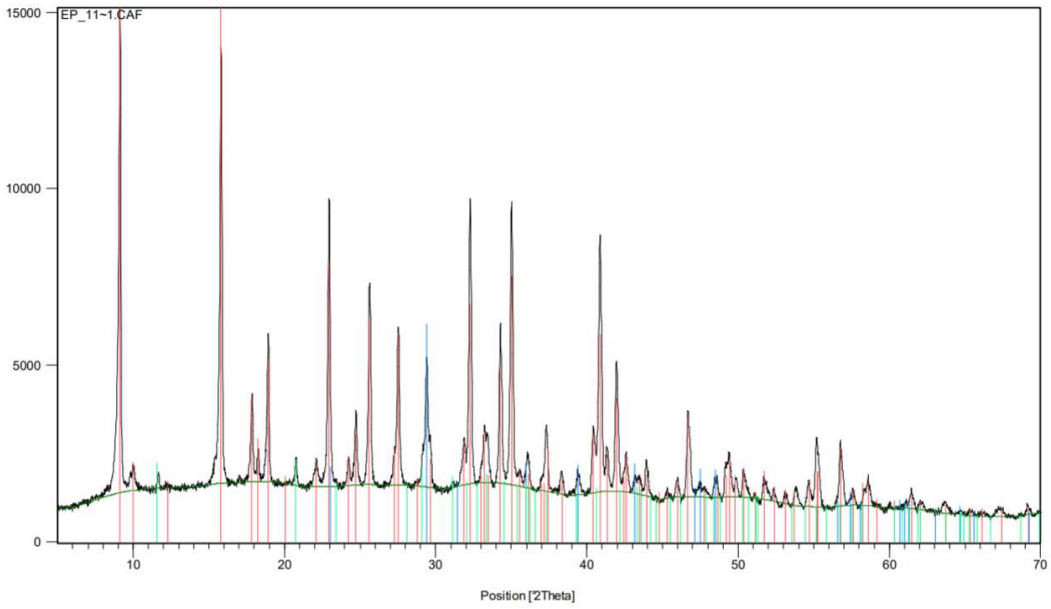


**Figure 7.A.5.-** XRD diffractogram of the solid obtained in EP 9 process

## 7.6. References


[1] A. Haghtalab, M. J. Kamali, A. Shahrabadi, *Fluid Phase Equilib.* **2014**, *373*, 43–54.
[2] J. Sun, L. Wang, G. Yu, *J. Chem. Eng. Data* **2015**, DOI 10.1021/acs.jced.5b00005.
[3] A. M. Cody, H. Lee, R. D. Cody, P. G. Spry, *Cem. Concr. Res.* **2004**, *34*, 869–881.
[4] S. Tait, W. P. Clarke, J. Keller, D. J. Batstone, *Water Res.* **2009**, DOI 10.1016/j.watres.2008.11.008.
[5] M. M. Emamjomeh, M. Sivakumar, A. S. Varyani, *Desalination* **2011**, *275*, 102–106.
[6] A. Mitra, SILICA DISSOLUTION AT LOW PH IN THE PRESENCE AND ABSENCE OF FLUORIDE, **2008**.
[7] P. Richard George, *PROCESS FOR THE TREATMENT OF HIGH SULPHATE WATERS*, **2015**, WO 2015/162540 A1.
[8] D. Damidot, U. A. Birnin-Yauri, F. P. Glasser, *Adv. Cem. Res.* **1994**, *7*, 129–134.
[9] D. Guimarães, V. de A. Oliveira, V. A. Leão, *J. Therm. Anal. Calorim.* **2016**, *124*, 1679–1689.
[10] P. Geldenhuys, A.J., Maree, J.P., de Beer, M., Hlabela, *J. South African Inst. Min. Metall.* **2003**, 345–354.
[11] M. Kotze, Z. Hendriette, *Improved Effluent Treatment Process for Sulphate Removal*, **2017**, CA 2993284.
[12] S. C. B. Myneni, T. J. Logan, G. A. Waychunas, **2021**, *31*, 1761–1768.
[13] C. J. Warren, E. J. Reardon, *Cem. Concr. Res.* **1994**, *24*, 1515–1524.
[14] R. Fischer, H. J. Kuzel, *Cem. Concr. Res.* **1982**, *12*, 517–526.
[15] V. S. Ramachandra, Z. Chun-Mei, *Mater. Struct.* **1986**, *19*, 437–444.
[16] M. W. . M. W. G. [Grafflin, *J. Chem. Educ.* **1929**, *6*, 1007.
[17] T. Grounds, H. G Midgley, D. V Novell, *Thermochim. Acta* **1988**, *135*, 347–352.
[18] T. Nishikawa, K. Suzuki, S. Ito, K. Sato, T. Takebe, *Cem. Concr. Res.* **1992**, *22*, 6–14.
[19] C. Hall, P. Barnes, A. D. Billimore, A. C. Jupe, X. Turrillas, *J. Chem. Soc. - Faraday Trans.* **1996**, *92*, 2125–2129.
[20] M. Fridrichová, K. Dvořák, D. Gazdič, J. Mokrá, K. Kulísek, *Adv. Mater. Sci. Eng.* **2016**, *2016*, DOI 10.1155/2016/9280131.
[21] Q. Zhou, E. E. Lachowski, F. P. Glasser, *Cem. Concr. Res.* **2004**, *34*, 703–710.
[22] Q. Zhou, F. P. Glasser, *Cem. Concr. Res.* **2001**, *31*, 1333–1339.
[23] V. Satava, O. Veprek, *J. Am. Ceram. Soc.* **1975**, *73*, 357–359.
[24] K. Ogawa, D. M. Roy, *Cem. Concr. Res.* **1981**, *11*, 741–750.
[25] A. Haghtalab, M. H. Badizad, *Fluid Phase Equilib.* **2016**, DOI 10.1016/j.fluid.2015.10.011.
[26] G. Azimi, V. G. Papangelakis, J. E. Dutrizac, *Fluid Phase Equilib.* **2007**, DOI 10.1016/j.fluid.2007.07.069.
[27] F. Visconti, J. M. De Paz, J. L. Rubio, *Eur. J. Soil Sci.* **2010**, *61*, 255–270.
[28] Z. Li, G. P. Demopoulos, *Ind. Eng. Chem. Res.* **2006**, *45*, 2914–2922.
[29] E. Rodil, J. H. Vera, *Fluid Phase Equilib.* **2001**, *187–188*, 15–27.
[30] A. Ferse, *J. Solid State Electrochem.* **2013**, *17*, 1321–1332.
[31] T. Yuan, J. Wang, Z. Li, *Fluid Phase Equilib.* **2010**, DOI 10.1016/j.fluid.2010.06.012.
[32] L. J. Kirwan, A. Hartshorn, J. B. McMonagle, L. Fleming, D. Funnell, *Int. J. Miner. Process.* **2013**, DOI 10.1016/j.minpro.2013.01.001.
[33] J. Ma, K. Zhai, Z. Li, *Hydrometallurgy* **2011**, DOI 10.1016/j.hydromet.2011.01.002.
[34] B. I. Whittington, B. L. Fletcher, C. Talbot, *Hydrometallurgy* **1998**, *49*, 1–22.
[35] A. M. Borreguero, I. Garrido, J. L. Valverde, J. F. Rodríguez, M. Carmona, *Energy Build.* **2014**, *76*, 631–639.
[36] Anhidritec, Minersa Group, "Industrial applications of anhydrite," can be found under https://www.anhydritec.com/, **2014**.
[37] AECOM, *Direct Potable Reuse Feasibility Study Report*, **2017**.
[38] R. . Bowell, in *IMWA Preceedings*, **2004**, pp. 329–342.
[39] A. M. Silva, R. M. F. Lima, V. A. Leão, *J. Hazard. Mater.* **2012**, *221–222*, 45–55.
[40] P. J. Usinowicz, B. F. Monzyk, L. Carlton, *Proc. Water Environ. Fed.* **2014**, *2006*, 139–153.
[41] J. . Smit, in *Int. Symp. Mine, Water Environ. 21st Century*, Seville, Spain, **1999**.
[42] International network for acid prevention, *Treatment of Sulphate in Mine Effluents*, **2003**.
[43] D. J. Hassett, G. J. McCarthy, P. Kumarathasan, D. Pflughoeft-Hassett, *Mater. Res. Bull.* **1990**, *25*, 1347–1354.
[44] R. Naidoo, K. Preez, Y. Govender-ragubeer, in *IMWA*, **2018**, pp. 215–220.

[45] E. T. Tolonen, T. Hu, J. Rämö, U. Lassi, *J. Environ. Manage.* **2016**, *181*, 856–862.
[46] M. L. D. Gougar, B. E. Scheetz, D. M. Roy, *Waste Manag.* **1996**, *16*, 295–303.
[47] M. Chrysochoou, D. Dermatas, *J. Hazard. Mater.* **2006**, *136*, 20–33.
[48] J. Kiventerä, K. Piekkari, V. Isteri, K. Ohenoja, P. Tanskanen, M. Illikainen, *J. Clean. Prod.* **2019**, *239*, DOI 10.1016/j.jclepro.2019.118008.
[49] B. Guo, K. Sasaki, T. Hirajima, *Cem. Concr. Res.* **2017**, *100*, 166–175.
[50] M. Zhang, E. J. Reardon, *Environ. Sci. Technol.* **2003**, *37*, 2947–2952.
[51] D. H. Moon, D. Dermatas, D. G. Grubb, *Environ. Monit. Assess.* **2010**, *169*, 259–265.
[52] G. J. McCarthy, D. J. Hassett, J. A. Bender, *MRS Proc.* **1991**, *245*, 129–140.
[53] H. Poellmann, S. Auer, H.-J. Kuzel, R. Wenda, *Cem. Concr. Res.* **1993**, *23*, 422–430.
[54] M. Niu, G. Li, Y. Wang, L. Cao, L. Han, Q. Li, Z. Song, *Constr. Build. Mater.* **2019**, *225*, 868–878.
[55] M. Niu, G. Li, Y. Wang, Q. Li, L. Han, Z. Song, *Constr. Build. Mater.* **2018**, *193*, 332–343.
[56] R. O. Abdel Rahman, D. H. A. Zin El Abidin, H. Abou-Shady, *Chem. Eng. J.* **2013**, *228*, 772–780.
[57] A. F. S. Gomes, D. L. Lopez, A. C. Q. Ladeira, *J. Hazard. Mater.* **2012**, *199–200*, 418–425.
[58] A. Al-obaidi, A. Al-Karawi, **1990**, pp. 1–6.
[59] D. Kartikaningsih, Y. J. Shih, Y. H. Huang, *Sustain. Environ. Res.* **2016**, *26*, 150–155.

# Chapter 8

Global conclusions and future work

# Table of contents

## 8.1. Introduction

This PhD thesis proposes an integrated process for salt cake Paval valorization (fluoride content reduction) through a hydrometallurgical process and the treatment of the produced effluent for its recycling, thus, reducing waste production. In this final chapter, the main conclusions are summarized and proposals for future research on the topic are suggested.

The effect of the main operating parameters (acidic and basic leaching agents, temperature, pH, reaction time and solid/liquid ratio) on the selective fluoride leaching from industrial Paval samples was studied while minimizing aluminum removal.

The above hydrometallurgical process produces a sulfate containing waste effluent. In order to reduce waste output, the purification of this stream and its reutilization into the hydrometallurgical process were studied. The scaling nature of the effluent required the adaptation and optimization of different sulfate removal methods.

In the next sections the main findings of the research are presented.

## 8.2. Hydrometallurgical process conclusions

After a thorough study of selective fluoride leaching, the main conclusions were:

- $H_2SO_4$ aqueous solutions were the most suitable leaching agent due to its high F removal selectivity and the possibility for Al/F leaching control.
- The main variables affecting the leaching process (temperature, $H_2SO_4$ concentration and their interaction) contributed to 95-100 % of the results' variance according to the ANOVA analysis.
- The selected leaching conditions (50 °C, 0.5 M $H_2SO_4$ and 59 minutes) reduced the F content in the sample from 1.2 to 0.7 wt% while only reducing the Al from 33 to 31 wt%.
- Samples of similar characteristics containing up to 1.6 wt% F could be treated with this process to achieve F contents below 1.0 wt%.

- The treated Salt Cake Paval is proposed as a good alternative to Bauxite in Europe based on availability and elemental and phase composition similarities.
- The hydrometallurgical treatment produces a liquid effluent, which could not be recycled into the circuit without prior treatment due to its scaling nature.

## 8.3. Effluent purification conclusions

The main conclusions of the waste effluent purification and reutilization research were:

- Sulfate concentration in the untreated effluent decreased from 42200 to 1748 mg/L, and metals to trace levels in 30 minutes with a 51 g/L lime dosage.
- With a 42 g/L limestone and 8.5 g/L lime dosage (GP'') equivalent results were obtained while reducing sludge production by 10 % and reactant costs by 50 %.
- With a 2.5 g/L lime and 1.1 g/L aluminum chloride dosage (EP) sulfate concentration decreased from 1748 to 70 mg/L in 30 minutes. Aluminum hydroxide inhibited ettringite formation due to its low solubility.
- GP'' effluent was found to be successfully reused for at least 9 recycles, regardless of the NaKCl and sulfate accumulation in the stream. The EP process successfully reduced sulfate concentration in GP'' 9 effluent to 140 mg/L, obtaining an effluent high in NaKCl and lime.
- As a result of these findings, an integrated process has been proposed, where:
    - The recycled effluent would be suitable to enter the Salt Slag processing after the ettringite precipitation and the carbonation steps to recover limestone and NaKCl respectively.
    - The gypsum or anhydrite recovered from the sulfate removal treatments could be commercialized for cement industry, Bayer red muds neutralization, screed mortar applications, contaminated soil recovery or mineral processing.

    - Ettringite could be commercialized as cementing compound, as sorbent, and dissolved by acid attack to produce aluminum hydroxide and gypsum.
- Alternatively, ettringite's complex crystal structure could be capitalized to immobilize hazardous chemicals from external effluents, providing an additional source of income.

## 8.4. Future work

A PhD is never an end, as it opens interesting new research paths. It is therefore important to highlight future research areas that could benefit from the present work:

- The fluoride content limit in the materials for the refractory manufacturing industry decreased from 1.0 to 0.5 wt% since the beginning of this research. Therefore, the current process parameters must be tailored to meet the current standards.
- As this research focused on the valorization of an industrial by-product, the process should be upscaled and upgraded from laboratory-scale batch processing to pilot/industrial (semi-)continuous operation mode. Prior to the upscaling and upgrading it would be interesting to:
    - Assess the possibility of one-pot gypsum precipitation where limestone and lime are added at different intervals to avoid one solid/liquid separation step.
    - Study the $CO_2$ recycling into the effluent carbonation step and the consecutive limestone recycling to further improve the environmental impact of the process.
    - Carry out an energetic, economic and environmental study of the integrated process.
- Study which effluents could be introduced in the ettringite precipitation step to be intertized.